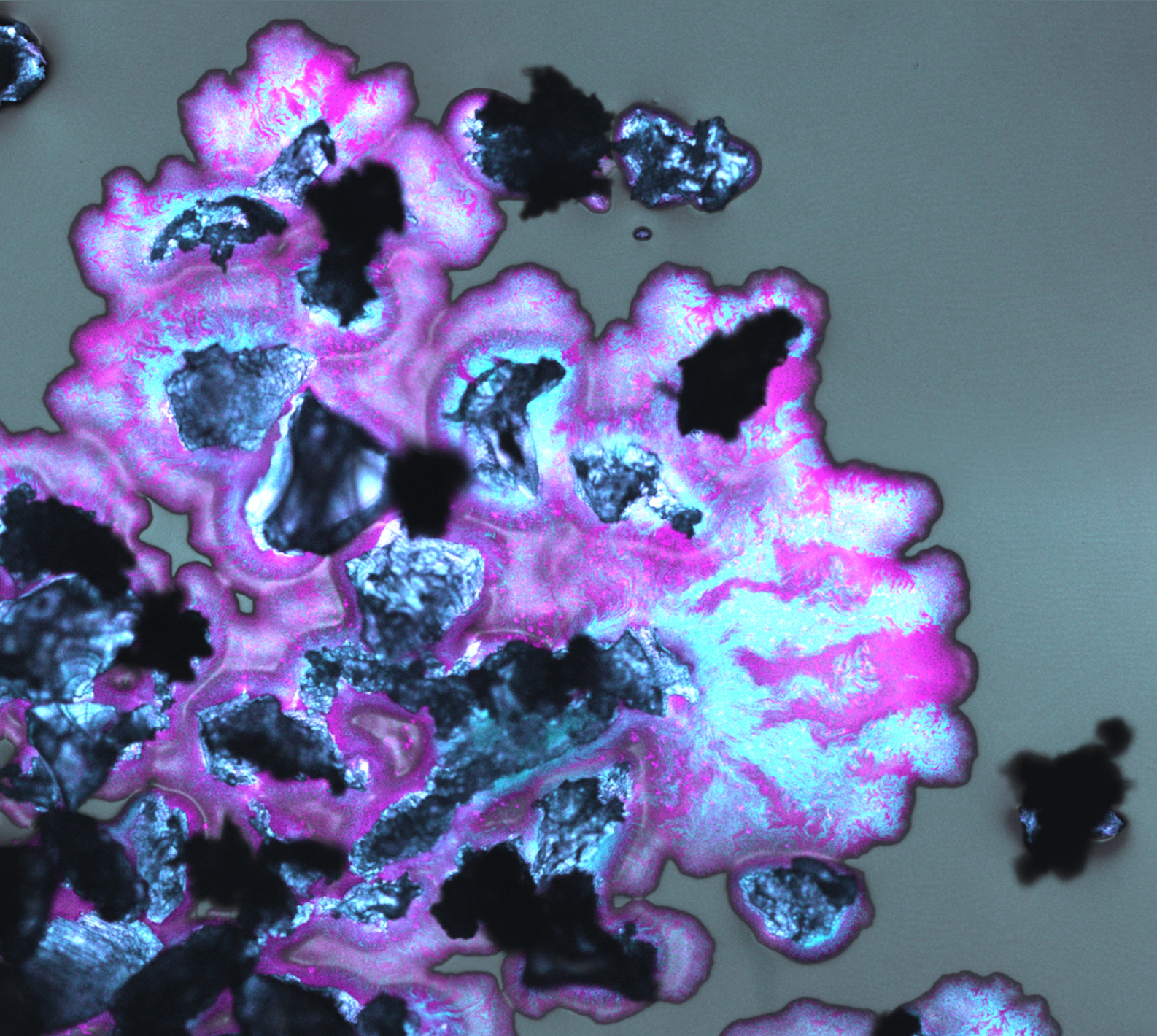


Influence of temporal and spatial heterogeneity on microbial spatial self-organization.

Davide Ciccarese

DISS. ETH NO. 26644



DISS. ETH NO. 26644

Influence of temporal and spatial heterogeneity on microbial spatial self-organization.

A thesis submitted to attain the degree of

DOCTOR OF SCIENCES of ETH ZURICH

(Dr. sc. ETH Zurich)

presented by

Davide Ciccarese

MSc, University of Milan

born on 08.03.1983

citizen of

Italy

accepted on the recommendation of

Prof. Dani Or	Examiner
Prof. Jan Roelof van der Meer	Co-examiner
Dr David R. Johnson	Co-examiner

2020

Dedicated to Sara

Table of Contents

Summary	6
Sommario	8
1. Introduction	10
2. Functional microbial landscapes	26
3. The right place at the right time – environmental feedbacks favor a few lucky individuals for proliferation during bacterial range expansion	51
4. Spatial jackpot events enable community persistence during fluctuations between mutualism and competition.	75
5. Interaction-dependent effects of surface structure on the spatial self-organization of microbial communities.	101
6. The strength of a metabolic interaction determines the establishment, proliferation, and spatial organization of local microbial populations	133
7. Discussion and outlook	152
Acknowledgements	165
Curriculum vitae	168

SUMMARY

In this thesis work, I investigated the influences of environmental heterogeneities on the spatial self-organization of microbial communities. I took a reductionist approach using isogenic cross feeding strains grown under controlled environmental conditions. The environmental heterogeneities investigated in this research study include local nutrient availability, temporal fluctuations in environmental conditions, physical structures, and spatial distance between interacting individuals. In Chapter 1, I describe the main knowledge gaps regarding spatiotemporal heterogeneities as drivers of microbial spatial organization and community composition. In Chapter 2, I review the methods and current state of research in synthetic ecology to investigate the causes and consequences of microbial spatial self-organization. I described the properties of patterns of self-organization and propose methods to quantify them. Finally, I give an overview on the existing methods to engineer the spatial organization of microbial communities. In Chapter 3, I co-authored a research article on the influence of local nutrient concentrations on spatial organization and the maintenance of diversity during expansion of a cross-feeding community. I provided an agent-based model developed by Benedict Borer (ETHZ, STEP) that describes the influence of spatial organization on the reproductive success of lineages with consequences on the maintenance of genetic diversity during range expansion. I contributed to the experimental results, to the formulation of the main research question, and to the writing of the manuscript. In Chapter 4, I investigate patterns of spatial self-organization that emerge during range expansion of a cross feeding community under temporal fluctuations in the available electron acceptor. I used an updated version of the model presented in Chapter 3 to explain the mechanisms that enable the persistence of the community during fluctuating conditions and preserve genetic diversity. In Chapter 5, I describe how physical objects on a surface influence spatial self-organization and interspecific diversity during range expansion. I found that physical objects have differing effects depending on the types of interactions (competition and mutualism) present between genotypes. More specifically, I found that competitive interactions maintain higher diversity at the expanding edge compared to mutualistic interactions. In Chapter 6, I illustrate how the strength of a mutualistic interaction determines whether individuals are likely to develop into colonies. More specifically, I show that colony abundance, size and interspecific distance all depend on the strength of the interaction. I found that the mutualistic component of the net interaction determines the number of colonies and interspecific distances while the competitive component of the net interaction determines colony

size. In Chapter 7, I discuss the main outcome of the research work and I describe new direction of future investigations.

SOMMARIO

In questo lavoro di ricerca ho investigato le influenze delle eterogeneità ambientali sull'organizzazione delle comunità microbiche. Mi sono servito di un approccio riduzionistico usando mutanti isogenici con dipendenza trofica. Le eterogeneità ambientali investigate in questo lavoro di ricerca, sono rispettivamente: disponibilità di nutrienti locale, fluttuazioni temporali, strutture fisiche e interazioni a distanza tra individui. Nel capitolo 1, descrivo le lacune di conoscenza relative alle eterogeneità spazio-temporali che determinano l'emergere delle strutture batteriche e che influenzano in fine la composizione comunitaria. Nel capitolo 2, illustro i metodi e lo stato attuale della ricerca dell'ecologia sintetica nello studio delle cause e conseguenze delle strutture batteriche. Ho descritto le proprietà degli struttura spaziali microbiche e ho proposto metodi per quantificare la loro disposizione spaziale. Infine, fornisco una panoramica dei metodi attualmente esistenti per ingegnerizzare le comunità microbiche. Nel capitolo 3, descrivo un lavoro di ricerca di cui sono stato coautore per studiare l'influenza della concentrazione locale di nutrienti sulla organizzazione microbica spaziale e sulle linee genetiche intraspecifiche durante l'espansione di comunità batteriche trofiche. Ho fornito un modello matematico basato sull'agente, sviluppato da Benedict Borer (ETHZ, STEP) capace di descrivere l'influenza delle strutture batteriche sul successo riproduttivo della diversità intraspecifica con conseguenze sulla deriva genetica nelle comunità in espansione. Ho contribuito ai risultati sperimentali, alla formulazione della domanda di ricerca principale e alla stesura del manoscritto. Nel capitolo 4 indago l'auto-organizzazione spaziale che emerge durante l'espansione delle comunità trofiche in condizioni atmosferiche fluttuanti. Ho usato una versione aggiornata del modello presentato nel capitolo 3 per spiegare i meccanismi che consentono la persistenza delle strutture batteriche capaci di preservare la diversità genetica in condizioni fluttuanti. Nel capitolo 5, descrivo come gli oggetti fisici su una superficie influenzano la diversità interspecifica nelle comunità in espansione. Diversi tipi di interazione (competizione e mutualismo) subiscono una diversa diminuzione della diversità genetica in presenza di oggetti fisici. Ho potuto osservare che le interazioni competitive mantengono una maggiore diversità ai margini in espansione rispetto alle interazioni mutualistiche. Nel capitolo 6, illustro il successo della colonizzazione come conseguenza della intensità delle interazioni trofiche. In questo capitolo, mostro che il numero relativo delle colonie dipende dall'interazione trofica a livello di comunità. Mentre a livello locale, l'interazione tra colonie vicine si dimostra essere una competizione di tipo

intraspecifica e interspecifica. Nel capitolo 7, discuto il risultato principale del lavoro di ricerca e ne descrivo gli sviluppi futuri.

CHAPTER 1: Introduction

Microbial spatial self-organization

Life on Earth is sustained by biogeochemical cycles powered by microbial communities [1–7]. One general feature that characterizes these communities is their incredibly biodiversity, and several mechanisms enable the coexistence of multiple genotypes [1, 8–13]. For example, different genotypes may perform different steps of the metabolic pathways (*i.e.*, division of metabolic labor) that contribute to these biogeochemical cycles [14–18]. The metabolically specialized genotypes can then occupy different niches and thus avoid competition [19, 20]. Genotypes could also change their surrounding environment (niche construction) creating favorable conditions for [21] or conversely leading to deleterious effects on other genotypes [22]. Because the vast majority of microbial life is found in spatially structured microbial communities (defined as surface attached communities) all of the above mechanisms could occur [1, 23, 24]. Living in densely packed communities results in inevitable interactions with other genotype, and these interactions may dictate the metabolic strategy that one genotype has evolved [11, 12, 25–30].

Eventually, interactions between different genotypes on a surface will result in the emergence of non-random patterns referred to as spatial self-organization [31, 32]. These spatial patterns will influence the evolutionary processes acting on and the ecological processes performed by the communities themselves [33–36]. Therefore, it is fundamental to understand the mechanisms that promote spatial self-organization in order to understand the functioning and behaviors of microbial communities. Yet, there is still a lack of understanding on how spatial self-organization emerges in the first place. Furthermore, there is a lack of knowledge regarding the mechanisms that promote the emergence of spatial self-organization and the effects of spatial self-organization on ecological processes. This knowledge gap limits our ability to understand microbial communities outside of laboratory conditions where multispecies interactions create complex spatial structures and challenge the interpretation of their functionality [37]. In Chapter 2, I review the methods and research that has been conducted to explore the spatial self-organization of microbial communities.

The emergence of microbial spatial self-organization leads the community to reach a functionality that depends on the genotypic assemblage and their local interactions with each other [38, 39]. The actual microbial spatial structures enable different genotypes to specialize at different steps of metabolic pathways that are otherwise impermissible [40]. Therefore, when the genotypes are assembled together, they form specific microbial landscape with new capabilities [41, 42].

Within microbial communities, interactions between genotypes can be so important that very often many genotypes cannot be cultivated alone because they required other genotypes to produce essential biosynthetic building blocks [43, 44]. In fact, the collective properties of a microbial community are typically greater than the sum of properties of the individual genotypes [45]. These properties are often referred to as emergent properties [45, 46]. However, the interplay between different genotypes is also mediated by the environment [22, 47]. Microbial populations create intimate connections with the surrounding environment that are often difficult to separate completely [47, 48], to the point that isolating single species from their original environment becomes impossible [49, 50]. Therefore, it is the interplay between biotic and abiotic factors that determine the composition of microbial communities [34, 51–55]. Yet, one great knowledge gap is to understand how biotic and abiotic factors contribute to the development of spatial self-organization of microbial communities [37, 42, 56].

To fill this knowledge gap, I took a reductionist approach where I used an experimental model system to explore how metabolic interactions between two isogenic cross-feeding mutants affect spatial self-organization under controlled environmental conditions. In my research, I identified four main aspects that describe environmental heterogeneity: local nutrient availability, temporal fluctuations in environmental conditions, physical structures, and spatial distance between interacting individuals [15, 57]. I independently investigated how each of these parameters influence spatial self-organization using a synthetic cross feeding community as model system.

The model system is based on the bacterium *Pseudomonas stutzeri* A1501, which is a facultative anaerobic denitrifier [58]. The isogenic mutants were constructed by deleting gene clusters that encode for different steps of the denitrification pathway [59]. By deleting the *nir* gene cluster, one isogenic mutant is unable to reduce nitrite (NO_2^-) to nitric oxide (NO), and I refer to this strain throughout the dissertation as the producer (*i.e.*, it produces NO_2^- from the reduction of NO_3^-) [59–61]. By deleting the *nar* gene cluster, a second isogenic mutant is unable to reduce nitrate (NO_3^-) to nitrite (NO_2^-), and I refer to this strain throughout the dissertation as the consumer (*i.e.*, it consumes

the NO_2^- produced by the producer) [52–54]. In addition, by also using a completely reducing strain that reduces nitrate to nitrogen gas, I can study competitive interactions under anaerobic conditions [62]. The three strains carry different fluorescent protein-encoding genes (*egfp* or *ecfp*) thus enabling me to distinguish them under the microscope and study their spatial arrangement [60, 61].

Our model system enables me to explore a variety of interactions (Fig. 1). When the producer and consumer are mixed to an equal ratio and deposited on an agar plate as described elsewhere [63], the bacterial cells expand and arrange themselves in space. Under anaerobic conditions, the two strains engage in a nitrite (NO_2^-) cross-feeding interaction [63, 64]. During expansion when nitrate (NO_3^-) is provided as the growth limiting substrate, the producer and consumer will expand sequentially (Fig. 1A and B) where the producer grows ahead of the consumer (Fig. 1C). Yet, the consumer could reach the edge of the expanding colony due to initial spatial positioning (Fig. 1C). The model system has an additional feature at pH 6.5, where nitrite (NO_2^-) becomes toxic [59], thus increasing the strength of the interaction between the producer and consumer. Conversely at pH 7.5 nitrite (NO_2^-) is less toxic, thus decreasing the strength of the interaction between the producer and consumer. Under aerobic conditions, the producer and consumer are metabolically independent and compete for oxygen. They consequently expand parallel to the axis of range expansion and form segregated sectors (Fig. 1D). The same pattern formation emerges if instead one would use two differently fluorescently tagged complete reducers (Fig. 1D). In Chapters 3, 4, 5 and 6, I investigate and discuss the ecological consequences of these different patterns of spatial self-organization.

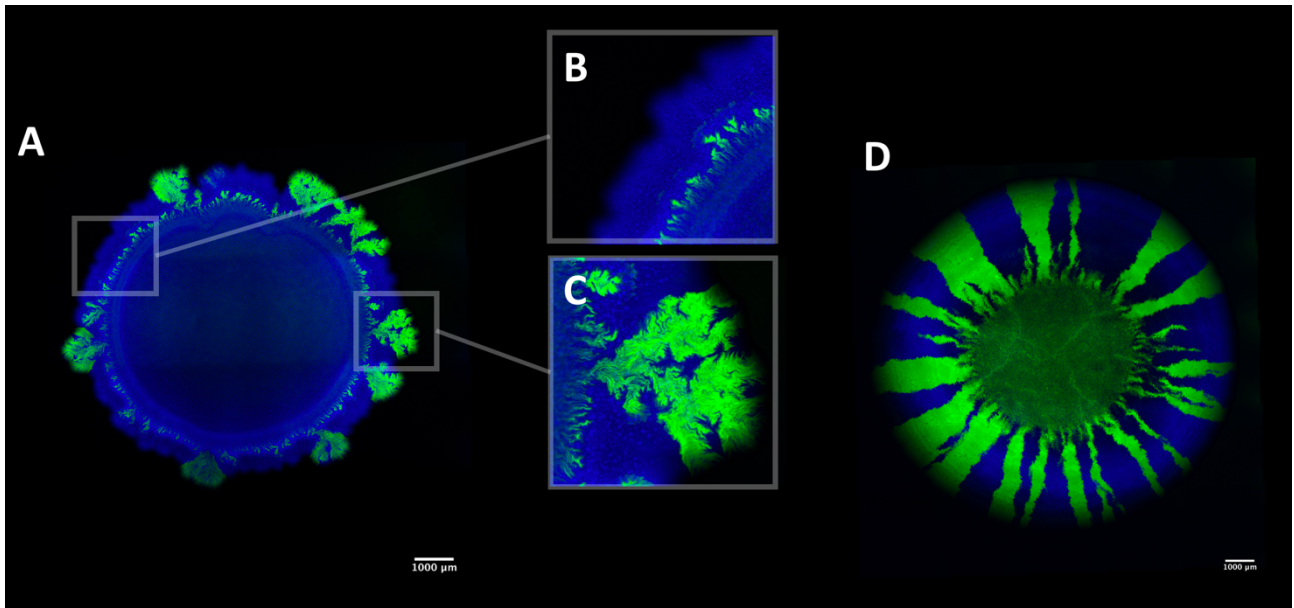


Figure 1. Patterns of spatial self-organization produced by our model system. *A)* Under anaerobic conditions when nitrate (NO_3^-) is provided as the growth-limiting substrate, the producer (expressing the cyan fluorescent protein) and the consumer (expressing the green fluorescent protein) grow sequentially (close-up picture *B*). However, in some area of the expansion, the consumer can reach the expanding edge due to initial spatial positioning of the consumer cells (close-up picture *C*). *D)* Under aerobic conditions, the producer (expressing the cyan fluorescent protein) and consumer (expressing the green fluorescent protein) grow simultaneously and create segregative sectors. The same pattern formation emerges when using two complete reducers.

Main knowledge gaps

Below I identify four main knowledge gaps regarding the causes and consequences of microbial spatial self-organization. All four knowledge gaps can be addressed using the experimental model system described above and serve as the motivation for my four research chapters.

Spatial self-organization mediated by local environmental feedbacks

Any sessile microbial community is intimately connected with its with their surrounding environment [47, 65]. Individual cells change their surrounding environment and create optimal conditions to proliferate [47]. In dense communities, these local interactions enable the spatial structuring and persistence of genotypes [66]. However, any sessile microbial assemblage poses great challenges to investigating how individual genotypes contribute to the maintenance of community diversity.

In the third chapter, I present how local nutrient concentrations influence pattern formation and genetic diversity using a mathematical model developed by Benedict Borer (ETHZ, STEP). In our cross-feeding model system (described above), the emergence of dendritic-like structures of the consumer enable their local population to remain at the edge of the colony (Fig. 1C). The emergence of these structure is favored by an initial spatial positioning of the consumer at the expanding edge. However, these structures seem to be an exception during successive expansion, and I therefore define them as spatial jackpot events in line with previous studies [67]. The mathematical model is able to describe how the metabolic interaction changes the local environment, creating heterogenous distributions of metabolites that influence spatial self-organization and population genetics. The model is then able to link the influence of jackpot events on the reproductive success of intraspecific lineages [68]. This result gives a better understanding of the interplay between spatial self-organization and population dynamics. More importantly, the model describes the intimate connection that spatial self-organization creates with the surrounding environment. Thus, suggesting a mechanism of growth rate differences due to heterogeneous local nutrient concentration within the expanding populations that drives the emergence of pattern formation.

Effects of spatial self-organization on community stability

The ecological stability of microbial communities is important in order to maintain its functioning over time [69]. However, periodic or sporadic changes in local environmental conditions pose a continuous challenge to this stability [70–73]. What are the mechanisms that prevent an ecosystem from collapsing in the face of these environmental changes? Does microbial spatial self-organization have a role in maintaining community stability over time?

The fourth chapter addresses this knowledge gap and builds upon to the previous one, as it investigates the emergence of the same pattern formation (spatial jackpot events) during temporal fluctuations in environmental conditions. The investigation of this specific heterogeneity is fundamental since every microbial community experiences fluctuating conditions that may affect community assembly [74, 75] and in turns their local spatial arrangement. It is then unclear how microbial spatial self-organization helps to maintain their ecological functionality under dynamically changing environmental conditions.

I wanted to fill this knowledge gap using our cross-feeding consortium to study the influence of temporal fluctuations on spatial self-organization. Specifically, our model system enables us to study changes in pattern formation as a response to fluctuating conditions (Fig.1). When the two isogenic cross-feeding mutants are exposed to anaerobic conditions, they expand successively (positive interactions) (Fig.1B). In contrast, when they are incubated in aerobic conditions, they become metabolically independent, enabling the emergence of simultaneous expansion patterns (negative interactions Fig. 1C). The underlying hypothesis is that such a change between two different spatial organizations can compromise the cross-feeding community over time. In the fourth chapter, I show that the cross feeding system is maintained over time as a consequence of the emergence and persistence of jackpot events. Moreover, I tested two different strengths of interactions. I found that the persistence of jackpot events increased as the strength of the interaction increased. This chapter sheds new light on how spatial self-organization helps to maintain the stability of trophic dependent microbial assembly during temporal fluctuation.

Effects of physical objects on spatial self-organization

The emergence of spatial self-organization in microbial communities is determined in part by abiotic factors [76]. In particular, in the natural environment spatial geometry can influence species distributions and community assembly [36, 77–83]. Any population that lives attached to a surface will inevitably undergo range expansion [1, 11, 84]. Therefore, the presence of physical structures on a surface can be a potentially important determinant of microbial spatial organization [85–89]. How does geometric heterogeneity influence microbial spatial arrangement during range expansion?

I addressed this question in Chapter 5 by comparing the effects of physical objects on spatial self-organization for two different types of interactions. More specifically, I determined the effects of physical objects for negative interactions (competitive interaction) between two complete reducers and positive interactions (mutualistic interactions) between the producer and consumer. I postulated that physical objects create deformities at the expanding edge, which in turn affects spatial self-organization [88]. Such deformations at the expansion edge would not only affect spatial self-organization and ecosystem functioning, but also population dynamics [88, 90]. This is novel, as previous studies of the influence of physical objects was only investigated for competitive interactions [88, 91], and thus did not consider trophic interactions. Comparing these different interactions is important, as the spatial arrangements of competing and metabolically dependent species can be fundamentally different [61, 92].

I extended this work in Chapter 5 to investigate how the presence of physical objects affects diversity at the expansion edge. I found that, geometric heterogeneity has a smaller impact on interspecific diversity for the negative interaction (competition) than for the cross-feeding interactions (mutualism). This chapter shows how geometric heterogeneity shapes interspecific diversity along expansion edges and highlights that the type of interaction is a key determinant to affecting community diversity during range expansion.

Effects of initial spatial positioning on spatial self-organization

When a population establishes on a new surface, the initial spatial positioning of individuals can determine individual fate and success at colonizing the new surface [93, 94]. For example, when two metabolically dependent strains are separated by space, the interactions between individuals are determined by the diffusion of exchanged metabolites [47, 95]. Therefore, the initial spatial positioning is particularly important for the success of trophically interacting strains that rely on metabolite diffusion [39, 47, 65, 96]. The local densities of individuals, for instance, affect the gradient of the metabolites [34, 77]. However, it is the initial positioning of individuals that modulate the resource allocation between individuals [65]. The spatial distribution of species depends on their local interactions influencing the overall community properties [65, 97]. The emergence of colonies and their establishment in pure competitive scenario has been showed to be a territorial competition for space where the winning genotype outcompete the others maximizing its spatial coverage to access to the resource [93]. Yet, when two strains compete, the distances between colonies is determined by the type of competing species and nutrient source [96].

In Chapter 6, I studied the effect of local interactions and community composition (colonization success) comparing strong and weak mutualism. This chapter shows that the final composition of a community depends on different types of interactions that act locally to define the spatial distances (competition) and globally to determine the final number of individuals that compose a community (mutualism).

Thesis outline

In Chapter 2, I provide a review on the state of knowledge regarding microbial spatial self-organization, including an overview of approaches to study spatial self-organization under laboratory conditions. I describe several synthetic ecology approaches that try to fill the knowledge gap on how the spatial self-organization influences community functioning, ecology, and evolution. In Chapter 3, I applied an agent-based model developed by Benedict Borer (ETHZ, STEP) to elucidate mechanisms that drive spatial self-organization in light of different trophic interactions. Furthermore, this study provides an explanation for how localized growth rate differences rooted in the underlying nutrient landscape promote the emergence of different patterns that influence the genetic diversity.

In Chapter 4, I show how spatial self-organization enables community persistence in the face of fluctuating environmental conditions. I further describe a potential mechanism for how self-organization bestows the observed stability.

In Chapter 5, I report how geometric heterogeneity influences the emergence of spatial patterns during mutualistic and competitive interactions. I show how physical objects can modulate spatial self-organization and, in turn, population diversity. I found that the type of interaction is a key determinant of interspecific diversity in presence of physical objects.

In Chapter 6, I present how the community composition is affected by the interplay between initial spatial positioning of individuals and local interactions. I found that the final community composition is determined by mutualistic interactions at the community level but by competition at the local level.

In Chapter 7, I discuss the main outcomes of the dissertation and provide an outlook that emerges from the collective body of my work. I identify key areas for future investigation and propose approaches to address these new areas of research. I finally discuss how my research outcomes may be generalizable to other types of microbial communities.

REFERENCES

1. Flemming HC, Wuertz S. Bacteria and archaea on Earth and their abundance in biofilms. *Nat Rev Microbiol* 2019; **17**: 247–260.
2. Lloyd KG, Steen AD, Ladau J, Yin J, Crosby L. Phylogenetically Novel Uncultured Microbial Cells Dominate Earth Microbiomes. *mSystems* 2018; **3**:pii: e00055-18
3. L.R. T, J.G. S, D. M, A. A, J. L, K.J. L, et al. A communal catalogue reveals Earth's multiscale microbial diversity. *Nature* 2017; **551**:457-463
4. Whitman WB, Coleman DC, Wiebe WJ. Prokaryotes: The unseen majority. *Proc Natl Acad Sci U S A* . 1998; **95**:6578-83
5. Locey KJ, Lennon JT. Scaling laws predict global microbial diversity. *Proc Natl Acad Sci U S A* 2016; **113**:5970-5.
6. Venter JC, Remington K, Heidelberg JF, Halpern AL, Rusch D, Eisen JA, et al. Environmental Genome Shotgun Sequencing of the Sargasso Sea. *Science (80-)* 2004; **304**:66-74
7. Planet of the microorganisms. *Nat Rev Microbiol* 2018; **16**: 257–257.
8. van Gestel J, Kolter R. When We Stop Thinking about Microbes as Cells. *J Mol Biol* . 2019; **431**:2487-2492
9. Nadell CD, Xavier JB, Foster KR. The sociobiology of biofilms. *FEMS Microbiol Rev* 2009; **33**: 206–224.
10. Mitri S, Xavier JB, Foster KR. Social evolution in multispecies biofilms. *Proc Natl Acad Sci* 2011; **108**: 10839–10846.
11. Mitri S, Richard Foster K. The Genotypic View of Social Interactions in Microbial Communities. *Annu Rev Genet* 2013; **47**: 247–273.
12. Crespi BJ. The evolution of social behavior in microorganisms. *Trends Ecol Evol* . 2001; **16**:178-183.
13. Foster KR. A defense of sociobiology. *Cold Spring Harb. Symp. Quant. Biol.* 2009; **74**:403-18
14. Ackermann M. A functional perspective on phenotypic heterogeneity in microorganisms. *Nat Rev Microbiol* 2015; **13**: 497–508.
15. Stubbendieck RM, Vargas-Bautista C, Straight PD. Bacterial communities: Interactions to scale. *Front Microbiol* 2016; **7**: 1–19.
16. Ponomarova O, Patil KR. Metabolic interactions in microbial communities: Untangling the Gordian knot. *Curr Opin Microbiol* 2015; **27**: 37–44.

17. Johnson DR, Goldschmidt F, Lilja EE, Ackermann M. Metabolic specialization and the assembly of microbial communities. *ISME J*. 2012; **6**:1985–91.
18. Dolinšek J, Goldschmidt F, Johnson DR. Synthetic microbial ecology and the dynamic interplay between microbial genotypes. *FEMS Microbiol Rev* 2016; **40**: 961–979.
19. Archidona-Yuste A, Wiegand T, Castillo P, Navas-Cortés JA. Spatial structure and soil properties shape local community structure of plant-parasitic nematodes in cultivated olive trees in southern Spain. *Agric Ecosyst Environ* 2020; **27**:104658
20. Peipoch M, Miller SR, Antao TR, Valett HM. Niche partitioning of microbial communities in riverine floodplains. *Sci Rep* 2019; **9**:16384
21. Herschend J, Koren K, Røder HL, Brejnrod A, Kühl M, Burmølle M. In Vitro Community Synergy between Bacterial Soil Isolates Can Be Facilitated by pH Stabilization of the Environment . *Appl Environ Microbiol* 2018; **84**: 1–15.
22. Ratzke C, Denk J, Gore J. Ecological suicide in microbes. *Nat Ecol Evol* 2018; **2**: 867–872.
23. Flemming H-C, Wingender J, Szewzyk U, Steinberg P, Rice SA, Kjelleberg S. Biofilms: an emergent form of bacterial life. *Nat Rev Microbiol* 2016; **14**: 563–575.
24. Flemming HC, Wingender J. The biofilm matrix. *Nat Rev Microbiol* . 2010; **8**:623-33
25. Hallatschek O, Hersen P, Ramanathan S, Nelson DR. Genetic drift at expanding frontiers promotes gene segregation. *Proc Natl Acad Sci* 2007; **104**: 19926–19930.
26. Van Gestel J, Weissing FJ, Kuipers OP, Kovács ÁT. Density of founder cells affects spatial pattern formation and cooperation in *Bacillus subtilis* biofilms. *ISME J* 2014; **8**: 2069–2079.
27. Muller MJI, Neugeboren BI, Nelson DR, Murray AW. Genetic drift opposes mutualism during spatial population expansion. *Proc Natl Acad Sci* 2014; **111**: 1037–1042.
28. Mitri S, Clarke E, Foster KR. Resource limitation drives spatial organization in microbial groups. *ISME J* 2016; **10**: 1471–1482.
29. Nadell CD, Drescher K, Foster KR. Spatial structure, cooperation and competition in biofilms. *Nat Rev Microbiol* 2016; **14**: 589–600.
30. McNally L, Bernardy E, Thomas J, Kalzqi A, Pentz J, Brown SP, et al. Killing by Type VI secretion drives genetic phase separation and correlates with increased cooperation. *Nat Commun* 2017; **8**: 14371.
31. Rietkerk M, van de Koppel J. Regular pattern formation in real ecosystems. *Trends Ecol Evol* 2008; **23**: 169–175.
32. Pringle RM, Tarnita CE. Spatial Self-Organization of Ecosystems: Integrating Multiple

- Mechanisms of Regular-Pattern Formation. *Annu Rev Entomol* 2017; **62**:359-377
- 33. Kim W, Racimo F, Schluter J, Levy SB, Foster KR. Importance of positioning for microbial evolution. *Proc Natl Acad Sci U S A* 2014; **111**: E1639-47.
 - 34. Cordero OX, Datta MS. Microbial interactions and community assembly at microscales. *Curr Opin Microbiol*. 2016; **31**:227-234
 - 35. Estrela S, Brown SP. Community interactions and spatial structure shape selection on antibiotic resistant lineages. *PLOS Comput Biol* 2018; **14**: e1006179.
 - 36. Neu L, Proctor CR, Walser J-C, Hammes F. Small-Scale Heterogeneity in Drinking Water Biofilms. *Front Microbiol* 2019; **10**: 2446.
 - 37. Tecon R, Mitri S, Ciccarese D, Or D, van der Meer JR, Johnson DR. Bridging the Holistic-Reductionist Divide in Microbial Ecology. *mSystems* 2019; **4**: e00265-18
 - 38. Bottery MJ, Passaris I, Dytham C, Wood AJ, van der Woude MW. Spatial Organization of Expanding Bacterial Colonies Is Affected by Contact-Dependent Growth Inhibition. *Curr Biol* 2019; **29**:3622-3634
 - 39. Nadell CD, Drescher K, Foster KR. Spatial structure, cooperation and competition in biofilms. *Nat Rev Microbiol* 2016; **14**: 589–600.
 - 40. Zerfaß C, Chen J, Soyer OS. Engineering microbial communities using thermodynamic principles and electrical interfaces. *Curr Opin Biotechnol*. 2018; **50**:121-127
 - 41. Madsen JS, Sørensen SJ, Burmølle M. Bacterial social interactions and the emergence of community-intrinsic properties. *Curr Opin Microbiol*. 2018. Elsevier Ltd. , **42**: 104–109
 - 42. Ciccarese D, Johnson DR. Functional Microbial Landscapes. *Compr Biotechnol* 2019; 42–51.
 - 43. Stewart EJ. Growing unculturable bacteria. *J Bacteriol*. 2012; **94**:4151-60
 - 44. Puspita ID, Kamagata Y, Tanaka M, Asano K, Nakatsu CH. Are uncultivated bacteria really uncultivable? *Microbes Environ* . 2012. **27**: 356–366
 - 45. Nadell CD, Foster KR, Xavier JB. Emergence of spatial structure in cell groups and the evolution of cooperation. *PLoS Comput Biol* 2010; **6**: e1000716
 - 46. Flemming HC, Wingender J, Szewzyk U, Steinberg P, Rice SA, Kjelleberg S. Biofilms: An emergent form of bacterial life. *Nat Rev Microbiol* . 2016; **14**:563-75
 - 47. Estrela S, Libby E, Van Cleve J, Débarre F, Deforet M, Harcombe WR, et al. Environmentally Mediated Social Dilemmas. *Trends Ecol Evol* 2019; **34**: 6–18.
 - 48. Odling-Smee FJ, Laland KN, Feldman MW. Niche construction: The neglected process in evolution. *Princeton University Press* . 2013; **30**: 191–202

49. Pham VHT, Kim J. Cultivation of unculturable soil bacteria. *Trends Biotechnol*. 2012; **30**:475-84
50. Ferrari BC, Binnerup SJ, Gillings M. Microcolony cultivation on a soil substrate membrane system selects for previously uncultured soil bacteria. *Appl Environ Microbiol* 2005; **71**:8714-20
51. Lee CK, Laughlin DC, Bottos EM, Caruso T, Joy K, Barrett JE, et al. Biotic interactions are an unexpected yet critical control on the complexity of an abiotically driven polar ecosystem. *Commun Biol* 2019; **2**:62
52. Ebrahimi A, Schwartzman J, Cordero OX. Cooperation and spatial self-organization determine rate and efficiency of particulate organic matter degradation in marine bacteria. *Proc Natl Acad Sci U S A* 2019; **116**: 23309–23316.
53. Wu X, Wang Y, Zhu Y, Tian H, Qin X, Cui C, et al. Variability in the Response of Bacterial Community Assembly to Environmental Selection and Biotic Factors Depends on the Immigrated Bacteria, as Revealed by a Soil Microcosm Experiment. *mSystems* 2019; **4**: e00496-19
54. Jiang X, Zerfaß C, Feng S, Eichmann R, Asally M, Schäfer P, et al. Impact of spatial organization on a novel auxotrophic interaction among soil microbes. *ISME J* 2018; **12**:1443–1456
55. Kassen R. The experimental evolution of specialists, generalists, and the maintenance of diversity. *J Evol Biol* 2002; **15**: 173–190.
56. Widder S, Allen RJ, Pfeiffer T, Curtis TP, Wiuf C, Sloan WT, et al. Challenges in microbial ecology: building predictive understanding of community function and dynamics. *ISME J* 2016; **10**: 2557–2568.
57. Ramette A, Tiedje JM. Multiscale responses of microbial life to spatial distance and environmental heterogeneity in a patchy ecosystem. *Proc Natl Acad Sci U S A* 2007; **104**: 2761–6.
58. Lalucat J, Bennasar A, Bosch R, Garcia-Valdes E, Palleroni NJ. Biology of *Pseudomonas stutzeri*. *Microbiol Mol Biol Rev* 2006; **70**: 510–547.
59. Lilja EE, Johnson DR. Metabolite toxicity determines the pace of molecular evolution within microbial populations. *BMC Evol Biol* 2017; **17**: 1–12.
60. Goldschmidt F, Regoes RR, Johnson DR. Metabolite toxicity slows local diversity loss during expansion of a microbial cross-feeding community. *ISME J* 2018; **12**: 136–144.
61. Goldschmidt F, Regoes RR, Johnson DR. Successive range expansion promotes diversity and

- accelerates evolution in spatially structured microbial populations. *ISME J* 2017; **11**:2112–2123
- 62. Lilja EE, Johnson DR. Segregating metabolic processes into different microbial cells accelerates the consumption of inhibitory substrates. *ISME J* 2016; **10**: 1568–1578.
 - 63. Goldschmidt F, Regoes RR, Johnson DR. Successive range expansion promotes diversity and accelerates evolution in spatially structured microbial populations. *ISME J* 2017; **11**: 2112–2123.
 - 64. Lilja EE, Johnson DR. Metabolite toxicity determines the pace of molecular evolution within microbial populations. *BMC Evol Biol* 2017; **17**: 52.
 - 65. Harcombe WR, Riehl WJ, Dukovski I, Granger BR, Betts A, Lang AH, et al. Metabolic resource allocation in individual microbes determines ecosystem interactions and spatial dynamics. *Cell Rep* 2014; **7**: 1104–1115.
 - 66. Nadell CD, Drescher K, Foster KR. Spatial structure, cooperation and competition in biofilms. *Nat Rev Microbiol* 2016; **14**: 589–600.
 - 67. Fusco D, Gralka M, Kayser J, Anderson A, Hallatschek O. Excess of mutational jackpot events in expanding populations revealed by spatial Luria-Delbrück experiments. *Nat Commun* 2016; **7**:12760
 - 68. Wright ES, Vetsigian KH. Stochastic exits from dormancy give rise to heavy-tailed distributions of descendants in bacterial populations. *Mol Ecol* 2019; **28**:3915–3928
 - 69. Li W, Stevens MHH. Community temporal variability increases with fluctuating resource availability. *Sci Rep* 2017; **7**: 45280
 - 70. Shenhav L, Furman O, Briscoe L, Thompson M, Silverman JD, Mizrahi I, et al. Modeling the temporal dynamics of the gut microbial community in adults and infants. *PLoS Comput Biol* 2019; **15**: e1006960
 - 71. Buscardo E, Geml J, Schmidt SK, Freitas H, Da Cunha HB, Nagy L. Spatio-temporal dynamics of soil bacterial communities as a function of Amazon forest phenology. *Sci Rep* 2018; **8**:4382
 - 72. Pett-Ridge J, Silver WL, Firestone MK. Redox fluctuations frame microbial community impacts on N-cycling rates in a humid tropical forest soil. *Biogeochemistry* 2006; **81**:95–110
 - 73. Tecon R, Ebrahimi A, Kleyer H, Erev Levi S, Or D. Cell-to-cell bacterial interactions promoted by drier conditions on soil surfaces. *Proc Natl Acad Sci* 2018; **115**: 9791–9796.
 - 74. Rodríguez-Verdugo A, Vulin C, Ackermann M. The rate of environmental fluctuations shapes ecological dynamics in a two-species microbial system. *Ecol Lett* . 2019; **22**:838-846

75. Doan HK, Leveau JHJ. Artificial Surfaces in Phyllosphere Microbiology. *Phytopathology* 2015; **105**: 1036–1042.
76. Green JL, Bohannan BJM, Whitaker RJ. Microbial biogeography: from taxonomy to traits. *Science* 2008; **320**: 1039–43.
77. Datta MS, Sliwerska E, Gore J, Polz MF, Cordero OX. Microbial interactions lead to rapid micro-scale successions on model marine particles. *Nat Commun* 2016; **7**:1196
78. Ettema CH, Wardle DA. Spatial soil ecology. *Trends Ecol Evol*. 2002; **17**:177-183
79. Ramette A, Tiedje JM. Multiscale responses of microbial life to spatial distance and environmental heterogeneity in a patchy ecosystem. *Proc Natl Acad Sci U S A* 2007; **104**:2761-2766
80. Tecon R, Or D. Cooperation in carbon source degradation shapes spatial self-organization of microbial consortia on hydrated surfaces. *Sci Rep* 2017; **7**: 1–11.
81. Borer B, Tecon R, Or D. Spatial organization of bacterial populations in response to oxygen and carbon counter-gradients in pore networks. *Nat Commun* 2018; **9**:769
82. Enke TN, Leventhal GE, Metzger M, Saavedra JT, Cordero OX. Microscale ecology regulates particulate organic matter turnover in model marine microbial communities. *Nat Commun* 2018; **9**:2743
83. Spiesman BJ, Stapper AP, Inouye BD. Patch size, isolation, and matrix effects on biodiversity and ecosystem functioning in a landscape microcosm. *Ecosphere* 2018; **9**: e02173.
84. Branda SS, Vik Å, Friedman L, Kolter R. Biofilms: The matrix revisited. *Trends Microbiol* 2005; **13**: 20–26.
85. Gralka M, Hallatschek O. Environmental heterogeneity can tip the population genetics of range expansions. *Elife* 2019; **8**: 1–24.
86. Burton OJ, Travis JMJ. Landscape structure and boundary effects determine the fate of mutations occurring during range expansions. *Heredity (Edinb)* 2008; **101**:329–340
87. Möbius W, Murray AW, Nelson DR. How Obstacles Perturb Population Fronts and Alter Their Genetic Structure. *PLoS Comput Biol* 2015; **11**: 1–30.
88. Beller DA, Alards KMJ, Tesser F, Mosna RA, Toschi F, Möbius W. Evolution of populations expanding on curved surfaces(a). *Epl* 2018; **123**:58005
89. Wang G, Or D. Trophic interactions induce spatial self-organization of microbial consortia on rough surfaces. *Sci Rep* 2014; **4**:6757
90. Kayser J, Schreck CF, Gralka M, Fusco D, Hallatschek O. Collective motion conceals fitness

- differences in crowded cellular populations. *Nat Ecol Evol* 2019; **3**: 125–134.
- 91. Möbius W, Murray AW, Nelson DR. How Obstacles Perturb Population Fronts and Alter Their Genetic Structure. *PLOS Comput Biol* 2015; **11**: e1004615.
 - 92. Goldschmidt F, Regoes RR, Johnson DR. Metabolite toxicity slows local diversity loss during expansion of a microbial cross-feeding community. *ISME J* 2018; **12**:136-144
 - 93. P. LD, J. AR. Competition for space during bacterial colonization of a surface. *J R Soc Interface* 2015; **12**: 20150608.
 - 94. Chacón JM, Möbius W, Harcombe WR. The spatial and metabolic basis of colony size variation. *ISME J* 2018; **12**: 669–680.
 - 95. Ghoul M, Mitri S. The Ecology and Evolution of Microbial Competition. *Trends Microbiol* 2016; **24**: 833–845.
 - 96. Chacón JM, Möbius W, Harcombe WR. The spatial and metabolic basis of colony size variation. *ISME J* . 2018. , **12**: 669–680
 - 97. Kerr B., Riley M.A., Feldman M.W., Bohannan B.J.M. Local dispersal promotes biodiversity in a real-life game of rock-paper-scissors. *Nature* 2002; **418**: 171–174.

CHAPTER 2: Functional Microbial Landscapes

A similar version of this chapter has been published as:

Ciccarese, Davide, & Johnson, R. David (2019). Functional microbial landscapes. In S. Agathos & B. Stenuit (Eds.), *Comprehensive biotechnology: Vol. 6. Environmental and related biotechnologies* (pp. 42-51). Elsevier

ABSTRACT

Surface-attached microbial communities are omnipresent on our planet. They play an important role in all major biogeochemical processes, provide valuable services to human society and our environment, and are utilized for biotechnological applications. An important feature of surface-attached microbial communities is that different microbial genotypes are typically not distributed randomly in space. Instead, they are typically distributed non-randomly in space and can arrange themselves into fascinating and intriguing patterns (*i.e.*, spatial self-organization). We refer to these non-random patterns of spatial self-organization as microbial landscapes. In this chapter, we first review the underlying causes of spatial self-organization and the emergence of microbial landscapes. We next describe how the emergence of a microbial landscape can affect the metabolic, ecological, and evolutionary properties and behaviors of microbial communities. We then provide an overview of how to quantitatively analyze microbial landscapes and discuss how such quantitative information can generate insights into the underlying causes and consequences of their emergence. We further discuss how laboratory experiments can inform us about the properties and behaviors of microbial landscapes in nature. Finally, we discuss how we might engineer microbial landscapes to achieve biotechnological objectives.

INTRODUCTION

An immense amount of microbial life on our planet exists in a spatially structured, sessile state attached to surfaces. One example is biofilms, where individual cells are embedded within an extracellular matrix or, in some cases, directly attached to neighboring cells [1, 2]. Surface-attached microbial communities can form on nearly every surface on our planet. This includes biotic surfaces, such as the human gastrointestinal tract [3] and plant roots [4], and abiotic surfaces, such as on soil particles [5], bioreactor components [6], industrial membranes [7], and water distribution pipes [8]. An important feature of surface-attached microbial communities is that cells are typically distributed non-randomly in space, resulting in higher-level functionalities and three-dimensional spatial organization. The formation of such non-random spatial distributions is referred to as spatial self-organization [9,10] and can result in the emergence of fascinating and intriguing spatial patterns [11-19] (Figure 1).

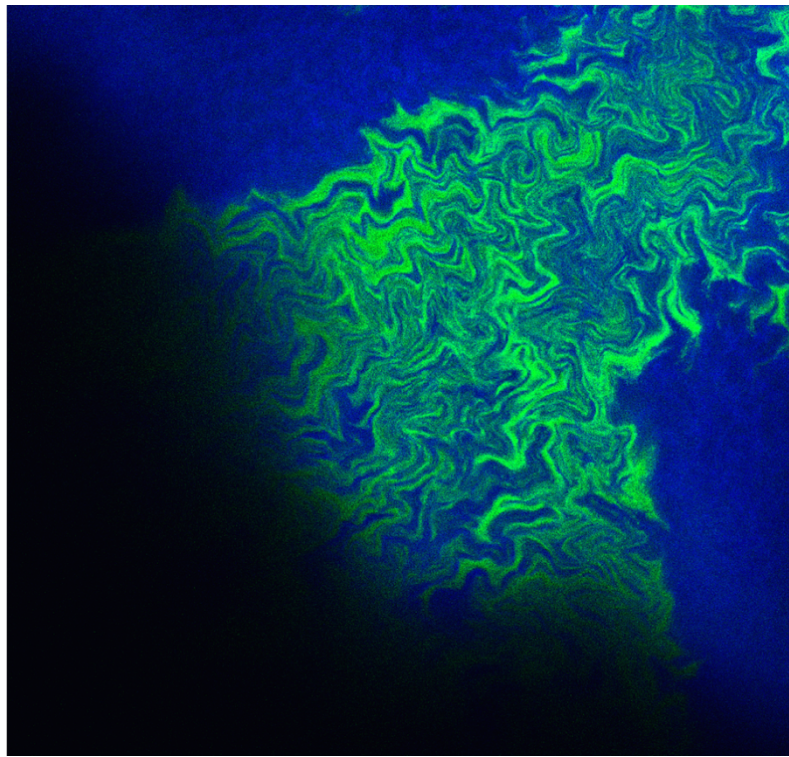


Figure 1. Spatial self-organization of a microbial community. This pattern emerges when two nitrite cross-feeding genotypes are supplied with nitrate as the growth-limiting substrate and expand together across a flat surface. The blue genotype contains a loss-of-function mutation in nitrite reductase and consumes nitrate but not nitrite. The green genotype contains a loss-of-function mutation in nitrate reductase and consumes nitrite but not nitrate. The two genotypes self-organize and produce fractal-like patterns during range expansion. The image is of the leading edge of community expansion and was obtained with confocal laser scanning microscopy.

What causes spatial self-organization to emerge across a surface? There are a multitude of potential causes, but they can broadly be delineated into abiotic and biotic determinants. Abiotic determinants include physical and chemical heterogeneities across the surface itself [20-23]. For example, patchy distributions of resources or local environmental conditions across the surface can cause different species to spatially aggregate together or segregate from each other more often than would be expected by chance, thus resulting in non-random distributions (Figure 2). Biotic determinants include interactions between different genotypes [11, 13, 14, 24]. Negative interactions (*i.e.*, competition, antagonism, *etc.*) can cause the genotypes to spatially segregate from each other, while positive interactions between genotypes (*i.e.*, mutualism, commensalism, *etc.*) can cause the genotypes to spatially aggregate together, both of which create non-random

spatial distributions (Figure 2). We refer to these non-random patterns of spatial self-organization as ‘microbial landscapes’ to emphasize this complexity, where a particular pattern of spatial self-organization may result from the abiotic conditions across the surface, the biotic properties of the resident genotypes, and interactions between those abiotic and biotic factors. Here, the concept of a microbial landscape is inspired from the central tenants of landscape ecology, which seeks to understand the reciprocal effects between patterns of spatial self-organization of ecological objects and the physical, chemical, and biological properties of the ecosystem [25].

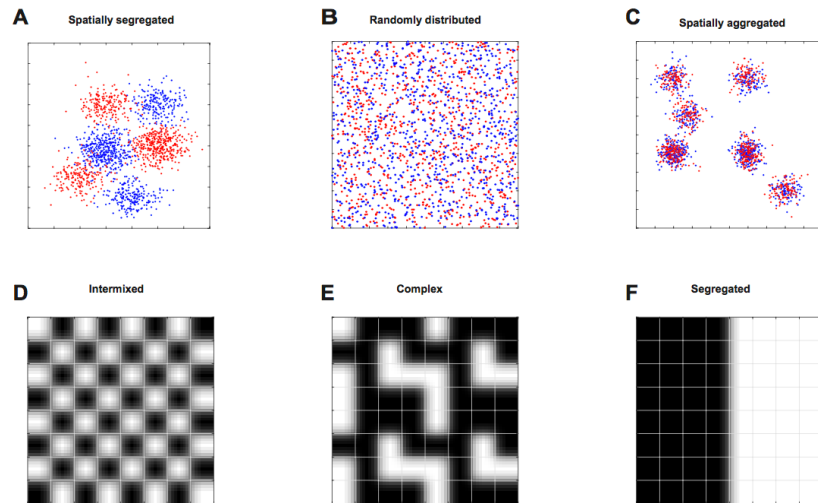


Figure 2. Examples of patterns of spatial self-organization. Consider two different genotypes (marked red and blue). These two genotypes may organize in one of three different patterns. (A) The two genotypes are segregated from each other in space. (B) The two genotypes are randomly distributed in space. (C) The two genotypes are aggregated together in space. The patterns of the two genotypes may also display higher-order properties. (D) The two genotypes are intermixed with a checkerboard pattern. This represents the maximum amount of intermixing but low complexity. (E) The two genotypes are intermixed with a complex pattern. The example is a self-similar fractal-like pattern with an intermediate amount of intermixing and high complexity. (F) The two genotypes are spatially segregated from each other with no intermixing and low complexity.

Properties of microbial landscapes

Why do we care about microbial landscapes? Importantly, a microbial landscape is not merely a fascinating pattern of spatial self-organization. Indeed, the microbial landscape itself can have profound effects on the properties and behaviors of the microbial community as a whole [2]. Below we summarize how the emergence of a microbial landscape can impact the metabolic, ecological, and evolutionary properties of a microbial community.

Metabolic properties

The emergence of a microbial landscape can enable metabolic processes that might otherwise be inefficient, unstable, or impermissible in a completely mixed environment, where microorganisms often exist in an spatially unstructured, planktonic state [26-28]. A canonical example is the enabling of metabolic pathways that would otherwise be thermodynamically unfavorable. Fermentation pathways involving interspecies electron transfer are one example [29]. Many fermentation pathways convert organic matter via the transfer of electrons to electron carriers, such as hydrogen. If hydrogen accumulates to sufficient concentrations, however, the fermentation process may no longer be thermodynamically favorable, consequently slowing or even ceasing operation of the process [29]. To overcome this limitation, genotypes often assemble together and form microbial landscapes that mitigate this effect, where hydrogen-producing genotypes lie in close spatial proximity to hydrogen-consuming genotypes (*i.e.*, spatial aggregation) [29]. The spatial aggregation of hydrogen-producing and -consuming genotypes maximizes the flux of hydrogen between them, thus minimizing the local accumulation of hydrogen and preventing the fermentation process from becoming thermodynamically unfavorable [29]. Another canonical example is the enabling of metabolic pathways that produce toxic intermediates. In investigations by Goldschmidt and coworkers [19, 30], a synthetic cross-feeding microbial community was engineered where one genotype metabolizes nitrate to nitrite while another genotype metabolizes the secreted nitrite. One challenge of this pathway is that nitrite is conditionally toxic [31]. When the genotypes are grown together, they form a specific microbial landscape, where the nitrite producing and consuming genotypes lie in close spatial proximity to each other [19, 30]. This results in increased growth rates of the microbial community as a whole, likely because the spatial aggregation of the different genotypes prevents the accumulation of nitrite and reduces its toxic effects [19, 30].

There are numerous other examples of how the emergence of a microbial landscape can enable otherwise impermissible metabolic processes to occur [26-28]. The recurring theme of these studies is that many metabolic processes require the exchange of metabolites between different genotypes. The emergence of microbial landscapes where the metabolite-exchanging genotypes lie in close spatial proximity to each other (*i.e.*, spatial aggregation) enhances the exchange of metabolites between the genotypes and/or reduces the negative effects of accumulated metabolites. Metabolite exchange thus represents a general mechanism by which the emergence of a microbial landscape can enable otherwise impermissible metabolic processes to occur.

Ecological properties

The emergence of a microbial landscape has strong relationships with the types of interactions that occur between different genotypes [11, 14, 16-18]. Importantly, interactions between different genotypes often depend on their spatial positioning to each other [11, 14, 16-18]. Two genotypes may interact positively (*i.e.*, mutualism, commensalism, *etc.*) if they have one particular spatial positioning, but may interact negatively (*i.e.*, competition, antagonism, *etc.*) if they have an alternative spatial positioning. This was elegantly illustrated with experiments conducted with two genotypes that cross-feed a metabolic intermediate. In those experiments, *Acinetobacter* strain C6 was assembled together with *Pseudomonas putida* strain R1 and the consortia was supplied with benzoyl alcohol as the growth-supporting substrate, where both strains can metabolize benzoyl alcohol via benzoate to CO₂ [32]. When grown together in a chemostat culture in the absence of spatial structure, and thus the absence of a microbial landscape, the two strains competed with each other and the *Acinetobacter* strain eventually reached high frequencies and dominated the culture. When grown together in a spatially structured environment, however, a clear microbial landscape emerged that promoted a more commensal interaction [32]. The *Acinetobacter* strain primarily metabolized benzoyl alcohol to benzoate while the *P. putida* strain metabolized the released benzoate, thus enabling *P. putida* to reach higher frequencies. Thus, the interaction switches from largely negative (*i.e.*, competition for benzoyl alcohol) to commensal (*i.e.*, cross-feeding of benzoate) when spatial structure is present and permits the emergence of a microbial landscape [32].

Another example is that the emergence of a microbial landscape can promote cooperative behaviors between genotypes via the release of metabolic products that are subsequently utilized by other individuals (*i.e.*, public goods). Extracellular polysaccharides (EPS), which are one of the most abundant components of the biofilm matrix, can be viewed as one of these public goods. While some individuals may divert metabolic resources from their own growth into producing and excreting EPS, other individuals may benefit from its release without investing their own resources into its production. In a study by van Gestel and coworkers [33], the authors tested whether EPS production is indeed a cooperative trait. Using mutant strains of *Bacillus subtilis* that differ in the production of EPS, the authors demonstrated that the microbial community as a whole benefits from the presence of mutant genotypes with higher levels of EPS production [33]. Moreover, they demonstrated that the initial relative abundance of different mutant genotypes (and thus different

levels of EPS production) affects the organization of the microbial landscape and other emergent properties of the microbial community [33].

The emergence of a microbial landscape can also have profound effect on the temporal stability of a microbial community. Namely, the small-scale spatial aggregation of different genotypes can stabilize their interactions over time [11, 14]. In a seminal study by Kerr and colleagues [11], the authors created a synthetic microbial community consisting of three genotypes of *Escherichia coli*: one produces colicin (genotype C), one is sensitive to colicin (genotype S), and one is resistance to colicin (genotype R). When propagated in batch culture without spatial structure, only genotype R persists, where it first displaces genotype S and then outcompetes genotype C. Genotype S is displaced due to the production of colicin while genotype C is displaced due to the costs of carrying the colicin-encoding plasmid. When propagated on agar plates that impose spatial structure, however, all three genotypes co-exist and form a distinct microbial landscape, where the three types dynamically invade each other [11]. Genotype C invades genotype S, genotype S invades genotype R, and genotype R invades genotype C. Thus, spatial structure promotes the emergence of a microbial landscape that stabilizes local interactions and enables all three genotypes to co-exist.

Importantly, the example above illustrates that spatial structure and the emergence of a microbial landscape can be a powerful force that maintains biodiversity by stabilizing local interactions between different genotypes [11]. However, the emergence of a microbial landscape can maintain and promote biodiversity via a wide range of additional mechanisms. Among the most intuitive mechanisms is heterogeneity in the local environmental conditions across the landscape that can promote local niche partitioning. If environmental heterogeneity is present, then this heterogeneity can create discrete niche spaces across the landscape, where different specialized genotypes can occupy and persist within different types of niches [20, 21, 24].

Perhaps a less intuitive mechanism for how interactions can maintain biodiversity is the role of the interactions themselves as a microbial community expands across space (*i.e.*, range expansion). In a seminal study by Hallatschek and coworkers [12], the authors constructed a synthetic microbial community consisting of two genotypes of *E. coli* that express different fluorescent proteins but are otherwise genetically identical. The two genotypes thus interact via pure competition. As the microbial community expands across space (*i.e.*, range expansion), only a few individuals emigrate

from the founding zone and contribute to community expansion, reflecting a massive loss of genetic diversity that might be present within the founding zone [12]. In analogous studies by Goldschmidt and coworkers [19, 30], however, the authors engineered communities where the two genotypes interact via metabolite cross-feeding rather than by pure competition. The authors hypothesized that metabolite cross-feeding should promote intermixing between the two genotypes, thus enabling more individuals to emigrate from the founding zone and contribute towards community expansion. Because more individuals would emigrate from the founding zone, this would maintain more of the potential genetic diversity present within the founding zone. Indeed, this outcome was experimentally observed [19, 30]. Thus, interactions that promote the emergence of microbial landscapes with increased intermixing also maintain more genetic diversity as a microbial community expands across space [18, 19, 30].

Finally, the emergence of a microbial landscape can have profound effects on the resistance and resilience of a microbial community to external perturbations. Antibiotic resistance bestowed by extracellular enzymes provides one illustrative example [34]. Assemblages of antibiotic resistant and non-resistant genotypes can co-exist in a spatially structured environment and collectively resist the negative impacts of antibiotic administration [34]. Briefly, when resistant and non-resistant genotypes are grown together in the absence of spatial structure, the resistant genotype displaces the non-resistant genotype after administration of antibiotics. However, when the resistant and non-resistant genotypes arrange themselves into a microbial landscape in a spatially structured environment, the microbial community as a whole can persist after administration of antibiotics. This is because the two genotypes aggregate together in space, and the resistant genotype produces sufficient local concentrations of the extracellular enzyme to confer resistance to the non-resistant genotype. The microbial community can exhibit improved growth as a whole when compared to either genotype growing in isolation, which may result from intrinsic tradeoffs between resistance and growth properties. The non-resistant genotype has improved growth performance because it does not pay the costs for resistance, which manifests into improved growth of the microbial community as a whole when the resistant genotype provides resistance to the non-resistant genotype. However, this effect only occurs when the genotypes grow in a spatially structured environment and form a microbial landscape that results in the spatial aggregation of the two genotypes, thus permitting the extracellular enzyme to accumulate to sufficiently high local concentrations to confer community-level resistance [34].

Evolutionary properties

The emergence of a microbial landscape can also affect the pace of molecular evolution within microbial communities [30, 35, 36]. In a study by Goldschmidt and coworkers [30], the authors found that certain types of microbial landscapes accelerate the pace of molecular evolution. The authors imposed a substrate cross-feeding interaction between two microbial genotypes that promote intermixing between the genotypes. The consequence of intermixing is that each genotype population fragments across space to form smaller local population sizes [30]. Because the local population sizes are smaller, beneficial mutations are more likely to establish within those smaller local populations. The consequence is that the pace of molecular evolution accelerates [30]. This principle is not unique to the substrate cross-feeding interaction imposed by the authors. Instead, it should be generalizable to any interaction or process that promotes the emergence of microbial landscapes where a larger population is spatially fragmented into smaller local population sizes.

Other types of microbial landscapes may decrease the pace of molecular evolution. In the seminal study reported by Hallatschek and coworkers [12], the authors demonstrated that only a few individuals located at the leading edge of an expanding microbial community contribute towards the production of new biomass as the microbial community expands across space (*i.e.*, range expansion). This has an important consequence on molecular evolution. If a beneficial mutation were to emerge behind the leading edge of expansion, it may not be able to establish even though it is beneficial. This is because the benefits of the mutation may not outweigh the unfavorable spatial positioning of the recipient individuals that lie behind the leading edge of expansion, where resources are less available. In other words, the probability that a beneficial mutation will establish depends not only on the benefits of the mutation itself, but also on the spatial arrangement of individuals across the microbial landscape.

Finally, the emergence of a microbial landscape may enable deleterious evolutionary trajectories as a microbial community expands across space (*i.e.*, range expansion) [37, 38]. The fundamental idea here is again that only a few individuals located at the front of an expanding microbial community contribute towards the production of new biomass. If one of those individuals contains a deleterious mutation, it may nevertheless establish within the microbial community. This is because the benefits of its favorable spatial positioning at the leading edge of expansion where resources are abundant

may outweigh the deleterious effects of the mutation itself. This has been referred to as “genetic surfing” and is a potentially generalizable mechanism for how deleterious mutations may spread across space and reach high frequencies [39, 40]. For example, it has been proposed as a mechanism for how deleterious mutations might have accumulated within human populations as they expanded across the planet [39, 41].

Quantifying microbial landscapes

Quantifying features of microbial landscapes is often a central task for many investigations. Quantification enables one to obtain a detailed description of a microbial landscape and generate hypotheses about the underlying processes or interactions that give rise to a particular microbial landscape [42]. The main premise here is that a microbial landscape contains information about the underlying processes or interactions [42]. If such information can be extracted in a quantitative manner, then the quantities can be compared to those expected or predicted for an appropriate null model [42]. Typically, a null model assumes that a microbial landscape emerges via purely random processes (Figure 2). However, more sophisticated null models can be developed, where one or more processes or interactions are assumed to operate [42]. By comparing a particular microbial landscape to an appropriate null model, one may then ask whether quantitative features of the observed microbial landscape are consistent with those expected when specific processes or interactions are incorporated into or removed from the null model. Importantly, comparing a microbial landscape to a null model cannot conclusively confirm or refute a particular process or interaction, as different processes and interactions can, in principle, give rise to quantitatively similar landscapes [42]. Instead, such comparisons are used to generate or refine hypotheses about specific processes or interactions, which ideally could then be directly tested via manipulative experimentation.

One-dimensional spatial intermixing

How do we extract quantitative information from a microbial landscape? There are a multitude of available analytical methods, of which spatial intermixing between two or more genotypes is arguably the simplest. Spatial intermixing is used to test whether two or more genotypes are spatially segregated or intermixed more than would be expected under an appropriate null model (Figure 2). If one observes deviations from that null model, then it can generate hypotheses about the processes or interactions that gave rise to the microbial landscape. For example, spatial

segregation of two genotypes may indicate that the two genotypes engage in a negative interaction (*i.e.*, competition, antagonism, *etc.*). In contrast, extensive spatial intermixing of two genotypes may indicate that the two genotypes engage in a positive interaction (*i.e.*, mutualism, commensalism, *etc.*). Spatial intermixing is often quantified along a one-dimensional line across a microbial landscape (*i.e.*, one-dimensional intermixing). Briefly, one defines an appropriate line and measures the number of transitions that occur between the two genotypes along that line. The number of transitions then provides a measure of the extent of intermixing between the two genotypes. Importantly, one-dimensional intermixing does not provide a global measure of intermixing, and caution must therefore be taken when using one-dimensional intermixing to draw conclusions about a two- or three-dimensional microbial landscape. Nevertheless, one-dimensional intermixing has been successfully applied in microbial ecology to generate novel insights into the causes and consequences of microbial landscapes [16, 19, 30, 43].

Two-dimensional spatial point-pattern analysis

The limitations of one-dimensional intermixing can, to some extent, be overcome using two-dimensional spatial point-pattern analysis methods. Spatial point-pattern analysis can be used to quantify the small-scale local correlational structure of different microbial genotypes across space [42]. As with one-dimensional intermixing, spatial point-pattern analysis can be used to test whether two or more genotypes are spatially aggregated closer together or segregated further apart than would be expected under an appropriate null model (Figure 2), where spatial aggregation may indicate positive interactions (*i.e.*, mutualism, commensalism, *etc.*) while spatial segregation may indicate negative interactions (*i.e.*, competition, antagonism, *etc.*) between the different genotypes. Among the simplest spatial point-pattern analysis methods are nearest neighbor methods [42]. In these approaches, a focal individual of one genotype is selected and the distance to the nearest (or k^{th} nearest) individual of another genotype is calculated. This is performed for a large number of focal individuals and the mean distance is compared to that predicted under an appropriate null model. If the mean distance is smaller than expected under an appropriate null model, then it indicates spatial aggregation of the genotypes. In contrast, if the mean distance is larger than expected under an appropriate null model, then it indicates spatial segregation of the genotypes. Many alternatives to the nearest neighbor methods have been proposed, such as the spherical contact distribution and pair-correlation function [42]. Importantly, all of these alternatives extract slightly different information on the local correlational structure of different

genotypes and can be used in conjunction with each other to obtain a more complete description of a particular microbial landscape [42].

While nearest neighbor methods quantify the two-dimensional correlation structure of a microbial landscape, they only capture the small-scale correlational structure of that landscape [42]. It is plausible that genotypes have a spatially aggregated or segregated correlational structure at one scale, but have the opposite correlational structure at a different spatial scale (*i.e.*, spatial segregation at small scales but spatial aggregation at larger scales) [42]. Many nearest neighbor-type methods would miss this scale dependence of the correlational structure, thus potentially generating misleading hypotheses about the underlying processes or interactions that give rise to a particular microbial landscape. To overcome this limitation, additional point-pattern analysis methods have been developed that quantify correlational structures across a wide range of spatial scales, such as Ripley's K function [44]. Briefly, the correlation metrics are quantified across a range of different spatial scales and the metrics are then plotted against the spatial scale. These methods not only allow one to observe whether the correlational structure differs across spatial scales, but also to identify the precise spatial scales at which differences may occur, thus leading to additional insights into the processes or interactions that cause the emergence of a particular microbial landscape [42].

Higher-order complexity

In some cases, one may not be interested in the local correlational structure of different genotypes, but may instead be interested in quantifying the global properties of a microbial landscape as a whole. For example, higher-order complexity may emerge, such as asymmetry (Figure 2). It is difficult to extract such higher-order complexity with simple one-dimensional intermixing or two-dimensional spatial point-pattern analysis methods because these methods primarily rely on quantifying distances between individuals. How then can we quantify properties of a pattern of spatial self-organization that contain information about higher-order complexity?

Information theory provides the basis for a class of approaches that extract information about higher-order complexity. Shannon entropy, which is built upon information theory, provides one approach. Shannon entropy quantifies the amount of disorder within a system, and several metrics have been developed based on Shannon entropy to describe spatial patterns. For example,

Kolmogorov complexity can be used to quantify the minimum information needed to describe a spatial pattern [45] while Grassberger complexity can be used to quantify how much information is distributed within a spatial pattern [46]. While potentially being extremely powerful for describing microbial landscapes, such approaches are to date not conventionally used in microbial ecology, possibly due to their computational and technical demands. Machine learning techniques might help to overcome some of these challenges. For example, Zieliński and coworkers [47] used a machine learning approach to classify colony shape and identify defined phenotypes. However, while such approaches are an important step forward, the challenge remains in that the metrics generated cannot be used as direct evidence for refuting or confirming the presence of certain types of processes or interactions. Further manipulative experimentation is typically required to draw such conclusions.

Many other types of metrics for quantifying higher-order complexity from microbial landscapes are available. For example, fractal-like branching patterns are often observed during the expansion of a microbial community across space (*i.e.*, range expansion) (Figure 1). These fractal-like branching patterns resemble patterns that emerge from the general process of diffusion-limited aggregation [19, 48, 49]. These patterns can be analyzed by calculating the fractal dimension of the pattern. The value of the fractal dimension may then give insights into the underlying processes that may be occurring, such as diffusion limited aggregation or local mechanical instabilities [19]. The main premise here is that different processes may give rise to different fractal dimensions, although caution is needed when drawing conclusions about processes from a simple measure of the fractal dimension [50, 51]. There are generally two classes of methods to quantify the fractal dimension, including matrix-based and vector-based methods. Among the matrix-based methods, a Euclidean distance map can be used to describe the shape of the interface between two genotypes and has the advantage in that it is reliable and quick to quantify [51, 52]. An alternative approach is box counting [51, 53], which imposes a defined box grid on a pattern to measure the scale-dependent properties of the pattern.

Despite the relative simplicity of the theory behind fractal analysis, a more universal method to describe a microbial landscape is warranted to prevent unbiased interpretations. One potentially universal method to describe a shape is the Fourier Descriptor. The specificity of a shape is characterized and sets of descriptors that specifically belong to that shape are used to compare it

to another shape. Because of its universality, the Fourier Descriptor can be readily applied to a microbial landscape, such as describing the space occupied by different genotypes. For example, Lloyd and coworkers [54] used the Fourier Descriptor to describe the shape of the patch occupied by a colony. Using the Voronoi tessellation, the authors determined the maximum space that the founder cells can cover and compared it to the Fourier descriptor for the colony to establish which of the colonies were able to cover the available space. Since the universality of the Fourier descriptor has great versatility to describe any shape, it can be used to describe nearly any pattern. However, as emphasized for other methods, linking a shape to a particular process or interaction requires reference datasets that are largely missing in microbial ecology [55].

A final measure that can be calculated is simply the space occupied by a microbial community or genotype relative to the total available space. This is an important quantity because it provides a measure of the unexploited space, which under certain conditions can be the limiting resource for a microbial community. Simple spatial metric tools such as the Voronoi tessellation can readily describe the potential unexploited space and therefore be used to compare how growth depends on the metabolic traits of different genotypes. Chacón and coworkers [56] defined a Voronoi response as the relative area covered by a colony to the available area defined by the Voronoi tessellation. This study linked the metabolic characteristics of two different genotypes to colony size variation. In a sense, the authors used the Voronoi tessellation to correlate spatial properties with an observed ecological scenario, where the genotypes competed for space and other resources.

Environmental relevance of experimental microbial landscapes

We have primarily focused on summarizing experiments or theoretical investigations with synthetic microbial communities consisting of two or a few genotypes growing under highly controlled environmental conditions. These reductionist-type investigations seek to minimize biotic and abiotic complexity, thus minimizing confounding factors and facilitating the identification of the underlying causes and consequences of microbial landscapes (Figure 3). This then raises an important question: Are the conclusions drawn from such investigations that minimize biotic and abiotic complexity relevant for understanding the causes and consequences of microbial landscapes under more complex natural environmental conditions (Figure 3)? Can the abiotic or biotic complexities present within natural environments modify the types of microbial landscapes likely to emerge and the properties of those microbial landscapes?

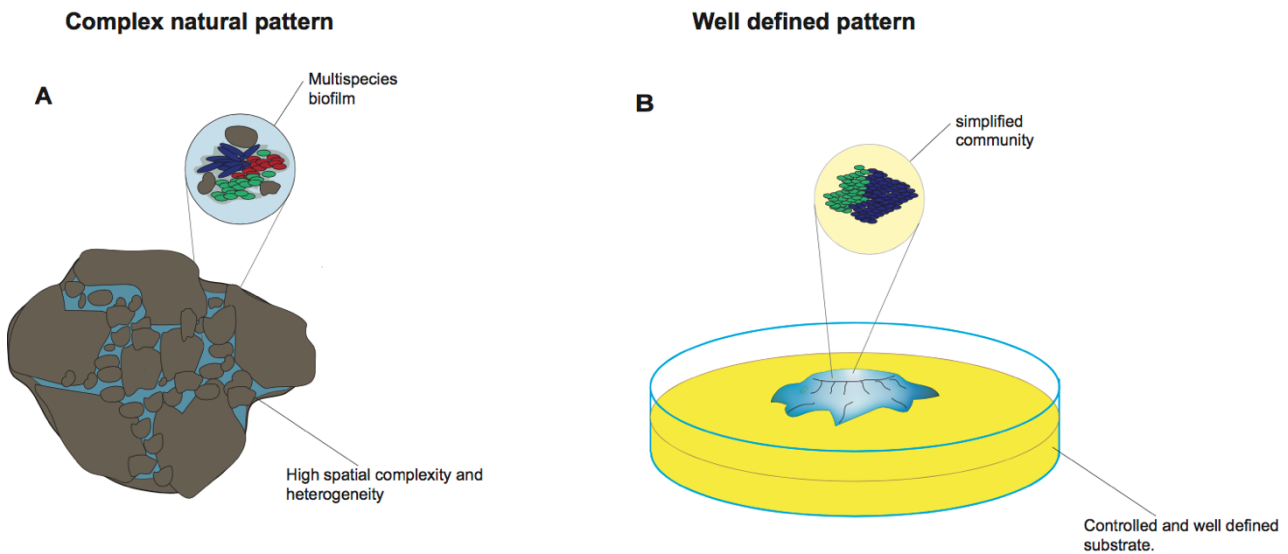


Figure 3. Comparison between natural and laboratory conditions. (A) Natural microbial landscapes contain a wide variety of physical, chemical, and biological complexity that is difficult to replicate under highly controlled laboratory conditions. (B) Laboratory microbial landscapes, such as those that might emerge as a two-genotype community expands in space across a flat surface, have reduced complexity. Reducing complexity in the laboratory facilitates identifying the underlying mechanisms that might promote the emergence of spatial self-organization. These mechanisms, however, might not be the important mechanisms that promote the emergence of spatial self-organization in nature.

One type of complexity that is typically removed from laboratory experiments is geometric complexity. Investigators typically propagate a microbial community over a flat surface. However, microbial communities in nature often confront substantial geometric complexity, such as the pore networks present in soils (Figure 3). Several investigations have sought to address this geometric complexity. For example, Dechesne and coworkers [57] grew cells on a porous surface where water availability could be experimentally controlled. When water saturates the surface, cell movement is geometrically unimpeded. However, as water availability is reduced, the geometric landscape becomes fragmented into localized regions of water saturation. This geometric fragmentation can then give rise to different types of microbial landscapes due to the reduced mobility of individuals. This principle can potentially be generalized, where any geometric complexity that impedes

microbial mobility could have profound effects on the types of microbial landscapes likely to emerge.

Another related complexity is the dimensionality of microbial landscapes. Most laboratory experiments only consider microbial landscapes in two dimensions (Figure 3). However, microbial landscapes are inherently three-dimensional (Figure 3). One challenge to observe and quantify three-dimensional microbial landscapes in geometrically complex environments is how to image cells through those geometric barriers. To overcome this challenge, Leis and coworkers [58] used a Nafion material that imposes physical barriers to microbial cells but is transparent to light, thus enabling microscopic imaging of microbial landscapes without optical obstacles. Several studies have used this material to impose geometric complexity and measure the consequences. For example, Nadell and coworkers [22] explored the effect of two competing strains of *P. aeruginosa* that differ in their ability to form biofilms, where the wild-type strain produces the matrix required for biofilm formation while a mutant strain does not. When propagated over a two-dimensional smooth surface, the wild-type strain displaces the mutant strain. However, when propagated in a complex three-dimensional environment created with Nafion to mimic a soil system, both strains persist in apparent co-existence. The authors hypothesized that the geometric complexity creates local spatial patches where both strains can persist, thus enabling their co-existence at the level of the microbial community. Other strategies also exist for imposing geometric complexity. For example, several studies used PDMS to synthesize an artificial leaf surface and found that geometric complexity provides space for certain individuals to avoid predation, thus promoting the emergence of a different type of microbial landscape [23].

As stated above, a main challenge of reproducing a natural environment in the laboratory is to recreate the three-dimensional space and its physical characteristics (Figure 3). Soil is a complex environment that can display heterogeneity in many different physical and chemical features, such as the simultaneous presence of the three characteristic states of liquid, gas and solid. To capture this physical and chemical heterogeneity, Borer and coworkers [59] used a glass pore network, described as a glass-etched micrometric pore network, to simultaneously incorporate all three characteristic states of liquid, gas, and solid. Using this system, the authors found that two species of *Pseudomonas* segregate and self-organize along gradients of carbon and oxygen, thus

demonstrating how heterogeneity in local conditions can promote coexistence and the emergence of complex microbial landscapes.

Another type of complexity that is typically minimized in laboratory experiments is species biodiversity. Natural microbial communities typically contain extraordinary species biodiversity that cannot be replicated in the laboratory. The huge number of potential interactions that may occur within these microbial communities could, in principle, result in multitude emergent behaviors and properties that would be difficult to investigate using synthetic microbial communities consisting of only two or a few genotypes. One way forward to bridge these enormous differences in species biodiversity would be to assemble incrementally more biodiverse communities in the laboratory and identify which processes and interactions remain relevant as species biodiversity increases. Thus far, however, there are few studies that have investigated incrementally more biodiverse communities [60, 61]. Yet, such experiments are critically important. For example, spatial positioning of multiple species in biodiverse communities can create complex diffusional gradients in numerous resources and metabolites simultaneously, while local and initial densities of different genotypes can impact their coexistence. Other difficulties emerge regarding higher-order interactions. One approach is to identify all possible pairwise interactions among a set of isolates and then test whether the pairwise interactions can predict behaviors in more complex assemblages. For example, Traxler and coworkers [62] tested the response of *Streptomyces coelicolor* to the presence of *Actinomyces* isolates. The colony morphology of *S. coelicolor* changed according to which isolate of *Actinomyces* was its nearest neighbor, suggesting that different isolates of *Actinomyces* release different metabolites and highlighting the possible complexity that higher-order diversity can trigger. Vetsigian and coworkers [63] observed similar observations, where the authors tested 64 pairwise interactions between *Streptomyces* isolates obtained from different soil samples. The authors found that isolates with identical 16S rRNA genes can give rise to different microbial landscapes, likely due to variation in the types of metabolites that they release.

Engineering microbial landscapes for biotechnological applications

Our summaries in this chapter largely focused on the underlying causes and consequences of microbial landscapes. This then raises an intriguing question: can the organization of a microbial landscape itself be used as a design parameter for biotechnological applications? Can we engineer or impose pre-defined microbial landscapes to achieve desired biotechnological objectives? To achieve such a task, it is essential to develop methodologies that physically embed individual cells at specific spatial positions and immobilize them over time.

Hydrogels provide one approach to achieve these tasks. Hydrogels allow one to construct precise two- or three-dimensional environments and embed cells at precise spatial locations. The advantage of hydrogels is that they are highly permeable, thus allowing molecules to be exchanged between individuals. Importantly, hydrogels are easy to use and can be constructed with simple modifications to commercial inkjet printers. For example, Roth and coworkers [64] used hydrogels to create complex patterns with automated and high spatial precision on the order of hundreds of microns. There are two main categories of inkjet printers that could be used, piezoelectric and thermal printers [65-66]. Notably, their application is not restricted to hydrogels, but can also be used to print two- or three-dimensional patterns using alginate, agar, and other biocompatible materials. Such approaches have been used to create defined microbial landscapes to investigate cell-cell communication, establish biofilms with novel properties, and perform antimicrobial assays [67-68].

While engineering microbial landscapes to achieve a desired biotechnological objective is tantalizing, it remains at its infancy. Much research has been conducted on understanding the underlying causes of microbial landscapes. However, predicting the consequences of a particular microbial landscape remains difficult. Additional investments are needed that translate experimental observations into mathematical predictions about the behaviors and properties of particular microbial landscapes. Given a microbial landscape, can we predict the emergent properties and behaviors of that landscape? How robust is the landscape to environmental perturbations or evolutionary processes? Only after we obtain mathematical models that generate accurate and precise predictions about the properties and behaviors of particular microbial landscapes will we be able to rationally engineer landscapes to achieve desired biotechnological objectives. While challenging, advances in individual-based modeling should contribute towards transitioning the field of microbial landscape ecology into a truly applied discipline with relevance for biotechnological applications.

REFERENCES

1. Hall-Stoodley L, Costerton JW and Stoodley P Bacterial biofilms: from the natural environment to infectious diseases. *Nature Reviews Microbiology* 2004; **2**: 95-108.
2. Flemming HC, Wingender J, Szewzyk U, Steinberg P, Rice SA and Kjelleberg S Biofims: an emergent form of bacterial life. *Nature Reviews Microbiology* 2016; **14**: 563-575.
3. Macfarlane S and Dillon JF Microbial biofilms in the human gastrointestinal tract. *Journal of Applied Microbiology* 2007; **102**: 1187-1196.
4. Ramey EB, Koutsoudis M, von Bodman SB and Fuqua C Biofilm formation in plant-microbe associations. *Current Opinion in Microbiology* 2004; **7**: 602-609.
5. Burmølle M, Kjøller A and Sørensen SJ An invisible workforce: biofilms in the soil, In: Lear G and Lewis G; (eds.) *Microbial Biofilms – Current Research and Applications*. Norfolk: Caister Academic Press International Journal of Food Microbiology; 2012; **155**: 61-71
6. Mulder A, van de Graaf AA, Robertson LA and Kukenen JG Anaerobic ammonium oxidation discovered in a denitrifying fluidized bed reactor. *FEMS Microbiology Ecology* 1995; **16**: 177-183.
7. Leiknes T and Ødegaard H The development of a biofilm membrane bioreactor. *Desalination* 2007; **202**: 135-143.
8. Hallam NB, West JR, Forster CF and Simms J The potential for biofilm growth in water distribution systems. *Water Research* 2001; **35**: 4063-4071.
9. Rohani P, Lewis TJ, Grünbaum D and Ruxton GD Spatial self-organization in ecology: pretty patterns or robust reality? *Trends in Ecology and Evolution* 1997; **12**: 70-74.
10. Lion S and Baalen MV Self-structuring in spatial evolutionary ecology. *Ecology Letters* 2008; **11**: 277-295.
11. Kerr B, Riley MA, Feldman MW and Bohannan BJM Local dispersal promotes biodiversity in a real-life game of rock-paper-scissors. *Nature* 2002; **418**: 171-174.
12. Hallatschek O, Hersen P, Ramanathan S and Nelson DR Genetic drift at expanding frontiers promotes gene segregation. *Proceedings of the National Academy of Sciences USA* 2007; **104**: 19926-19930.
13. Hansen SK, Rainey PB, Haagensen JA and Molin S Evolution of species interactions in a biofilm community. *Nature* 2007; **445**: 533-536.

14. Kim HJ, Boedicker JQ, Choi JW and Ismagilov RF Defined spatial structure stabilizes a synthetic multispecies bacterial community. *Proceedings of the National Academy of Sciences USA* 2008; **105**: 18188-18193.
15. Dekas AE, Poretsky RS and Orphan VJ Deep-sea archaea fix and share nitrogen in methane-consuming microbial consortia. *Science* 2009; **326**: 422-426.
16. Momeni B, Brileya KA, Fields MW and Shou W Strong inter-population cooperation leads to partner intermixing in microbial communities. *eLife* 2013; **2**: e00230.
17. Momeni B, Waite AJ and Shou W Spatial self-organization favors heterotypic cooperation over cheating. *eLife* 2013; **2**: e00960.
18. Müller MJI, Neugeboren BI, Nelson DR and Murray AW Genetic drift opposes mutualism during spatial population expansion. *Proceedings of the National Academy of Sciences USA* 2014; **111**: 1037–1042.
19. Goldschmidt F, Regoes RR and Johnson DR Successive range expansion promotes diversity and accelerates evolution in spatially structured microbial populations. *The ISME Journal* 2017; **11**: 2112-2123.
20. Vos M, Wolf AB, Jennings SJ and Kowalchuk GA Micro-scale determinants of bacterial diversity in soil. *FEMS Microbiology Reviews* 2013; **37**: 936-954.
21. Wang G and Or D Hydration dynamics promote bacterial coexistence on rough surfaces. *The ISME Journal* 2013; **7**: 395-404.
22. Nadell CD, Ricaurte D, Yan J, Drescher K and Bassler BL Flow environment and matrix structure interact to determine spatial competition in *Pseudomonas aeruginosa* biofilms. *eLife* 2017; **6**: e21855.
23. Doan HK and Leveau JHJ Artificial surfaces in phyllosphere microbiology. *Phytopathology* 2015; **104**: 1036-1042.
24. Wang G and Or D Trophic interactions induce spatial self-organization of microbial consortia on rough surfaces. *Scientific Reports* 2014; **4**: 6757.
25. Turner MG and Gardner RH *Landscape Ecology in Theory and Practice: Pattern and Process*, 2nd edn. New York: Springer. 2015
26. Kindaichi T, Tsushima I, Ogasawara Y, Shimokawa M, Ozaki N, Satoh H and Okabe S *In situ* activity and spatial organization of anaerobic ammonium-oxidizing (anammox) bacteria in biofilms. *Applied and Environmental Microbiology* 2007; **73**: 4931-4939.

27. Satoh H, Miura Y, Tsushima I and Okabe S Layered structure of bacterial and archaeal communities and their *in situ* activites in anaerobic granules. *Applied and Environmental Microbiology* 2007; **73**: 7300-7307.
28. Breugelmans P, Barken KB, Tolker-Nielsen T, Hofkens J, Dejonghe W and Springael D Architecture and spatial organization in a triple-species bacterial biofilm synergistically degrading the phenylurea herbicide linuron. *FEMS Microbiology Ecology* 2008; **64**: 271-282.
29. Schink B Energetics of syntrophic cooperation in methanogenic degradation. *Microbiology and Molecular Biology Reviews* 1997; **61**: 262-280.
30. Goldschmidt F, Regoes RR and Johnson DR Metabolite toxicity slows local diversity loss during expansion of a microbial cross-feeding community. *The ISME Journal* 2018; **12**: 136-144.
31. Lilja EE and Johnson DR Segregating metabolic processes into different microbial cells accelerates the consumption of inhibitory substrates. *The ISME Journal* 2016; **10**: 1568-1578.
32. Christensen BB, Haagensen JAJ, Heydorn A and Molin S Metabolic commensalism and competition in a two-species microbial consortium. *Applied and Environmental Microbiology* 2002; **68**: 2495-2502.
33. van Gestel J, Vlamakis H and Kolter R From cell differentiation to cell collectives: *Bacillus subtilis* uses division of labor to migrate. *PLoS Biology* 2015; **13**: e1002141.
34. Vega NM and Gore J Collective antibiotic resistance: mechanisms and implications. *Current Opinion in Microbiology* 2014; **21**: 28-34.
35. Xavier JB, Martinez-Garcia E and Foster KR Social evolution of spatial patterns in bacterial biofilms: when conflict drives disorder. *The American Naturalist* 2009; **174**: 1-12.
36. Madsen JS, Burmølle M, Hansen LH and Sørensen SJ The interconnection between biofilm formation and horizontal gene transfer. *FEMS Immunology & Medical Microbiology* 2012; **65**: 183-195.
37. Hallatschek O and Nelson DR Gene surfing in expanding populations. *Theoretical Population Biology* 2008; **73**: 158-170.
38. Hallatschek O and Nelson DR Life at the front of an expanding population. *Evolution* 2010; **64**: 193-206.
39. Klopfstein S, Currat M and Excoffier L The fate of mutations surfing on the wave of a range expansion. *Molecular Biology and Evolution* 2005; **23**: 482-490.

40. Travis JM, Münkemüller T, Burton OJ, Best A, Dytham C and Johst K Deleterious mutations can surf to high densities on the wave front of an expanding population. *Molecular Biology and Evolution* 2007; **24**: 2334-2343.
41. Excoffier L, Foll M and Petit RJ Genetic consequences of range expansions. *Annual Review of Ecology, Evolution, and Systematics* 2009; **40**: 481-501.
42. Wiegand T and Moloney KA *Handbook of Spatial Point-Pattern Analysis in Ecology*. Boca Raton: CRC Press. 2014
43. Mitri S, Clarke E and Foster KF Resource limitation drives spatial organization in microbial groups. *The ISME Journal* 2016; **10**: 1471-1482.
44. Ripley BD The second-order analysis of stationary point processes. *Journal of Applied Probability* 1976; **13**: 255-266.
45. Ming L and Vitányi PMB *An Introduction to Kolmogorov Complexity and its Applications*, 3rd edn. New York: Springer. 2008
46. Grassberger P Toward a quantitative theory of self-generated complexity. *International Journal of Theoretical Physics* 1986; **25**: 907-928.
47. Zieliński B, Plichta A, Misztal K, Spurek P, Brzychczy-Włoch M and Ochońska D Deep learning approach to bacterial colony classification. *PLoS ONE* 2017; **12**: e0184554.
48. Matsushita M, Wakita J, Itoh H, Watanabe K, Arai T, Matsuyama T, Sakaguchi H and Mimura M Formation of colony patterns by a bacterial cell population. *Physica A: Statistical Mechanics and its Applications* 1999; **274**: 190-199.
49. Mimura M, Sakaguchi H and Matsushita M Reaction-diffusion modeling of bacterial colony patterns. *Physica A: Statistical Mechanics and its Applications* 2000; **282**: 283-303.
50. Dubuc B, Quiniou JF, Roques-Carmes C, Tricot C and Zucker SW Evaluating the fractal dimension of profiles. *Physical Review A* 1989; **39**: 1500-1512.
51. Berubé D and Jebrak M High precision boundary fractal analysis for shape characterization. *Computers & Geosciences* 1999; **25**: 1059-1071.
52. Rudge TJ, Federici F, Steiner PJ, Kan A and Haseloff J Cell polarity-driven instability generates self-organized, fractal patterning of cell layers. *ACS Synthetic Biology* 2013; **2**: 705-714.
53. Matsuyama T and Matsushita M Fractal morphogenesis by a bacterial cell population. *Critical Reviews in Microbiology* 1993; **19**: 117-135.
54. Lloyd DP and Allen RJ Competition for space during bacterial colonization of a surface. *Journal of the Royal Society Interface* 2015; **12**: 0608.

55. Rice KP, Saunders AE and Stoykovich MP Classifying the shape of colloidal nanocrystals by complex Fourier Descriptor analysis. *Crystal Growth & Design* 2012; **12**: 825-831.
56. Chacón JM, Möbius W and Harcombe WR The spatial and metabolic basis of colony size variation. *The ISME Journal* 2018; **12**: 669-680.
57. Dechesne A, Wang G, Gülez G, Or D and Smets BF Hydration-controlled bacterial motility and dispersal on surfaces. *Proceedings of the National Academy of Sciences USA* 2010; **107**: 14369-14372.
58. Leis AP, Schlicher S, Franke H and Strathmann M Optically transparent porous medium for nondestructive studies of microbial biofilm architecture and transport dynamics. *Applied and Environmental Microbiology* 2005; **71**: 4801-4808.
59. Borer B, Tecon R and Or D Spatial organization of bacterial populations in response to oxygen and carbon counter-gradients in pore networks. *Nature Communications* 2018; **9**: 769.
60. Jia X, Liu C, Song H, Ding M, Du J, Ma Q and Yuan Y Design, analysis and application of synthetic microbial consortia. *Synthetic and Systems Biotechnology* 2016; **1**: 109-117.
61. Said SB and Or D Synthetic microbial ecology: engineering habitats for modular consortia. *Frontiers in Microbiology* 2017; **8**: 1125.
62. Traxler MF, Watrous JD, Alexandrov T, Dorrestein PC and Kolter R Interspecies interactions stimulate diversification of the *Streptomyces coelicolor* secreted metabolome. *mBio* 2013; **4**: e00459-13.
63. Vetsigian K, Jajoo R and Kishony R Structure and evolution of *Streptomyces* interaction networks in soil and *in silico*. *PLoS Biology* 2011; **9**: e1001184.
64. Roth EA, Xu T, Das M, Gregory C, Hickman JJ and Boland T Inkjet printing for high-throughput cell patterning. *Biomaterials* 2004; **25**: 3707-3715.
65. Calvert P Inkjet printing for materials and devices. *Chemistry of Materials* 2001; **13**: 3299-3305.
66. Allain LR, Stratis-Cullum DN and Vo-Dinh T Investigation of microfabrication of biological sample arrays using piezoelectric and bubble-jet printing technologies. *Analytica Chimica Acta* 2004; **518**: 77-85.
67. Basu S, Gerchman Y, Collins CH, Arnold FH and Weiss R A synthetic multicellular system for programmed pattern formation. *Nature* 2005; **434**: 1130-1134.
68. Choi WS, Ha D, Park S and Kim T Synthetic multicellular cell-to-cell communication in inkjet printed bacterial cell systems. *Biomaterials* 2011; **32**: 2500-2507.

CHAPTER 3: The right place at the right time – environmental feedbacks favor a few lucky individuals for proliferation during bacterial range expansion

Borer Benedict, Ciccarese Davide, Johnson R David, Or Dani

Author contribution: I contributed to the experimental results presented in Figs. 1, to the formulation of the main research question, to the analysis of the data, and to the writing of the manuscript.

ABSTRACT

Bacterial communities that support key global biogeochemical cycles are spatially organized to fulfill their ecological functions. The processes that promote and sustain spatial self-organization of sessile bacterial assemblages remain difficult to resolve experimentally due to limitations to visualizing and tracking individual cells within large colonies. In contrast to liquid cultures, surface attached range expansion fosters genetic segregation of the population where cells residing at the expanding periphery are favored due to preferential access to nutrients. In this study, we elucidate mechanisms that shape spatial organization of cross-feeding bacterial communities using a mathematical model describing individual cells that inhabit a spatially resolved nutrient landscape. Our model can reproduce a number of well-documented observations in bacterial range expansion and provides a mechanistic, unified explanation in localized growth rate differences mediated by the underlying nutrient landscape, which is highly sensitive to the type of trophic interaction. We visualize the consequences of dynamic range expansion for individual cell lineages in homogeneous and spatially structured environments and identify scenarios where trophic dependencies induce counterintuitive reproductive advantages. Bacterial community organization is influenced by the scale of rare events at the single cell level where the frequency and propagation of selected lineages exerts a disproportional influence on the community, and potentially, on its functioning.

INTRODUCTION

Bacterial life in natural environments is predominantly associated with sessile assemblages of cells that form aggregates or surface-attached biofilms [1–5]. The confinement of bacterial cells in sessile colonies and their limited relocation opportunities makes positioning in space a critical factor for access to nutrients [6], exchange of metabolites [7], protection from phage infection [8] or protection from predation [9]. Within such highly constrained systems, scenarios emerge in which a few cells contribute disproportionately to the long term community biomass [10] supporting the notion of “survival of the luckiest”. Evidence in the form of genetic segregation of initially mixed communities is observed frequently in colonies growing on surfaces [11–18] or observations of detrimental mutations accumulating at the assemblage periphery that are rapidly lost in homogeneous environments such as liquid cultures [19]. During sessile growth, bacterial cells are essentially fixed in space and depend on diffusional fluxes dictated by heterogeneous nutrient landscapes (governed by the surface and their neighbors) that ultimately shape the resulting bacterial assemblage [6]. In contrast to advection dominated planktonic life style, bacterial cells in diffusion dominated systems often self-engineer their immediate surroundings (a process frequently termed niche construction [20]). For example, single species biofilms engage in cross-feeding interactions through divergent behavior of spatially segregated subpopulations experiencing fundamentally different growth conditions [21, 22]. Overall, trophic interactions have the potential to shape the emerging community patterns during bacterial range expansion. When competing for the same resource, the front of an expanding population offers advantages due to preferential nutrient access and reduced competition that permit the unhindered expansion of individual cell lineages, forming genetically segregated sectors [11]. In contrast, cross-feeding interactions where one species relies on nutrients or modification of its imminent surroundings provided by another species within the assemblage [23] add constraints by the need for close proximity to the interacting partner. The signature of such interactions is seen in the spatial organization of cells within the assemblage [24–27] with the potential of sequential expansion if trophic interactions are unilateral [28]. Interestingly, these sequential patterns can be interrupted by a second pattern [28] where large monoclonal sectors emerge due to rare nucleation events (where monoclonal sectors are seeded due to a combination stochastic but mostly deterministic conditions). These patterns mediate various aspects of community functioning and their disturbance or in the absence of spatial structure, a community may lose ecosystem functions [7,

29, 30]. Experimentally identifying mechanisms that give rise to the different expansion patterns poses a challenge resulting from the difficulties in visualizing and tracking individual cells and limitations to capture the underlying nutrient landscape. Turning to mathematical models that simulate both the nutrient conditions and bacterial processes at the relevant scale to individual cells provides an opportunity to unveil mechanisms giving rise to experimentally observed community patterns at the macro scale. We hypothesize that the spatial organization of sessile, cross-feeding bacterial assemblages undergoing range expansion is shaped by highly localized and dynamic growth rate differences that are reinforced by self-engineered nutrient landscape underlying the assemblage. To systematically and quantitatively evaluate the hypothesis and the mechanisms postulated, we developed an agent-based model that combines Monod type growth kinetics with a simple mechanical shoving algorithm for bacterial growth in homogeneous and structured habitats similar to experimental setups used for independent validation. The detailed description of chemical and metabolite diffusion at high spatial resolution links localized nutrient conditions and spatially variable growth rates as a key driver that promote community pattern formation. Finally, we discuss the influence of obstacles such as found in structured habitats (porous media or rough surfaces) on the spatial self-organization, community proliferation and genetic segregation. These insights are used to visualize the importance of the spatial dimension in shaping the community composition concerning individual “lucky” bacterial lineages and potential ramification for evolutionary mechanisms.

RESULTS

Dynamic nutrient landscapes mediate colony spatial self-organization

We use a synthetic community containing two isogenic mutants of *P. stutzeri* A1501 [28, 31] cross-feeding nitrite in the denitrification pathway (Fig. 1a) to systematically investigate mechanisms that shape the spatial self-organization of trophically interacting bacterial colonies during range expansion. Nitrite toxicity at lower ambient pH modify the type of trophic interactions from competition (complete reducer growing anaerobically on nitrate, bilateral disadvantage), via weak mutualism (producer and consumer cross-feeding nitrite anaerobically at pH 7.5, unilateral benefit) to strong mutualism (producer and consumer cross-feeding nitrite anaerobically at pH 6.5, bilateral advantage). Two fundamentally different expansion mechanisms have been observed experimentally depending on the type of trophic interactions.

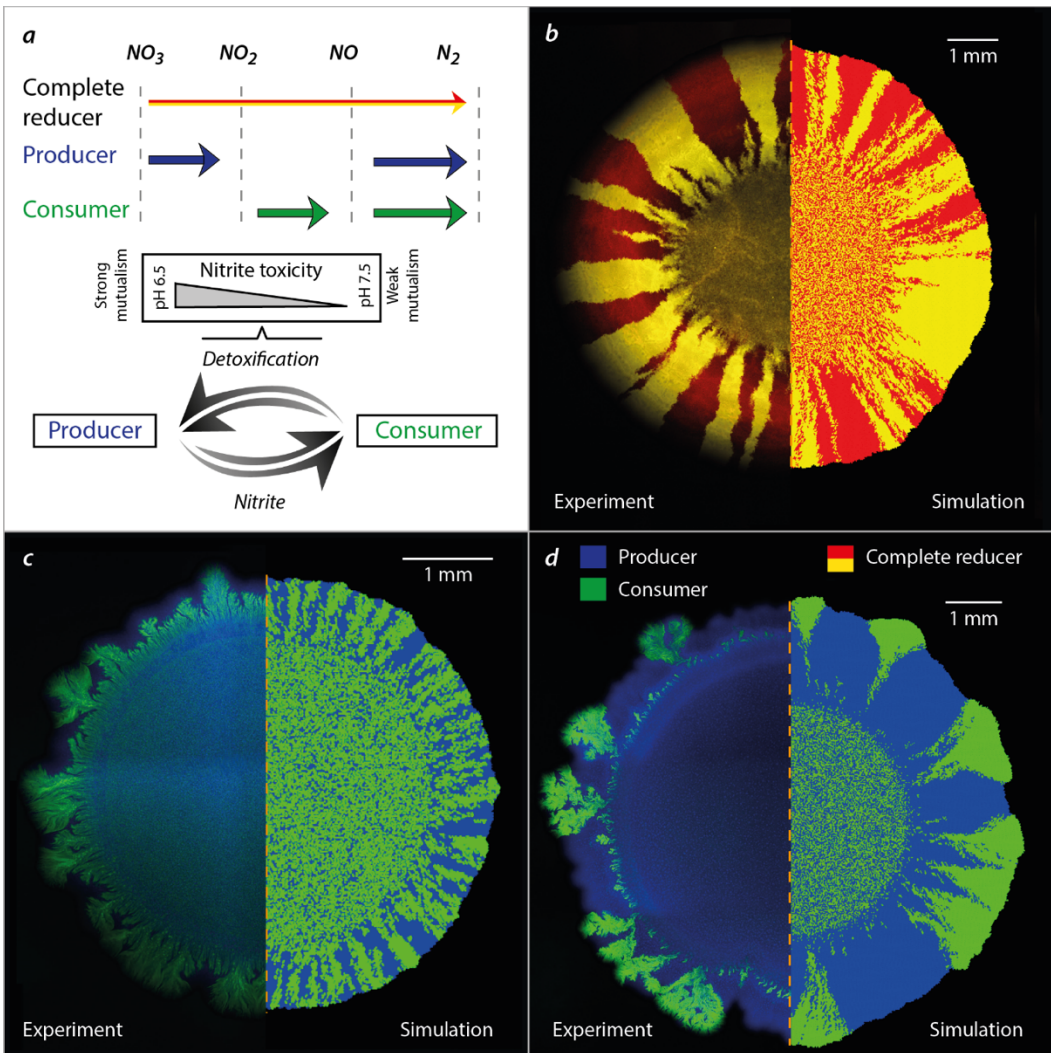


Figure 1. Spatial patterns emerging from different trophic interactions among members of a synthetic bacterial community grown on agar surfaces. a) The denitrification metabolic pathway of the complete reducer and the producer and consumer used in this study. The complete reducer *P. stutzeri* A1601 employs the entire denitrification pathway, reducing nitrate (NO_3^-) all the way to dinitrogen gas (N_2). Two nitrite cross-feeders derived from the complete reducer were used to form a mutualistic consortium: (i) a producer converts nitrate to nitrite (NO_2^-) but is unable to complete the denitrification pathway due to a lack of nitrite reductase; (ii) a consumer unable to use nitrate directly as an electron acceptor (lacking the enzyme nitrate reductase) and thus depends on the producer supplying nitrite. The toxicity of the intermediate metabolite nitrite promotes a mutualistic relationship where the strength of the interaction is controllable due to the variable toxicity of nitrite depending on local pH (acidity). b) Comparison of experimental and simulation

data of a competitive scenario represented by two complete reducer *P. stutzeri* strains. Simultaneous expansion of the two isogenic but fluorescently tagged strains creates visible sectors of strains tagged with the same fluorescence. *c)* Comparison of experimental and simulation data of a mutualistic interaction where producer is tagged with CFP (blue) and consumer with GFP (green). Due to the higher toxicity of nitrite the community is more intermixed. *d)* Comparison of experimental and simulation data of a weak mutualistic (pH 7.5) scenario where producer is tagged with *ecfp* (blue) and consumer with *egfp* (green). The colony follows sequential expansion lead by the producer with visible sectors of consumers emerging.

Competition for the same resource fosters segregation and the formation of well-defined sectors of each bacterial strain (Fig. 1b). Similar patterns have been observed frequently in other studies [11, 28, 31]. The onset of strong mutualistic interactions promote an increased intermixing of the two strains (Fig. 1c) that we attribute to the need for reducing diffusion distances between interacting partners [30, 31]. Weak mutualistic growth invokes two distinct spatial patterns: a sequential pattern where producer cells dominate the colony periphery [28, 31] and in certain rare cases where large consumer branches emerge at the colony periphery (Fig. 1d) . The dynamics of super-sectors (defined as the rare but large monoclonal sectors observed in weak mutualistic scenarios contributing disproportionately to colony expansion) are difficult to investigate experimentally and require insights into the spatially variable growth rates and shoving mechanisms.

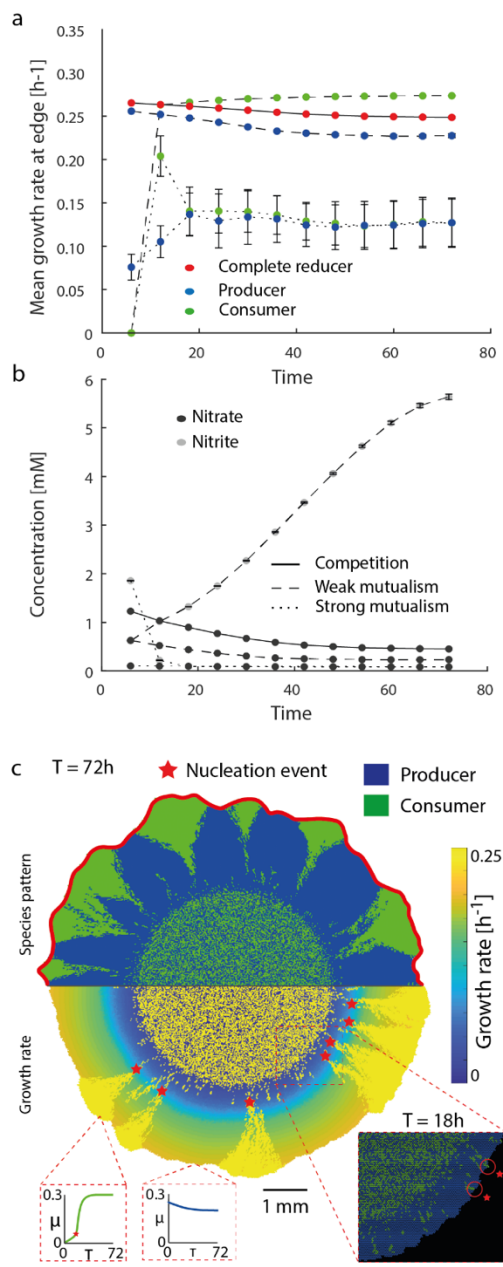


Figure 2. The underlying chemical landscape governs local growth rates of the bacterial colony.

Nutrient concentrations and growth rates within the growth layer for all trophic interactions (red zone in panel c). a) In the competitive scenario, predicted growth rates are equal for the complete reducers having the same kinetic parameters. Weak mutualism is characterized by a relative growth rate advantage due to the ubiquitous nitrite availability. In mutualistic scenario, both strains have a lower but equal growth rate due to nitrite toxicity, emphasizing their mutualistic interaction. b) Competition results in a slow decline of nitrate with no nitrite produced (complete reducer). Weak mutualistic conditions promote the accumulation of nitrite as there is negligible toxicity in this

condition. Strong mutualism results in a rapid decline of nitrate (toxicity acts on the yield), with overall low nitrite levels (removed by consumer cells in close proximity). c) Spatial distribution of the two species community in weak mutualistic conditions (top) in relation to the predicted growth rates (bottom) at the end of the simulation time. Following individual cells within the simulation reveals different growth rate histories depending on the strain and location. Growth rates of producer cells are dictated by nitrate availability and proximity to the colony periphery (due to nitrate diffusion). Consumer cells initially cannot grow due to nitrite limitation and subsequently proliferate if remaining sufficiently close to the colony periphery through shoving. Rare nucleation events indicate the creation of large monoclonal sectors that arise due to favorable spatial positioning (initially shoved by the producer cells) and nutrient conditions.

The mathematical model reveals links between the underlying nutrient landscape and associated localized growth rates and the emerging colony patterns (Fig. 2). When observing the nutrient conditions in the proximity of the expanding colony edge (indicated by the red rim in Fig. 2c), both complete reducer strains experience the same nitrate concentrations and hence equal growth rates as they are essentially isogenic strains in the competitive scenario (Fig. 2a). Strong mutualism (nitrite being toxic, pH 6.5) results in an overall lower but similar growth rate (converging) of the two strains and thus smaller colony size for the same incubation time when compared to the competition scenario. A significantly different pattern characterizes the weak mutualistic consortium. After an initial lag phase due to nitrite unavailability, the consumer strain benefits from an overall higher growth rate compared to the producer strain in the weak mutualistic scenario (Fig. 2a). This mechanism is rooted in the underlying nutrient landscape (Fig. 2b). At pH 6.5, nitrite toxicity controls the proliferation of the consumer strain and equal production and consumption keep nitrite concentrations low. At pH 7.5, nitrite is non-toxic and begins to accumulate during the early stages of colony growth due to the sequential expansion of the producer followed by the consumer. In some rare cases, consumers are pushed ahead by the proliferating producers (Fig. 2c) and remain in the actively growing colony periphery. Once sufficient nitrite is available, these consumer cells residing at the periphery proliferate disproportionately due to their relative growth rate advantage and create large monoclonal consumer sectors. This process, remaining at the periphery through passive motion until favorable conditions enable emergence of super sectors, is further defined as “nucleation of super-sectors” for simplicity. These differences become apparent when visualizing dynamic growth rates of individual agents during the simulation depending on the location and strain (Fig. 2c). Producer cells remaining at the colony periphery retain high growth rates throughout the simulation slightly declining due to nitrate diffusive limitations. Consumer cells on the other hand have an initial disadvantage owing to the lack of nitrite which fir needs to be provided by the producer cells. Thus, consumer cells are reliant on proliferation and shoving from producer cells to stay at the colony periphery. Once the surrounding producers provide sufficient nitrite, the cells which managed to remain at the colony periphery proliferate into large sectors of kin cells due to a relative growth rate advantage compared to the surrounding producers (no substrate limitation). These observations highlight how stochastic effects (shoving of the consumer cells through producer proliferation) and deterministic processes (higher relative growth rate of the relocated consumer cells resulting in concave sector boundaries) manage to govern the two different observed patterns in weak mutualistic conditions.

Lineage tracking reveals lucky individuals and spatial genetic bottlenecks

The mechanistic model provides opportunities that are not yet possible experimentally to track lineages of bacterial “virtual” cells within the complex and spatially varying community. The assumption is that variations in reproductive success of the ancestral population (inoculated cells) results in some cell lineages (defined as the ancestral inoculated cell and all of its progeny) that contribute disproportionately to the final colony biomass as depicted as pseudo-colors in Fig. 3. For competitive trophic interactions, the model predicts a clear segregation of the two strains into sectors that prominently persist into the colony periphery (as also observed experimentally shown in Fig. 1a and in other studies).

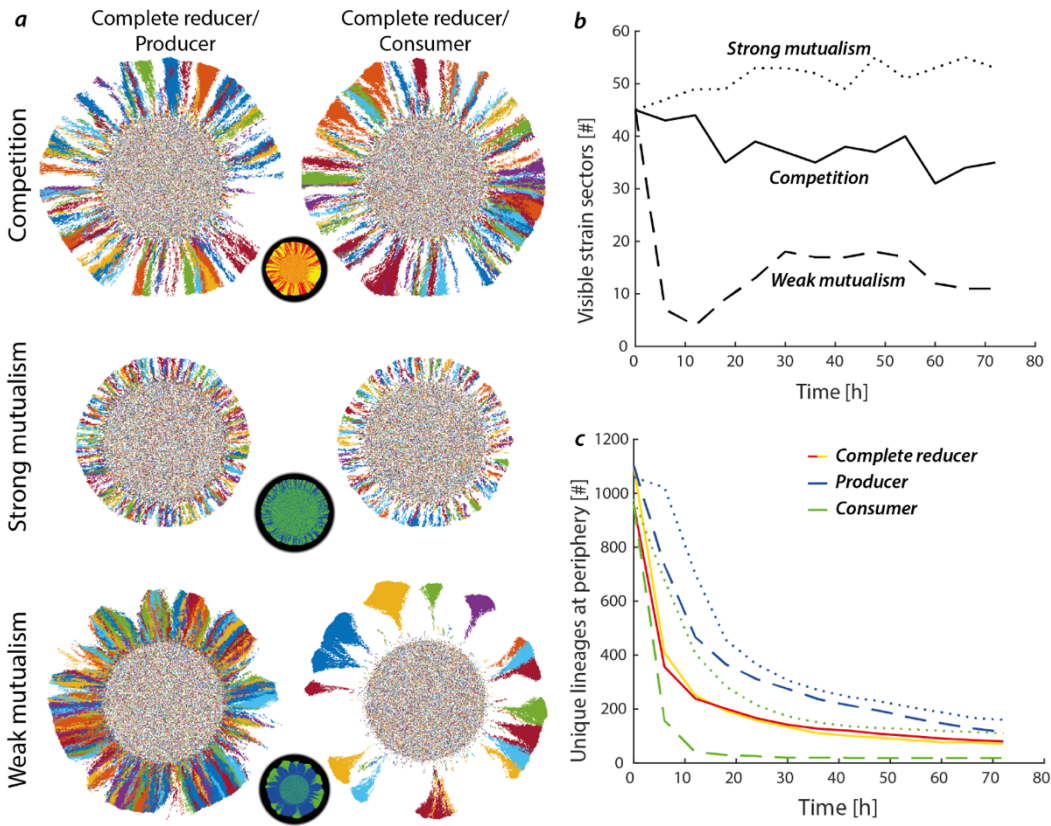


Figure 3. Trophic interactions alter the reproductive success of individual cells. a) Reproductive success of individual lineages with associated spatial patterns of demixing depending on trophic interaction. Competition results in well-defined sectors where one sector typically contains multiple ancestral lineages. Strong mutualism favors intermixing of the two strains resulting thin sectors. In case of weak mutualism, the producer strain primarily engages in competitive patterns due to nutrient competition with its kin. Large consumer sectors emerge where individual ancestral lineages become dominant and produce monoclonal sectors. b) The number of interspecies boundaries remains stable in the competitive scenario. In weak mutualistic scenario, the number of interspecies boundaries shows a decline due to the loss of most consumer branches. An increase in the number of interspecies boundaries in the strong mutualistic case is attributed to branches bifurcating and thus increased intermixing of the two strains. c) The total number of unique lineages residing at the colony periphery shows a steep decrease during early colony development asymptotically reaching steady state once sectors have developed. The decrease follows different patterns depending on trophic interactions mediated by the varying mechanisms of range expansion (sequential versus simultaneous).

An important observation that could not be directly resolved in the experiment is that a single sector containing the same strain does not consist of a single ancestor (i.e. not originating from the same inoculated cell). Strong mutualism favors intermixing of the two strains with considerably thinner sectors compared to the trophic competition scenario. Sequential expansion as observed under weak mutualistic interactions alters the observed pattern. For the majority of the colony, the producer expands radially (perpendicular to the colony periphery) with no penetration of consumer sectors similar to the pattern observed in the competitive scenario (essentially equal patterns since producers compete for nitrate). Super sectors that penetrate the layer of producers are typically monoclonal, owing to the fact that they typically nucleate from a single cell. In between consumer branches, an increased rate of coalescence of producer lineages can be observed that arise from spatial bottlenecks imposed by the flanking consumer sectors. The degree to which a community de-mixes during range expansion experiments is commonly quantified by counting the number of transitions between different strain sectors at the colony periphery, and can be tracked dynamically in the simulation (Fig. 3b, legend in Fig. 3c). For competitive trophic interactions, the total visible sectors remain stable throughout the simulation with a slight negative trend due to coalescence events where individual sectors are pinched and buried behind the colony expansion front. Sequential expansion of two strains promotes rapid demixing for weak mutualistic interactions, with some more branches resurging in the later stages of the simulation.

For the strong mutualistic interactions scenario, the tight association between the two strains favors intermixing and thus an overall higher number of individual branches is seen at the end of the simulations. This analysis follows capabilities of experimental systems where distinction between sectors can only be made based on fluorescent differentiation. By quantifying the unique lineages that proliferate to the colony periphery, differences in demixing dynamics between the strains become evident. When competing for the same resource, the two strains demix very rapidly, as they are essentially equivalent except for the fluorescent label (Fig. 3c). In the case of strong mutualism, demixing of both strains is slower compared to the competitive case where more individual lineages manage to proliferate at the colony periphery in the case of the consumer strain. Weak mutualism promotes a strong demixing of the consumer strain whereas the producer has a slower demixing with time compared to the competitive scenario since more space is available initially lacking growth by the consumer until sufficient nitrite has accumulated. Overall, from the inoculated cells residing within the actively growing layer at the colony periphery, approximately

80% of all cell lineages are lost during range expansion which increases to 99% when taking into account all inoculated cells (i.e. cells at the colony center). The loss of lineages during colony expansion underlines the variation in reproductive success of individual lineages where a fraction of the initial inoculum ($0.31\% \pm 0.02\%$, $0.32\% \pm 0.03\%$, $4.96\% \pm 0.06\%$ for the competitive, weak mutualistic and strong mutualistic scenario, respectively) contributes more than 50% of the final community biomass.

Spatial structure mediates self-organization with genetic consequences

Definitive studies for disentangling the effects of structured environments (porous media or rough surfaces) from those induced by trophic interactions on the resulting spatial organization and genetic lineages are rare. We have used the model to simulate, for identical trophic scenarios (competition, weak mutualism, strong mutualism) the resulting community patterns expanding in structured environments with varying density of obstacles simulated as solid particles (Fig. 4).

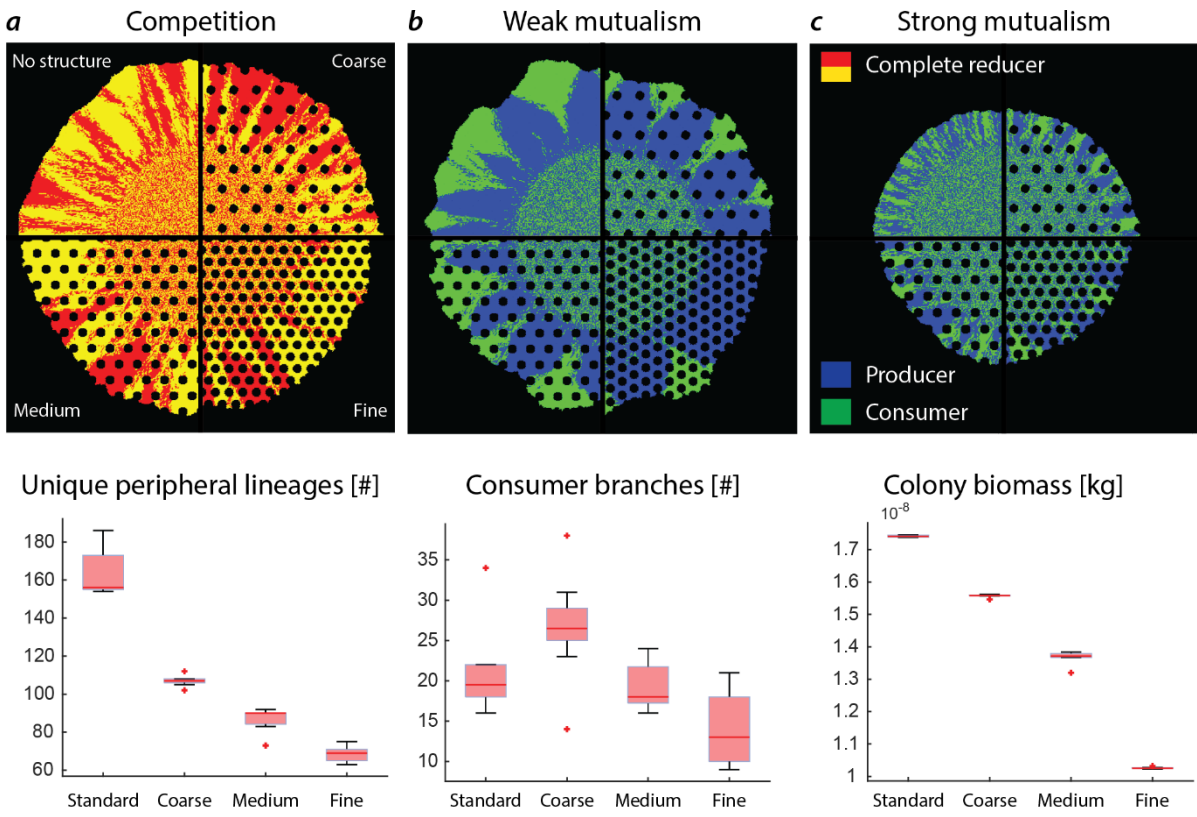


Figure 4. Simulated two-species bacterial colony expansion into domains with different spatial structures – impacts on lineage proliferation with potential ecological and evolutionary consequences. a) When competing, the addition of structures reduce the number of cell lineages proliferating to the periphery due to trapping of cell lineages in front of the obstacle. This leads to greater genetic segregation of the community and fewer lineages persisting to the assemblage periphery. b) Weak mutualistic conditions result in a similar picture concerning producers. Consumer branches that nucleate in front of an obstacle are limited in their persistence due to spatial constraints and the total number of proliferating branches decrease with increasing obstacle density changing the ecological functioning of the assemblage. Interestingly, the introduction of obstacles to a homogeneous habitat increases the number of consumer branches (although statistically not significant, p-value of 0.12, two-sample t-test). c) In mutualistic conditions, the increased segregation of the two strains is detrimental to the function of the whole community due to the increased diffusion distance between the strains resulting in an overall lower expansion rate of the community.

An increase in obstacle density results in a higher genetic segregation of the two strains when competing for the same nutrient (Fig. 4a, competition) with fewer individual cell lineages persisting to the colony periphery. A similar effect is expected for the producer strain in weak mutualistic conditions as they are equally dependent on the diffusion of nitrate from the periphery. The increase in obstacles has a varying effect on the consumer strain branches in the weak mutualistic case (Fig. 4b). Although a similar number of monoclonal consumer branches emerge in the early stages of colony expansion, obstacles hindering the proliferation of these branches results in a limited number persisting to the colony periphery in medium and fine structured habitats. Interestingly, more consumer branches persist to the periphery in coarse conditions compared to a homogeneous habitat. Emerging consumer branches are pushed through bottlenecks by surrounding producer cells, which facilitates their persistence to the periphery. In contrast to the medium and fine structured habitats, these branches do not encounter many additional obstacles that may inhibit their proliferation. Strong mutualistic conditions favor a higher degree of intermixing resulting in shorter average diffusion lengths. Including obstacles in the simulation results in decreased intermixing of the two strains and thus longer average diffusion lengths expressed in an overall lower total biomass created during colony growth (Fig. 4c).

DISCUSSION

Trophic interactions modify nutrient landscapes and affect colony patterns

It has been frequently documented that changes in trophic interactions invoke fundamentally different spatial self-organization and expansion mechanisms such as simultaneous expansion when competing for the same resource [11, 28, 31], simultaneous expansion at higher intermixing ratios during strong mutualistic growth [30–32] or sequential expansion for cross-feeding an intermediate metabolite with unilateral benefit of the interacting species [28]. In the latter case, two significantly different patterns are observed within the same colony: (i) sequential expansion where the producer strain advances first and the consumer strain follows and (ii) localized super-sectors of the consumer strain having a higher growth rate compared to the surrounding producer strain [28, 31]. Important questions concerning these super-sectors are the mechanisms that promote the emergence of the super sectors and their persistence at the colony periphery. In order for super sectors to emerge, two conditions are required: an initial phase where consumers manage to stay at the periphery despite a growth rate disadvantage and a subsequent phase where consumers have a growth rate advantage indicated by the curved sector boundaries. In the simulations, growing producer cells initially shove consumers located at the colony periphery until sufficient nitrite is produced for them to proliferate. A similar delay in consumer proliferation has been observed experimentally . The mechanism enabling the consumer individuals to proliferate at the colony periphery is embedded within the underlying nutrient landscape where localized relative growth rate differences between the two strains emerge dynamically (Fig. 2c). In contrast to the producer, the consumer strain is not dependent on diffusion of peripheral nitrate and has a ubiquitous supply of nitrite provided by the more abundant producer, resulting in a higher growth rate relative to the producer in the later stages of colony expansion (Fig. 2b). The shape of the emerging super sector has previously been linked to the relative growth rate advantages [33]. Similar observations have been made in studies focusing on the mechanical forces shaping the spatial patterns of mutant strains with relative growth rate differences during range expansion [17, 18]. In both cases, cells having a growth rate disadvantage managed to stay at the colony periphery through mechanical interactions and shoving of the surrounding faster growing cells. Although the resulting colony pattern in our system is similar to the above-mentioned studies, the mechanism is fundamentally different (growth rate difference imposed via mutations versus the mechanism of emerging localized growth rate advantages due to the underlying diffusion landscape). This highlights the

interplay of biotic and abiotic factors during community assembly of sessile bacterial assemblages and the importance of localized growth rates as a key driver for emerging spatial self-organization.

Lineage tracking reveals segregation dynamics depending on trophic interaction

Genetic segregation of fluorescently labelled strains in experiments suggests a strong reduction in genetic diversity compared to the ancestral population [11]. Limited by the availability of differentiable fluorescent proteins, experimental observations are restricted to a coarse resolution and are not capable of resolving individual lineages, although efforts have been made to include multiple fluorescent proteins [13], high temporal resolution imaging [34] and also three dimensional tracking [35]. An individual-based model on the other hand is capable to resolve the segregation dynamics based on individual inoculated cells and enabled us to quantify the number of individual cell lineages persisting at the expanding colony edge depending on trophic interaction. Interestingly, comparison of demixing dynamics show a similar trend for strong mutualism and competition when looking at individual lineages compared to the strain-based differentiation, i.e. a higher intermixing in the case of the mutualistic scenario versus competitive (Fig. 3b and 3c). In the weak mutualistic case, the producer benefits from the reduced competition for space (since the consumer initially does not grow due to the lack of nitrite) resulting in more individual cell lineages proliferating and persisting at the colony periphery. Only once the consumer super-sectors begin to emerge do they begin to pose a barrier for the producer cells resulting in coalescence events and an overall reduction of observed producer cell lineages at the colony periphery. For the case of consumer cells, weak mutualistic growth results in a few “lucky cells” that are able to proliferate and contribute disproportionately to the colony expansion. These cell lineages, despite being dependent on another strain, profit from the weak mutualistic growth, which highlights the somewhat counterintuitive situation of having a higher reproductive success compared to any other scenario despite an initial growth rate disadvantage.

Structured habitats modulate evolutionary processes in natural environments

Bacterial assemblages rarely grow on homogeneous surfaces. The influence of single objects and rough agar on the proliferation of cell lineages has been observed both experimentally and *insilico* [36–38]. Some recent studies include the interrelation of structure and flow environment on biofilm growth [39], the influence of hydration conditions [40] and boundary deformities on the spatial organization of trophically interacting communities [40] and the influence of heterogeneous

environments on population genetics [38]. Simplified, cell lineages directly in front of the obstacles are outgrown by lineages close to the obstacle boundary, posing spatial genetic bottlenecks [19, 36, 37]. When growing in a habitat populated by numerous solid obstacles, this effect is amplified and results in a more pronounced genetic segregation compared to the homogeneous environment void of obstacles with an overall reduction of individual cell lineages residing at the colony periphery. Within the simulations, cells were treated as isogenic without any genetic variation or potential for mutations. In natural bacterial assemblages, a higher number of individual cell lineages containing genetic variation and potential mutations at the expanding edge increases the opportunity for natural selection to shape the final community structure [41]. It has been shown previously that allele surfing promotes adaptation of bacterial colonies using a mutation with tunable selective advantage [34]. Again, one of the main differences between this and our system is the fact that the relative growth rate advantage is a dynamic emergent property of the underlying nutrient landscape. Thus, the observed mechanisms of localized growth rates shaping the dynamics of individual cell lineages has the potential of modulating evolutionary processes by determining the standing genetic variation of the expanding edge in natural bacterial assemblages. This in turn accelerates (increased beneficial mutations at the periphery) or decelerates (burying beneficial mutations behind the expanding front) the pace of evolution in bacterial assemblages undergoing range expansion [34]. It is generally thought that a balance between genetic drift and natural selection shapes the population genetics of range expanding communities. We here showed in addition how trophic interactions and nutrient availability underlying bacterial communities can shape the proliferation of individual cells through localized growth rate advantages and thus alter evolutionary mechanisms acting within the growth layer. Spatially structured habitats mediate the reproductive success of individual lineages and highlight the importance of chance relative to natural selection for trophically interacting bacterial communities. Our simulations and experimental validation emphasize the importance of growth rate differences as a key driver in pattern formation and final genetic population diversity and the importance of microbes as “environmental engineers” playing a crucial role in not only shaping their imminent surroundings but also having far-reaching consequences for community structure and local ecosystem functioning.

MATERIALS AND METHODS

Experimental observations using a synthetic bacterial community

A synthetic cross-feeding bacterial ecosystem composed of two isogenic mutant strains of the bacterium *Pseudomonas stutzeri* A1501 [28, 42] was used as a model community (Fig. 1). Briefly, the producer strain is able to reduce nitrate to nitrite but not further to nitrous oxide. The consumer on the other hand can only reduce nitrite to nitrous oxide but is unable to use nitrate. When grown together with nitrate as the growth-limiting resource, the two strains engage in a nitrite cross-feeding interaction. Nitrite is toxic at pH 6.5 but not at pH 7.5 [43–46], thus the cross-feeding interaction can be fine-tuned between weak mutualism and stronger mutualism by adjusting the pH of the growth medium or agar plate. When growing aerobically, the manipulated range of pH does not have any experimentally observable effect on liquid growth capabilities [42]. The two strains also contain an IPTG-inducible green or cyan fluorescent protein-encoding gene [28], which enables us to distinguish and quantify the abundance of each strain when grown together [28, 31]. Two complete reducers differentiated by the same IPTG-inducible fluorescent proteins are used to create a scenario where both strains compete for nitrate (competition) [47].

Experimental range expansion

The range expansion experiments were performed as described in [28]. We prepared overnight cultures of the complete reducers alone and the cross-feeding isogenic mutants alone in lysogeny broth (LB) medium for a period of 12 h in a shaking incubator at 37°C at 220 rpm. When the cultures reached stationary phase, the optical density at 600 nm (OD_{600}) was adjusted to one. In order to adjust the OD, the cultures were centrifuged at 3615 g for eight minutes, the supernatants were discarded, and the remaining cells were suspended in 1000 μ l of 0.9% (w/v) NaCl solution. We then transferred the cultures into a glove box (Coy Laboratory Products, Grass Lake, MI) containing a nitrogen (N_2):hydrogen (H_2) (97:3) anaerobic atmosphere. Two strains (two complete reducers or producer and consumer) were mixed at a ratio of 1:1 and 1 μ l were then deposited onto the center of anaerobic LB agar plate amended with 1 mM of sodium nitrate ($NaNO_3$) and adjusted to pH 7.5 (weak mutualistic conditions) or 6.5 (strong mutualistic conditions) with 0.5 M NaOH or 30% v/v HCl. Plates were incubated in the anaerobic glove box for a period of 2 weeks at room temperature. The colonies were subsequently imaged using a Leica TCS SP5 II confocal microscope (Etzlar,

Germany). The colonies were exposed to aerobic conditions for 1 h preceding image acquisition to allow for maturation of the fluorescent proteins.

Agent-based mathematical model

The mathematical model combines numerical pseudo two-dimensional nutrient diffusion with an on-grid individual-based representation of bacterial cells following local growth conditions determined using Monod-type kinetics [7, 48, 49]. A circular domain of 5 mm radius composed of a hexagonal lattice with side length of 20 microns is used as a backbone for diffusion calculation based on one-dimensional Fickian diffusion between nodes whilst respecting mass balance at each node (Equation 1):

$$\frac{\partial C}{\partial t} = D \frac{\partial^2 C}{\partial x^2} - R \quad 1$$

where C is the concentration [mol/m³], t is time [s], D the diffusion coefficient [m²/s], x the spatial coordinate along the bond [m] and R the bacterial consumption of the nutrient (mol/m³/s)

Details of all parameters are given in Table 1. Only nitrate and nitrite are included in the simulation since other nutrients are provided in non-limiting concentrations. A constant peripheral source for nitrate is included (1 mM) whereas nitrite is produced locally solely by bacterial metabolism. Due to the size of each hexagon, bacterial cells are essentially represented as super agents [50] and each grid node is inhabited by a single cell (i.e. strains are mutually exclusive).

Bacterial cells are inoculated at the center (inoculation radius of 2 mm) where each node is attributed randomly with a producer or consumer strain. A random inoculation mass for each super-agent is chosen between 10% and 100% of the mass at division.

Bacterial cells consume nutrients depending on the trophic interaction. In the competitive scenario, both strains only consume nitrate where the growth rate for a super-agent i (i.e. node i of the grid) is calculated using Equation 2:

$$\mu_{cd,i} = \mu_{max} * \frac{C_{NO3,i}}{C_{NO3,i} + K_{NO3}} \quad 2$$

where $\mu_{cd,i}$ is the local growth rate of the complete reducer (1/s) at node i, μ_{max} the maximum growth rate (1/s), K_{NO3} the Monod half-saturation coefficient for nitrate (mM) and $C_{NO3,cd}$ the nitrate concentration (mM) at node i. When cross feeding on nitrite (weak mutualism, i.e. no nitrite

toxicity), the growth rates of the producer and consumer are described by Equation 3 and 4, respectively:

$$\mu_{prod,i} = \mu_{max} * \frac{C_{NO3,i}}{C_{NO3,i} + K_{NO3}} \quad 3$$

$$\mu_{cons,i} = \mu_{max} * \frac{C_{NO2,i}}{C_{NO2,i} + K_{NO2}} \quad 4$$

where $\mu_{prod,i}$ is the local growth rate of producer cell (1/s) at node i, $\mu_{cons,i}$ is the local growth rate of consumer cell (1/s) at node i, K_{NO2} the Monod half-saturation coefficient for nitrite (mM), and $C_{NO2,i}$ the nitrite concentration (mM) at node i. Biomass dynamics follow a simple exponential model as described by Equation 5:

$$m_{t+1,i} = m_{t,i} + \mu_i * m_{t,i} * \Delta t \quad 5$$

where $m_{t+1,i}$ and $m_{t,i}$ is the biomass (kg) in time step t and t+1 at node i, respectively, and Δt the numerical time step (s). The total nutrient consumed is related to the gain in biomass at node i following a biomass yield coefficient described by Equation 6:

$$\vartheta_{n,i} = \frac{\mu_i * m_{t,i}}{Y_i} \quad 6$$

where $\vartheta_{n,i}$ is the consumption rate of nutrient n at node i (mol/s) and Y_i the biomass yield coefficient (kgDW/mol). In the case of nitrate consumption by the producer, an equivalent amount of nitrite is produced following stoichiometry. Nitrite toxicity has been shown to affect the growth yield [51]. Thus, for the mutualistic conditions, the biomass yield coefficient for both strains is calculated using Equation 7:

$$Y_i = \begin{cases} (Y_{max} - Y_{min}) * \frac{K_{inh}}{K_{inh} + C_{NO2,i}} + Y_{min}, & pH = 6.5 \\ Y_{max}, & pH = 7.5 \end{cases} \quad 7$$

where Y_{max} is the maximum biomass yield (kgDW/mol), Y_{min} the minimum biomass yield (kgDW/mol) and K_{inh} the nitrite inhibition coefficient (mM).

Colony expansion in the mathematical model is a combination of cell division and a simple on-grid shoving algorithm. From the location of a dividing cell, the shortest path distance to the colony periphery is calculated. If the distance is sufficiently small (<100 microns, 5 grid cells) all cells along the shortest path are shoved towards the colony periphery where the current peripheral cell is assigned a new node at random from any unoccupied neighboring nodes. The total simulated time is 72 h using a 60 s time step.

REFERENCES

1. Hall-Stoodley L, Costerton JW, Stoodley P. Bacterial biofilms: From the natural environment to infectious diseases. *Nat Rev Microbiol*. 2004; **2**: 95-108.
2. Kolter R, Greenberg EP. Microbial sciences: The superficial life of microbes. *Nature*. 2006; **441**: 300-2.
3. Monds RD, O'Toole GA. The developmental model of microbial biofilms: ten years of a paradigm up for review. *Trends Microbiol*. 2009; **17**: 73-87.
4. Nadell CD, Xavier JB, Foster KR. The sociobiology of biofilms. *FEMS Microbiol Rev* 2009; **33**: 206–224.
5. Flemming HC, Wuertz S. Bacteria and archaea on Earth and their abundance in biofilms. *Nat Rev Microbiol* 2019; **17**: 247-260.
6. Stewart PS. Diffusion in biofilms. *J Bacteriol*. 2003; **185**: 1485-91.
7. Borer B, Tecon R, Or D. Spatial organization of bacterial populations in response to oxygen and carbon counter-gradients in pore networks. *Nat Commun* 2018; **9**: 769.
8. Testa S, Berger S, Piccardi P, Oechslin F, Resch G, Mitri S. Spatial structure affects phage efficacy in infecting dual-strain biofilms of *Pseudomonas aeruginosa*. *Commun Biol* 2019; **4**: 405.
9. Justice SS, Hunstad DA, Cegelski L, Hultgren SJ. Morphological plasticity as a bacterial survival strategy. *Nat Rev Microbiol* 2008; **6**: 162-8.
10. Hallatschek O, Nelson DR. Population genetics and range expansions. *Phys Today* 2009; **62**: 42–47.
11. Hallatschek O, Hersen P, Ramanathan S, Nelson DR. Genetic drift at expanding frontiers promotes gene segregation. *Proc Natl Acad Sci U S A* 2007; **104**: 19926-30.
12. Weber MF, Poxleitner G, Hebisch E, Frey E, Opitz M. Chemical warfare and survival strategies in bacterial range expansions. *J R Soc Interface* 2014; **11**: 172.
13. Weinstein BT, Lavrentovich MO, Möbius W, Murray AW, Nelson DR. Genetic drift and selection in many-allele range expansions. *PLoS Computational Biology*. 2017; **13**: e1005866.
14. Van Gestel J, Weissing FJ, Kuipers OP, Kovács ÁT. Density of founder cells affects spatial pattern formation and cooperation in *Bacillus subtilis* biofilms. *ISME J* 2014; **8**: 2069–2079.
15. Mitri S, Clarke E, Foster KR. Resource limitation drives spatial organization in microbial groups. *ISME J* 2016; **10**: 1471–1482.

16. Müller MJI, Neugeboren BI, Nelson DR, Murray AW. Genetic drift opposes mutualism during spatial population expansion. *Proc Natl Acad Sci U S A* 2014; **111**: 1037–42.
17. Giometto A, Nelson DR, Murray AW. Physical interactions reduce the power of natural selection in growing yeast colonies. *Proc Natl Acad Sci* 2018; **115**: 11448–11453.
18. Kayser J, Schreck CF, Gralaka M, Fusco D, Hallatschek O. Collective motion conceals fitness differences in crowded cellular populations. *Nat Ecol Evol* 2019; **3**: 125–134.
19. Travis JMJ, Münkemüller T, Burton OJ, Best A, Dytham C, Johst K. deleterious mutations can surf to high densities on the wave front of an expanding population. *Mol Biol Evol* 2007; **24**: 2334–43.
20. Odling-Smee FJ, Laland KN, Feldman MW. Niche Construction. *Am Nat* 1996; **147**: 641.
21. Cole JA, Kohler L, Hedhli J, Luthey-Schulten Z. Spatially-resolved metabolic cooperativity within dense bacterial colonies. *BMC Syst Biol* 2015; **9**: 15.
22. Dal Co A, Ackermann M, van Vliet S. Metabolic activity affects the response of single cells to a nutrient switch in structured populations. *J R Soc Interface* 2019; **16**: 182.
23. Estrela S, Libby E, Van Cleve J, Débarre F, Deforet M, Harcombe WR, et al. Environmentally Mediated Social Dilemmas. *Trends Ecol Evol* 2019; **34**: 6–18.
24. Rohani P, Lewis TJ, Grünbaum D, Ruxton GD. Spatial self-organization in ecology: Pretty patterns or robust reality? *Trends Ecol Evol.* 1997; **12**: 70-4.
25. Camazine S, Deneubourg J-L, Franks NR, Sneyd J, Theraulaz G, Bonabeau E. Self-Organization in Biological Systems. Princeton University Press, Princeton, USA, Princeton, USA. 2001
26. Lion S, Baalen M Van. Self-structuring in spatial evolutionary ecology. *Ecol Lett.* 2008; **11**: 277–295.
27. Dong X, Fisher SG. Ecosystem spatial self-organization: Free order for nothing? *Ecol Complex* 2019; **38**: 24-30.
28. Goldschmidt F, Regoes RR, Johnson DR. Successive range expansion promotes diversity and accelerates evolution in spatially structured microbial populations. *ISME J* 2017; **11**: 2112–2123.
29. Haagensen JAJ, Hansen SK, Christensen BB, Pamp SJ, Molin S. Development of spatial distribution patterns by biofilm cells. *Appl Environ Microbiol* 2015; **81**: 6120–6128.
30. Tecon R, Or D. Cooperation in carbon source degradation shapes spatial self-organization of microbial consortia on hydrated surfaces. *Sci Rep* 2017; **7**: 43726.
31. Goldschmidt F, Regoes RR, Johnson DR. Metabolite toxicity slows local diversity loss during

- expansion of a microbial cross-feeding community. *ISME J* 2018; **12**: 136–144.
- 32. Momeni B, Brileya KA, Fields MW, Shou W. Strong inter-population cooperation leads to partner intermixing in microbial communities. *Elife* 2013; **2013**: 1–23.
 - 33. Farrell FD, Gralka M, Hallatschek O, Waclaw B. Mechanical interactions in bacterial colonies and the surfing probability of beneficial mutations. *J R Soc Interface* 2017; **14**: 73.
 - 34. Gralka M, Stiewe F, Farrell F, Möbius W, Waclaw B, Hallatschek O. Allele surfing promotes microbial adaptation from standing variation. *Ecol Lett* 2016; **19**: 889–898.
 - 35. Díaz-Pascual F, Hartmann R, Lempp M, Vidakovic L, Song B, Jeckel H, et al. Breakdown of *Vibrio cholerae* biofilm architecture induced by antibiotics disrupts community barrier function. *Nat Microbiol.* 2019; **4**: 2136–2145.
 - 36. Möbius W, Murray AW, Nelson DR. How Obstacles Perturb Population Fronts and Alter Their Genetic Structure. *PLOS Comput Biol* 2015; **11**: e1004615.
 - 37. Beller DA, Alards KMJ, Tesser F, Mosna RA, Toschi F, Möbius W. Evolution of populations expanding on curved surfaces(a). *Epl* 2018; **123**, 58005.
 - 38. Gralka M, Hallatschek O. Environmental heterogeneity can tip the population genetics of range expansions. *Elife* 2019; **12** pii: e44359.
 - 39. Nadell CD, Ricaurte D, Yan J, Drescher K, Bassler BL. Flow environment and matrix structure interact to determine spatial competition in *Pseudomonas aeruginosa* biofilms. *Elife* 2017; **13**: pii: e21855.
 - 40. Borer B, Tecon R, Or D. Spatial organization of bacterial populations in response to oxygen and carbon counter-gradients in pore networks. *Nat Commun* 2018; **9**: 769.
 - 41. Kayser J, Schreck CF, Yu Q, Gralka M, Hallatschek O. Emergence of evolutionary driving forces in pattern-forming microbial populations. *Philos Trans R Soc B Biol Sci* 2018; **373**: 20170106.
 - 42. Lilja EE, Johnson DR. Segregating metabolic processes into different microbial cells accelerates the consumption of inhibitory substrates. *ISME J* 2016; **10**: 1568–1578.
 - 43. Almeida JS, Reis MAM, Carrondo MJT. Competition between nitrate and nitrite reduction in denitrification by *Pseudomonas fluorescens*. *Biotechnol Bioeng* 1995; **46**: 194–201.
 - 44. Sijbesma WFH, Almeida JS, Reis MAM, Santos H. Uncoupling effect of nitrite during denitrification by *Pseudomonas fluorescens*: An in vivo ³¹P-NMR study. *Biotechnol. Bioeng.* 1996; **52**: 176–82.
 - 45. Baumann B, Van Der Meer JR, Snozzi M, Zehnder AJB. Inhibition of denitrification activity but not of mRNA induction in *Paracoccus denitrificans* by nitrite at a suboptimal pH. *Antonie van*

Leeuwenhoek, Int J Gen Mol Microbiol 1997; **72**: 183–189.

46. Zhou Y, Oehmen A, Lim M, Vadivelu V, Ng WJ. The role of nitrite and free nitrous acid (FNA) in wastewater treatment plants. *Water Res* 2011; **45**: 4672-82.
47. Lilja EE, Johnson DR. Metabolite toxicity determines the pace of molecular evolution within microbial populations. *BMC Evol Biol* 2017; **17**: 52.
48. Ebrahimi A, Or D. Hydration and diffusion processes shape microbial community organization and function in model soil aggregates. *Water Resour Res* 2015; **51**: 9804-9827.
49. Kim M, Or D. Individual-Based Model of Microbial Life on Hydrated Rough Soil Surfaces. *PLoS One* 2016; **11**: e0147394.
50. Scheffer M, Baveco JM, Deangelis DL, Rose KA, Vannes EH. Super-individuals a simple solution for modeling large populations on an individual basis. *Ecol Modell* 1995; **80**: 161–170.
51. Thatipamala R, Rohani S, Hill GA. Effects of high product and substrate inhibitions on the kinetics and biomass and product yields during ethanol batch fermentation. *Biotechnol Bioeng* 1992; **40**: 289-97.

CHAPTER 4: Spatial jackpot events enable community persistence during fluctuations between mutualism and competition

Ciccarese Davide, Micali Gabriele, Borer Benedict, Or Dani, Johnson R. David.

ABSTRACT

All surface attached microbial communities consist of different genotypes that organize themselves non-randomly across surfaces (referred to as spatial self-organization). These patterns of spatial self-organization can bestow microbial communities with properties that are not otherwise obtainable to any single genotype. We hypothesize here that these patterns are important determinants of community persistence in the face of temporal fluctuations in environmental conditions. To test this hypothesis, we used two trophically dependent isogenic strains of *Pseudomonas stutzeri* to study their spatial self-organization under fluctuating environmental conditions. We performed range expansion experiments where we alternated the environment between anaerobic and aerobic conditions, where anaerobic conditions promote mutualistic cross-feeding while aerobic conditions promote competition between the two strains. We found that specific localized patterns of spatial self-organization emerge that enable the microbial community to persist during the fluctuations, which we refer to as spatial jackpot events. We further applied an agent based mathematical model to identify the underlying mechanism that enables the persistence of these spatial jackpot events. Finally, we show that community composition changes in response to the temporal fluctuations, but that the community eventually reaches a new steady state that depends on the strength of the mutualistic interaction. Together, our results demonstrate that spatial self-organization is indeed an important determinant of community persistence in the face of fluctuations in environmental conditions.

INTRODUCTION

Every microbial community experiences perturbations or temporal fluctuations in their local environmental conditions [1–6]. These changes in environmental conditions can have important consequences, such as modulating the types of interactions that occur between different genotypes (*i.e.*, mutualism, commensalism, competition, *etc.*) [7–9] and how different genotypes arrange themselves across space (referred to hereafter as spatial self-organization) [10–13]. These changes in interactions and spatial self-organization can, in turn, affect community-level properties and behaviors [14–19]. For example, they can determine the metabolic processes performed by microbial communities [7, 20, 21], the resistance and/or resilience of those metabolic processes to additional environmental changes [22], and the evolutionary processes acting on microbial communities [23–25]. Thus, a better understanding of how changes in environmental conditions affect microbial interactions and spatial self-organization is critically important for our basic understanding of the structure, functioning, and evolution of microbial communities.

We hypothesize here that temporal fluctuations in environmental conditions that change interactions between mutualism and competition can compromise long-term community persistence. Our hypothesis is based on the following two assumptions: 1) environmental conditions that promote mutualism or competition will result in the emergence of fundamentally different patterns of spatial self-organization, and 2) the patterns of spatial self-organization that emerge under one set of environmental conditions (*i.e.*, that promote mutualism) are detrimental to the community as a whole under the other set of environmental conditions (*i.e.*, that promote competition). If these two assumptions are satisfied, then temporal fluctuations between the different environmental conditions could compromise the long-term persistence of the community and, under certain conditions, could lead to its eventual collapse.

To test this hypothesis, we performed experiments and mathematical simulations with a synthetic microbial community that satisfies both of the above-mentioned assumptions. The community is composed of two isogenic mutant strains of the facultative anaerobic denitrifying bacterium *Pseudomonas stutzeri* [25–27] (Fig. 1A). The two strains contain different loss-of-function deletions in the denitrification pathway, which allows us to impose an environmentally-dependent trophic interaction [11, 25, 27–29]. Under anaerobic environments with nitrate (NO_3^-) as the growth-limiting

resource, one strain consumes nitrate and releases nitrite (NO_2^-) (referred to hereafter as the producer) while the other strain consumes the released nitrite (referred to hereafter as the consumer) [27] (Fig. 1A). They therefore engage in a nitrite cross-feeding interaction. Additionally, nitrite is conditionally toxic with an increasing effect at lower pH [27]. Thus, the producer depends on the consumer to remove potentially toxic nitrite whereas the consumer depends on the producer to provide nitrite [27]. At pH 7.5 when nitrite is relatively non-toxic, we refer to this interaction as a weak mutualism [29]. In contrast, at pH 6.5 when nitrite is highly toxic, we refer to this interaction as a strong mutualism [29].

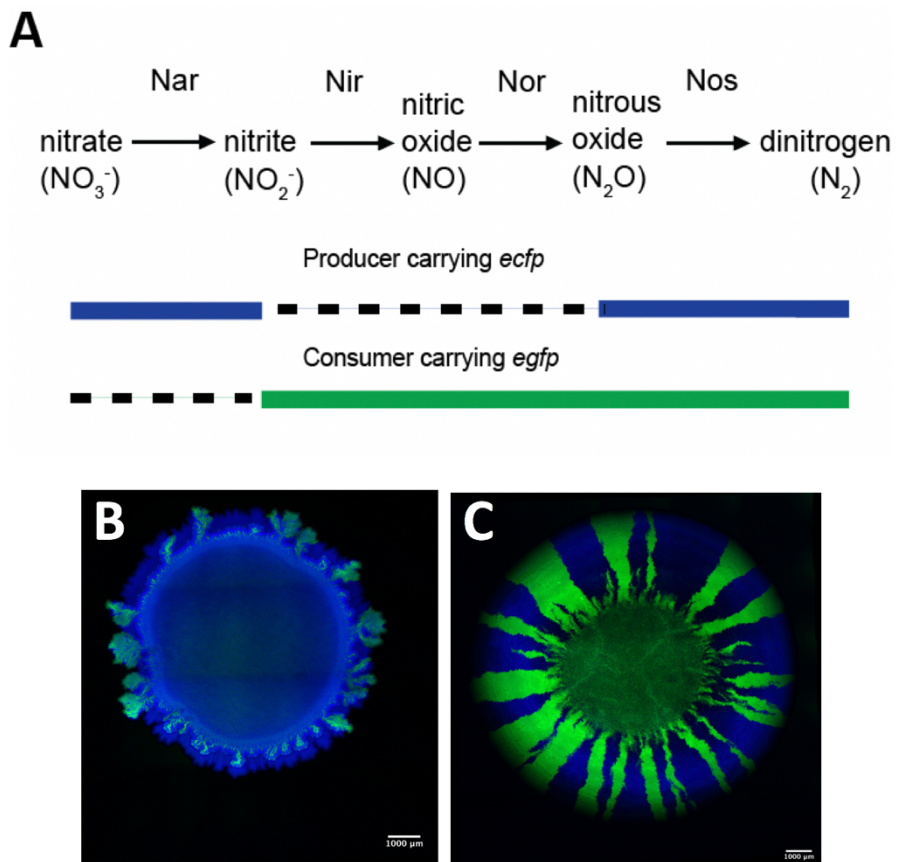


Figure 1. Synthetic microbial community used in this study. **A** The synthetic community is composed of two isogenic mutant strains of *P. stutzeri* that differ in their ability to reduce nitrate (NO_3^-) and nitrite (NO_2^-). The producer has a deletion in the *nir* gene cluster and can reduce nitrate but not nitrite. The consumer has a deletion in the *nar* gene cluster and can reduce nitrite but not nitrate. The two strains also carry either the *ecfp* or *egfp* fluorescent protein encoding gene. Thick horizontal bars indicate the nitrogen oxides that can be reduced by each strain. The color of the bar indicates the fluorescent protein-encoding gene carried by each strain. Dashed lines indicate the nitrogen oxides that can be reduced by each strain. **B** Pattern of spatial self-organization formed after two weeks of expansion under anaerobic conditions. **C** Pattern of spatial self-organization formed after two weeks of expansion under aerobic conditions.

Importantly, anaerobic (mutualism) and aerobic (competition) conditions promote the emergence of fundamentally different patterns of spatial self-organization during range expansion [11] (Fig. 1B and C), thus satisfying the first assumption discussed above. Under anaerobic (mutualism) conditions, the two strains expand sequentially, where the producer expands first and the consumer follows [25] (Fig. 1B). This is because the producer can grow immediately due to the exogenous supply of nitrate (NO_3^-) while the consumer can only grow later after the producer releases sufficient amounts of nitrite (NO_2^-). Under aerobic (competition) conditions, both strains (producer and consumer) expand simultaneously [11] (Fig. 1C). This is because both strains compete for oxygen and have equivalent phenotypic capabilities.

For this experimental system, we predict that the patterns of spatial self-organization that emerge during range expansion under anaerobic (mutualism) conditions are detrimental to the community as a whole under aerobic (competition) conditions and vice versa (Fig. 2), thus satisfying the second assumption discussed above. Sequential expansion during anaerobic (mutualism) conditions results in the producer positioned at the expansion frontier [11, 25, 28] (Fig. 2A). If the environment changes to aerobic (competition) conditions, the producer will then have preferential access to resources, which are supplied via diffusion from the periphery. The consequence is that the producer has a growth advantage over the consumer resulting in a decrease in the ratio of consumer to producer cells (Fig. 2C). If the environment switches back to anaerobic conditions, the smaller number of consumer cells will result in increased nitrite (NO_2^-) accumulation, as there are relatively fewer consumer cells to consume nitrite. Over a series of anaerobic (mutualism)/aerobic (competition) transitions, we therefore expect a gradual decrease in the ratio of consumer to producer cells and an increase in nitrite accumulation (Fig. 2C). As nitrite increasingly accumulates, it will eventually impose deleterious effects on the community as a whole and, under certain conditions (*i.e.*, strong mutualism when nitrite is highly toxic), compromise the long-term persistence of the community and potentially lead to its collapse.

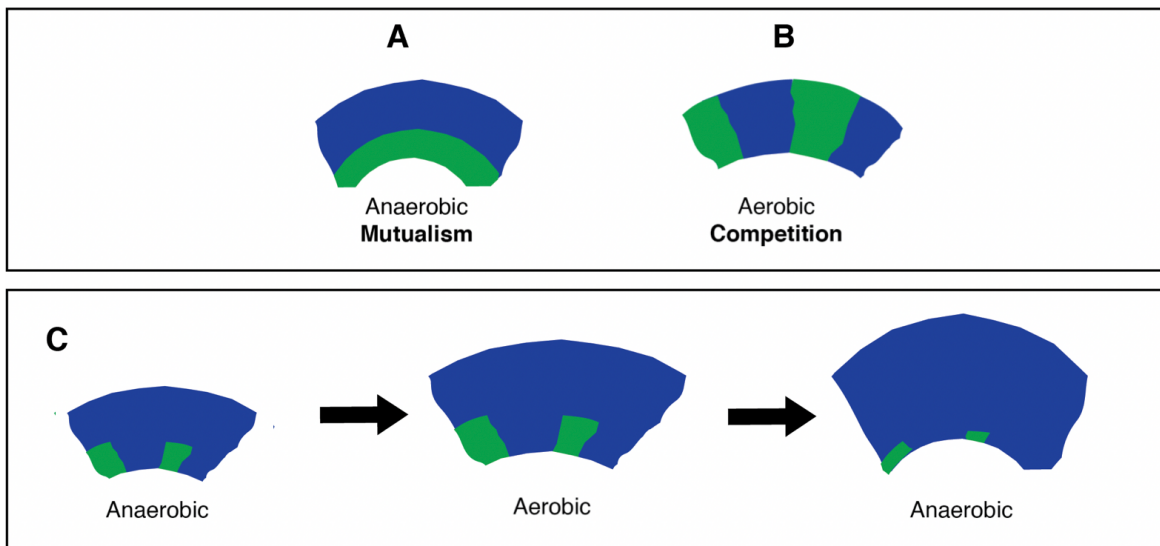


Figure 2. Predicted effect of repeated anaerobic/aerobic transitions on community dynamics. **A** Anaerobic (mutualism) conditions result in the sequential expansion of the two strains. This is because the producer can grow immediately via the exogenously added nitrate (NO_3^-) while the consumer cannot grow until nitrite (NO_2^-) accumulates to sufficient concentrations. **B** Aerobic (competition) conditions result in the simultaneous expansion of the two strains. This is because they compete for oxygen and have equivalent phenotypic capabilities. **C** We predict that repeated transitions between anaerobic and aerobic conditions will result in the gradual decrease in the ratio of consumer to producer cells, thus potentially leading to the accumulation of nitrite to toxic concentrations. This is due to the preferential spatial positioning of the producer at the onset of aerobic conditions.

To test this expectation, we conducted range expansion experiments with the synthetic microbial community described above (Fig. 1) and elsewhere [11, 25, 28] while imposing repeated transitions between anaerobic (mutualism) and aerobic (competition) conditions. We then quantified the influence of these transitions on community composition and expansion, where we expected a gradual decrease in the ratio of consumer to producer cells, as well as a decrease in interspecific intermixing and an increase in nitrite (NO_2^-) accumulation. Moreover, when subjected to environmental conditions that promote strong mutualism (*i.e.*, at pH 6.5 when nitrite is highly toxic), we expect the repeated transitions to slow community expansion and eventually compromise long-term community persistence. Our experimental design mimics a natural scenario; soil denitrifying microorganisms are often subjected to anaerobic/aerobic fluctuations due to, for example,

intermittent rainfall events, where anaerobic conditions can develop in saturated soils while aerobic conditions develop in unsaturated soils [9]. More generally, the principle that we investigate here may be relevant for any type of environmental fluctuation that satisfies the two assumptions discussed above (*i.e.*, the different environmental conditions promote the emergence of different patterns of spatial self-organization and the patterns of spatial self-organization that emerge under one set of environmental conditions are detrimental under other set of environmental conditions).

MATERIALS AND METHODS

Bacterial strains

The synthetic cross-feeding microbial community consists of two isogenic mutant strains of the bacterium *Pseudomonas stutzeri* A1501 [25, 26] (Fig. 1A). One strain carries a single loss-of-function deletion in the *nirS* gene and can reduce nitrate (NO_3^-) to nitrite (NO_2^-) but cannot reduce nitrite to nitrous oxide (N_2O) (referred to hereafter as the producer). The other strain carries a single loss-of-function deletion in the *narG* gene and cannot reduce nitrate to nitrite but can reduce nitrite to nitrous oxide (referred to hereafter as the consumer). When grown together with nitrate as the growth-limiting resource under anaerobic (mutualism) conditions, the two strains engage in a mutualistic nitrite cross-feeding interaction [27]. When grown together under aerobic (competitive) conditions, the two strains engage in a competitive interaction [11]. The two strains differ at only single genetic loci [27], thus preventing potential confounding effects that might otherwise emerge if more distantly related strains were used. In order to avoid recombination between the two strains when grown together, both strains carry a single loss-of-function deletion in the *comA* gene [27]. Finally, each strain carries an IPTG-inducible *ecfp* or *egfp* fluorescent protein-encoding gene (Fig. 1), which enables us to distinguish the strains when grown together [25, 27].

Range expansion experiments and temporal fluctuations

We performed range expansion experiments as described elsewhere [25]. We first grew the producer and consumer independently in aerobic lysogeny broth (LB) medium overnight in a shaking incubator at 37°C at 220 rpm. After reaching stationary phase, we centrifuged the cultures at 7000 rpm for 8 minutes at room temperature, discarded the supernatants, suspended the remaining cells in 1 ml of saline solution (0.89% NaCl, v/w) and adjusted the densities of the producer and consumer independently to an optical density of 1 at 600 nm (OD_{600}). We then mixed the producer and consumer at a volumetric ratio of 1:1 (producer:consumer) and deposited 1 μl of each mixture onto the center of a separate LB agar plate containing 1 mM sodium nitrate (NaNO_3). Since the producer and consumer are isogenic mutants with identical optical properties, equivalent OD_{600} values correspond to equivalent cell numbers. Prior to inoculating the LB agar plates, we adjusted the pH of the plates to 6.5 or 7.5 as described elsewhere [25], with four replicates per condition.

We imposed transitions between anaerobic (mutualism) and aerobic (competition) conditions for fifteen cycles ($n = 4$ for each pH condition). A single cycle consisted of incubation for 36 hours under anaerobic conditions inside a glove box (Coy Laboratory Products, Grass Lake, USA) containing an anaerobic nitrogen (N_2):hydrogen (H_2) atmosphere (97:3) followed by incubation for 12 hours under aerobic conditions in ambient air. We chose these incubation times to provide the strains with approximately equivalent expansion opportunity under aerobic and anaerobic conditions. More specifically, the aerobic growth rates of the two strains are approximately three-fold faster when compared to their anaerobic growth rates [27], and we therefore provided approximately three-fold more time to expand under anaerobic conditions than under aerobic conditions. We performed oxygen measurements and confirmed that all available oxygen had diffused out of the LB agar plate within 12 hours of transferring the plates back into the glove box as reported in supporting material. We note, however, that our main predictions (*i.e.*, that repeated transitions between anaerobic and aerobic conditions can compromise community persistence) are independent of the time spent under either of those conditions (Fig. 2D).

Microscopy and image acquisition

We obtained tile scans of the range expansions with a Leica TCS SP5 II confocal microscope (Etzlar, Germany) as described in detail elsewhere [11, 25, 28]. We scanned the range expansions at every transition from anaerobic to aerobic and from aerobic to anaerobic. We exposed the agar plates to ambient air for 1 h preceding image acquisition to allow for maturation of the fluorescent proteins as described elsewhere [25].

Quantitative image analysis

We processed images using ImageJ and Matlab R2017a as described elsewhere [11, 25, 28]. We quantified community composition and local spatial arrangement at the expansion frontier using two measurements; the surface ratio of consumer to producer and the intermixing index. We quantified the surface ratio within a ring located at the expansion frontier using a circular windowing approach, where the outer edge of the ring is located at the expansion frontier and the inner edge is located 100 pixels behind the outer edge. We selected this area because it avoids overlap with the previous time point, and thus measures the surface ratio only within the desired time window. We quantified the intermixing index, which defines the degree of spatial intermixing between the two strains, as described elsewhere [25, 30, 31].

Statistical analyses.

We used parametric methods for all of our statistical tests and considered $P < 0.05$ to be statistically significant. We reported the type of statistical test, the sample size for each test, and the exact P for each test in the results section.

RESULTS

Effect of temporal fluctuations on community composition and intermixing

We first tested the effects of repeated transitions between anaerobic (mutualism) and aerobic (competition) conditions on community composition and interspecific mixing. We expected that, over a series of anaerobic (mutualism)/aerobic (competition) transitions, the surface ratio of consumer to producer at the expansion frontier and the degree of intermixing would both decrease (Fig. 2C). To test this, we performed range expansions where we repeatedly transitioned the environment between anaerobic (mutualism) and aerobic (competition) conditions for 15 cycles. We performed these experiments at both pH 6.5 (strong mutualism) ($n = 4$) and pH 7.5 (weak mutualism) ($n = 4$) and measured the surface ratio of consumer to producer and the intermixing index along the expansion frontier immediately before each transition.

We found that, as expected, the surface ratio of consumer to producer and the intermixing index both decreased over the series of anaerobic (mutualism)/aerobic (competition) transitions (Fig. 3). The changes in these quantities appear to have two distinct dynamic phases; a first phase with a relatively steep decay and a second phase with a shallower decay. We therefore modeled their dynamics using a two-phase linear regression model [32–34] (See the SI for a complete description of the model). During the first phase, the surface ratio of consumer to producer cells decreased significantly more rapidly at pH 7.5 (weak mutualism) ($R^2 = 0.90$, $P = 2 \times 10^{-9}$, coeff = -0.0374, 95%CI = [-0.038, -0.0368]) than at pH 6.5 (strong mutualism) ($R^2 = 0.94$, $P = 1 \times 10^{-7}$, coeff = -0.0103, 95%CI = [-0.0108, -0.0097]) (Fig. 3A). We observed consistent results for the intermixing index, where it also decreased significantly more rapidly at pH 7.5 (weak mutualism) ($R^2 = 0.90$, $P = 2 \times 10^{-9}$, coeff = -0.0289, 95%CI = [-0.0295, -0.0284]) than at pH 6.5 (strong mutualism) ($R^2 = 0.93$, $P = 9 \times 10^{-8}$, coeff = -0.01, 95%CI = [-0.0109, -0.0098]) (Fig. 3B). During the second phase, the change in the surface ratio of consumer to producer cells did not significantly differ between pH 7.5 (weak mutualism) ($R^2 = 0.90$, $P = 2 \times 10^{-9}$, coeff = 0.0008, 95%CI = [0.0002, 0.0014]) and pH 6.5 (strong mutualism) ($R^2 = 0.94$, $P = 1 \times 10^{-7}$, coeff = 0.0003, 95%CI = [-0.0002, 0.0008]) (Fig. 3A). However, we observed that the decrease in the intermixing index was significantly different between pH 7.5 (weak mutualism) ($R^2 = 0.94$, $P = 2 \times 10^{-9}$, coeff = 0.0018, 95%CI = [0.0013, 0.0024]) and pH 6.5 (strong mutualism) ($R^2 = 0.94$, $P = 8 \times 10^{-8}$, coeff = -0.0019, 95%CI = [-0.0025, -0.0013]). Overall, the final surface ratio of consumer to producer is smaller at pH 7.5 (weak mutualism) (mean = 0.0163, SD = 0.01) than at pH 6.5 (strong

mutualism) (mean = 0.052, SD = 0.02) (two-sample two-sided t-test; P = 0.03, n = 4) (Fig. 3). Consistently, the final intermixing index is also smaller at pH 7.5 (weak mutualism) (mean = 0.0039, SD = 0.0032) than at pH 6.5 (strong mutualism) (mean = 0.0107, SD = 0.0049) (two-sample two-sided t-test; P = 0.05, n = 4) (Fig. 3).

There are two important outcomes of the above described experiment. First, the modelled two-phase linear regression of the surface ratio of consumer to producer and the intermixing index both depended on the pH, where the initial rate of decay was faster at pH 7.5 (weak mutualism) than at pH 6.5 (strong mutualism) (Fig. 3). Thus, as the strength of interdependency increases, the decay of the surface ratio and intermixing index are slowed. Second, at pH 6.5 (strong mutualism) we never observed the complete loss of the consumer from the expansion frontier (*i.e.*, neither the surface ratio of consumer to producer nor the intermixing index reached zero) (Fig. 3). These observations that the consumer to producer ratio and the intermixing index did not reach zero are counter to our initial expectations, where we expected that the producer would obtain a preferential spatial positioning at the expansion frontier under anaerobic conditions, which should then lead to a decrease in the surface ratio of producer to consumer and the eventual complete displacement of the consumer from the expansion frontier (Fig. 2C).

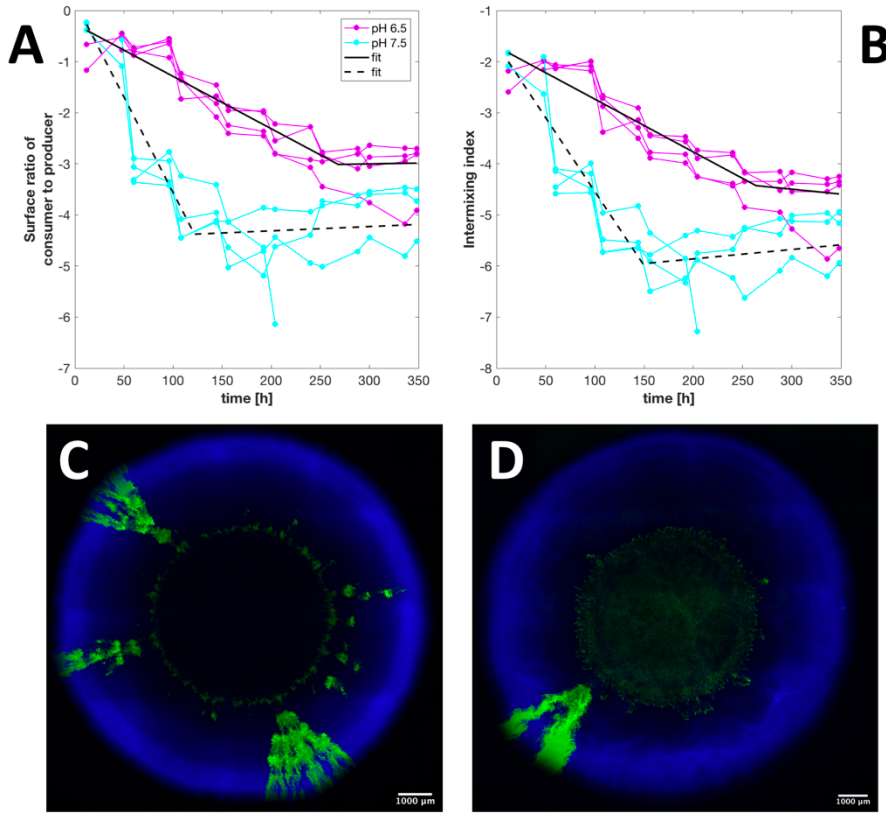


Figure 3. Dynamics of community composition and intermixing during repeated anaerobic (mutualism)/aerobic (competition) transitions. **A** Community composition measured as the surface ratio of consumer to producer. **B** Intermixing between the consumer and producer measured as the intermixing index. Experiments were performed at pH 6.5 (strong mutualism) (magenta datapoints) and pH 7.5 (weak mutualism) (cyan datapoints). Each data series is for an independent replicate ($n = 4$). The solid black lines are the two-phase linear regression models (log axis) for pH 6.5 (strong mutualism) while the dashed black lines are the two-phase linear regression models for pH 7.5 (strong mutualism). **C** Pattern of spatial self-organization formed at pH 6.5 after 350h of expansion under fluctuating conditions. **D** Pattern of spatial self-organization formed at pH 7.5 after 350h of expansion under fluctuating conditions.

Spatial jackpot events enable persistence of the consumer at the expansion frontier.

How did the consumer manage to persist at the expansion frontier over the series of anaerobic (mutualism)/aerobic (competition) transitions? It was previously reported that spatial patterns can bifurcate due to small differences in the initial spatial positioning of individual cells (Goldschmidt *et al.*, *in review*). This results in two fundamentally different patterns of spatial self-organization that emerge at the same time and length scale. The dominant pattern is sequential expansion, where the producer expands first and the consumer follows. The rare pattern is concurrent expansion, where the producer pushes the consumer forward and the producer and consumer expand approximately at the same time (Fig. 4B, white arrows).

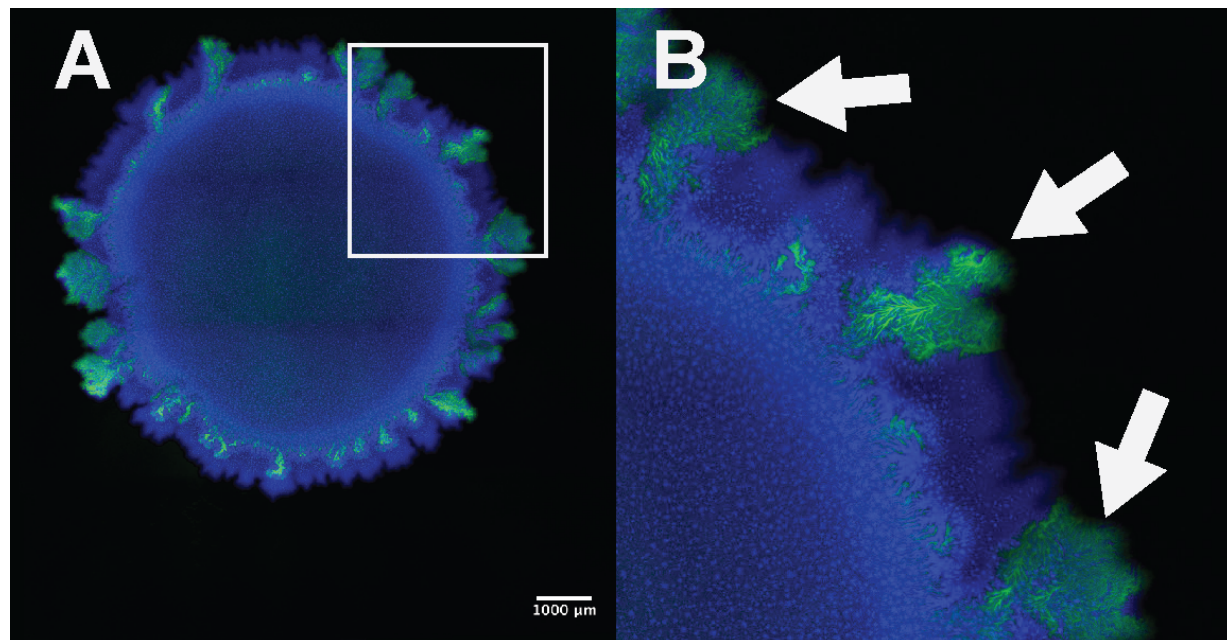


Figure 4. Multiple spatial jackpot events emerge during range expansion under anaerobic (mutualism) conditions. **A** Multiple concurrent expansion patterns events (spatial jackpot events) emerge after two weeks of range expansion. These spatial jackpot events enable the consumer to maintain a spatial position at the expansion frontier. **B** Magnification of the expansion frontier. The white arrows indicate spatial jackpot events.

In our experiments, we indeed observed these rare concurrent expansion patterns (Fig. 4), and we propose here that it is these concurrent expansion patterns enable the consumer to persist at the expansion frontier in the face of repeated anaerobic (mutualism)/aerobic (competition) transitions. By enabling the consumer to maintain a spatial position at the expansion frontier, these rare

concurrent expansion patterns could provide a continuous sink for nitrite (NO_2^-) and therefore enable the prolonged persistence of the community, even at pH 6.5 when nitrite is severely toxic. In this study, we refer to these rare concurrent expansion patterns as spatial jackpot events.

A clear expectation that emerges from these arguments is that the number of spatial jackpot events should increase as the toxicity of nitrite increases. This is because spatial jackpot events enable the consumer to persist at the expansion frontier and consume nitrite, and should therefore have a growth advantage. To test this, we quantified the number of spatial jackpot events at the end of the series of anaerobic (mutualism)/aerobic (competition) transitions. We found that, indeed, the number of spatial jackpot events was higher at pH 6.5 (strong mutualism) than at pH 7.5 (weak mutualism). We observed mean numbers of spatial jackpot events of 3.5 (SD = 1.3, n = 4) at pH 6.5 and 1 (SD 0.5, n = 4) at pH 7.5, and these mean numbers are significantly different from each other (two-sample two-sided t-test; P = 0.0073, n = 4). Thus, we conclude that the increased number of spatial jackpot events at pH 6.5 (strong mutualism) slows the observed decay in the surface ratio of consumer to producer and the intermixing index over repeated transitions between anaerobic (mutualism)/aerobic (competition) conditions (Fig. 3).

To provide further support that these spatial jackpot events can enable the consumer to persist in the face of an anaerobic (mutualism)/aerobic (competition) transitions, we simulated range expansions using an agent based mathematical model (Fig. 6). Details of the model are reported elsewhere (Chapter 3) and its implementation in this study in the SI. The model revealed two important outcomes. First, the model is able to simulate the emergence of spatial jackpot events (Fig. 6), where consumer cells that lie at the expansion frontier are able to maintain their spatial positioning and achieve a higher local growth rate (Fig. 7). Second, after formation, the spatial jackpot events persisted at both pH 6.5 (strong mutualism) and pH 7.5 (weak mutualism) even in the face of anaerobic (mutualism)/aerobic (competition) transitions, which is again consistent with our experimental observations (Fig. 6). We empathise that spatial jackpot events emerge in the simulations purely as a consequence of local favourable spatial positioning and do not require genetic changes, which is consistent with previous experimental observations (Goldschmidt *et al.*, submitted).

The model simulations are also consistent regarding the accumulation of nitrite (NO_2^-) over the anaerobic (mutualism)/aerobic (competition) transitions. The simulations show that nitrite accumulates to lower concentrations at pH 6.5 (strong mutualism) (Fig. 7A) than at pH 7.5 (weak mutualism) (Fig. 7B). This is explained by a lower metabolic activity of producer cells at pH 6.5 due to the toxicity of nitrite (Fig. 7). Regardless of the pH, the consumer cells located within spatial jackpot events have larger growth rates and disproportionately contribute to the production of consumer biomass, and thus represent a persistent sink for nitrite (Fig. 7).

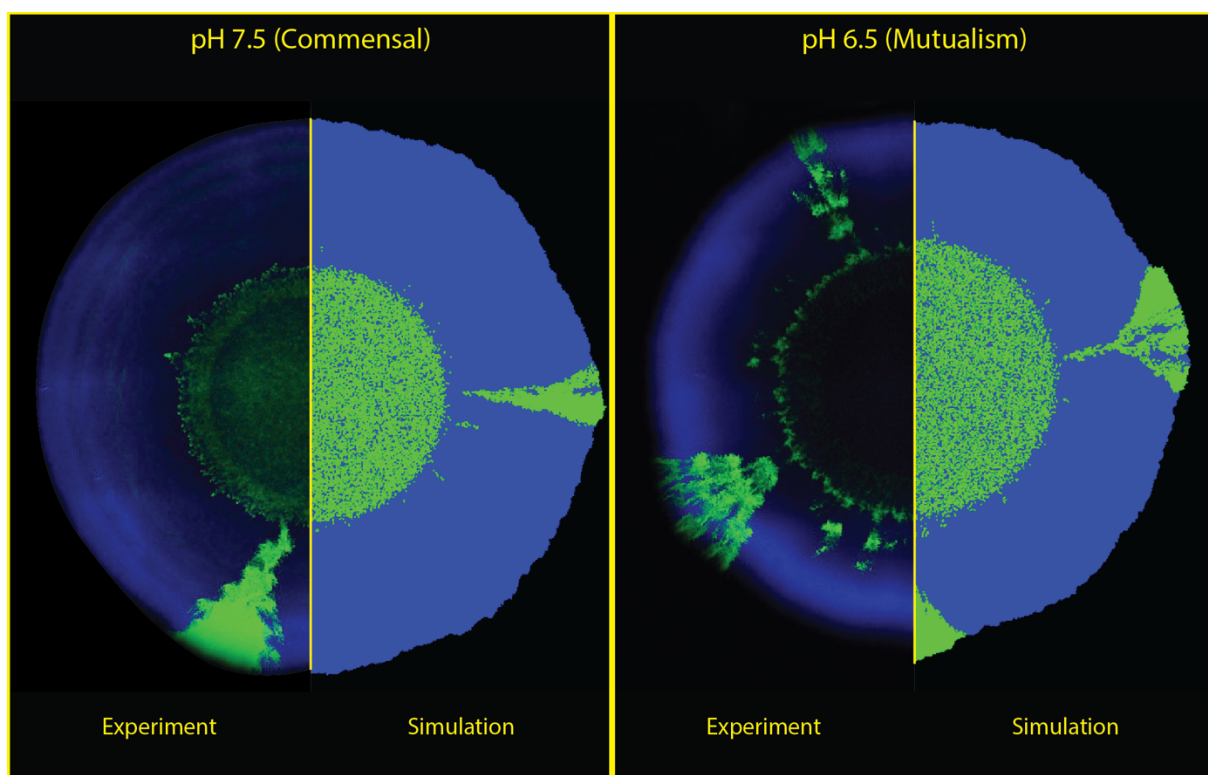


Figure 6. Comparison of experimental and simulated range expansions. At both **A** pH 7.5 (weak mutualism) and **B** pH 6.5 (strong mutualism) conditions, the sequential expansion pattern dominates the expansion region. However, under both conditions, spatial jackpot events emerge consisting of sequential expansion patterns.

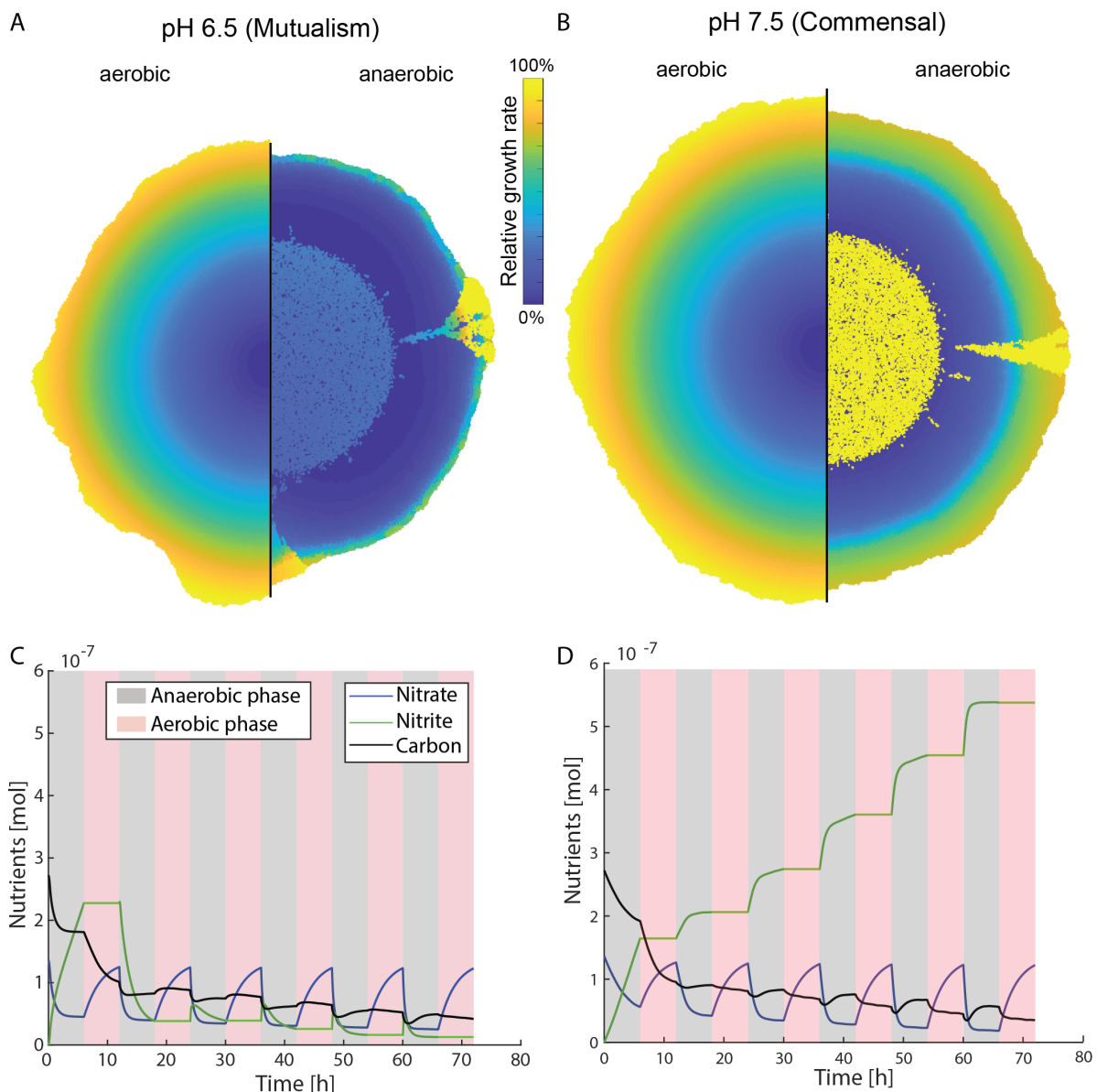


Fig. 7. Local growth rates and nutrient dynamics during range expansion. Spatially visualised relative growth rate for **A** strong mutualistic and **B** weak mutualistic conditions. In aerobic conditions (competition), growth rates decline radially from the periphery to the center due to carbon being the only limiting nutrient. In anaerobic conditions, the produces show a similar radial decline due to nitrate limitation whereas the consumer benefits from the ubiquitous availability of nitrite. **C** and **D** Dynamic total nutrient content in the simulated domain for strong mutualistic and weak mutualistic conditions, respectively. In comparison to static anaerobic conditions, nitrate limitation is less prominent due to diffusion of nitrate into the colony during aerobic phases. **C** In strong mutualistic conditions, nitrite concentrations are low due to the overall higher relative abundance of consumers. **D** In weak mutualistic conditions, nitrite accumulates within the domain lacking strong nitrite toxicity.

Divergent trajectories of community composition and spatial self-organization.

We finally tested whether the dynamic trajectories of the communities depend on the pH (and thus the strength of the mutualistic interaction). To test this, we constructed phase diagrams of the surface ratio of consumer to producer cells and the intermixing index over time. When tracking the two quantities over the fifteen anaerobic (mutualism)/aerobic (competition) transitions, we observed two important outcomes. First, for both pH 6.5 (strong mutualism) and pH 7.5 (weak mutualism), the travel distances between transitions were relatively large over the first three transitions. Thereafter, the travel distances reduced and the quantities began to circulate around a centroid. This suggests that the communities reached a new approximately stable state, and this new stable state emerged as a consequence of the anaerobic(mutualism)/aerobic (competition) transitions. Second, the positions of the new approximately stable states differed depending on the pH, where the new stable state at pH 6.5 (strong mutualism) is located closer the origin than the new stable state at pH 7.5 (weak mutualism). The new steady state at pH 6.5 (strong mutualism) has a larger surface ratio of consumer to producer cells and a larger intermixing index. This suggests that the producer is strongly dependent on the consumer when nitrite toxicity is high, and there are therefore strong benefits for maintaining more balanced ratios of consumer to producer cells and increased intermixing (*i.e.*, the producer advances slowly without the consumer in close spatial proximity to consume nitrite). In contrast, the new steady state at pH 7.5 (weak mutualism) has a smaller surface ratio of consumer to producer cells and a smaller intermixing index. This is intuitive, as the producer is less dependent on the consumer when nitrite toxicity is low, and there are therefore weaker benefits for maintaining balanced ratios of consumer to producer and intermixing (*i.e.*, the producer can advance without the consumer).

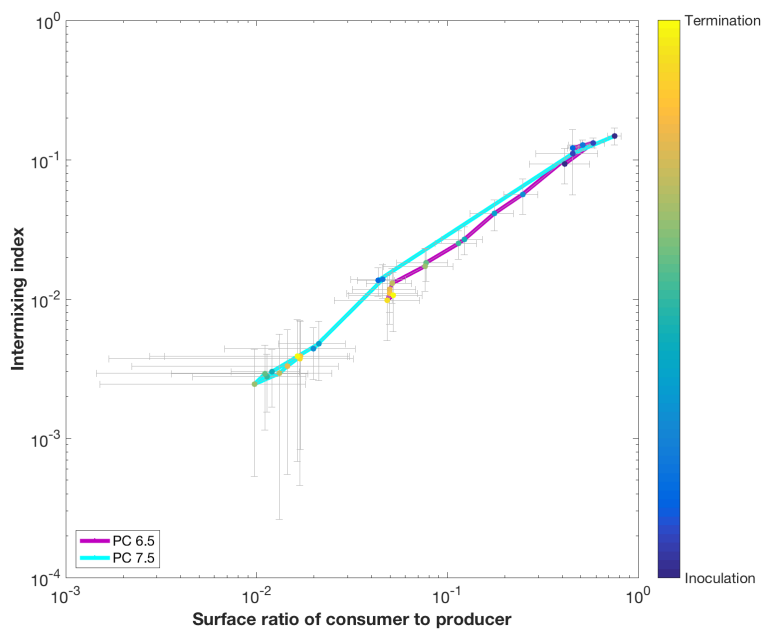


Figure 8 Interaction strength determines the location of the new persistent state. In the phase space, we keep track of the local intermixing index and the surface ratio of producer to consumer over the series of anaerobic (mutualism)/aerobic (competition) transitions. The communities start from the same position in phase space and evolve towards two distant new persistent states. The magenta line is for communities grown at pH 7.5 and the cyan line is for communities grown at 6.5.

DISCUSSION

Counter to our initial expectation (Fig. 2C), we found that our microbial community can persist in the face of repeated transitions between anaerobic (mutualism)/aerobic (competition) conditions. The underlying cause of this persistence is the emergence of spatial jackpot events. These jackpot events enable the consumer to persist at the leading edge of the expansion frontier under anaerobic (mutualism) conditions, and thus also enable it to persist after transition to aerobic (competition) conditions. Thus, spatial jackpot events may be an important mechanism that enables community resilience and resistance to environmental perturbations. In essence, spatial jackpot events generate local spatial pattern diversity within microbial communities. Thus, just as genetic and functional diversity can provide resistance and resilience to microbial communities, spatial pattern diversity can also contribute towards resistance and resilience.

Why do spatial jackpot events emerge, and what enables their propagation? The term “jackpot event” has typically been used in relation to genotypic events, where rare mutations can emerge and enable new genotypes to proliferate and persist [35–37]. In our case, spatial jackpot events do not have a genetic basis, but instead emerge due to variation in the initial spatial positioning of individuals . They then propagate and are further maintained by local conditions (i.e., high local growth rates within those jackpot events) (Chapter 3). In our model system, consumer cells located within a spatial jackpot event have a local growth advantage due to their close spatial proximity to the most metabolically active producer cells (Fig. 7). Thus, stochastic processes determine the initial spatial positioning of individuals, while deterministic process then act on those individuals and can generate a range of spatial patterns with different growth rates and behaviours.

How widespread are spatial jackpot events likely to occur in nature? We argue that such spatial jackpot events may be typical features of nearly every self-organizing microbial community. When any surface is colonized by microbial cells, individuals will not be distributed uniformly. Instead, all colonized surfaces will contain local differences in the initial spatial positioning of individuals. These differences, in turn, can create pattern diversity, where some of the patterns may provide new community-level properties such as resistance or resilience to environmental changes. Thus, spatial jackpot events may not just be widespread, they may be inevitable features of any surface-attached microbial community.

ACKNOWLEDGEMENTS

We thank Sara Mitri, and Robin Tecon for helpful discussions and Jan Dolinšek for helping on the oxygen quantification with the microsensor.

REFERENCES

1. Voreades N, Kozil A, Weir TL. Diet and the development of the human intestinal microbiome. *Front Microbiol* 2014; **5**: 494.
2. Bleuven C, Landry CR. Molecular and cellular bases of adaptation to a changing environment in microorganisms. *Proc R Soc B Biol Sci* 2016; **283**.
3. Mathis R, Ackermann M. Response of single bacterial cells to stress gives rise to complex history dependence at the population level. *Proc Natl Acad Sci U S A* 2016; **113**:4224-9.
4. Kraemer SA, Boynton PJ. Evidence for microbial local adaptation in nature. *Mol Ecol* 2017; **26**:1860-1876.
5. Jaggi R, Jiang J, Momoh AO, Alderman A, Giordano SH, Buchholz TA, et al. Seasonal Cycling in the Gut Microbiome of the Hadza Hunter-Gatherers of Tanzania. *Science (80-)* 2017; **357**: 802–806.
6. Rodríguez-Verdugo A, Vulin C, Ackermann M. The rate of environmental fluctuations shapes ecological dynamics in a two-species microbial system. *Ecol Lett* 2019; **22**: 838–846.
7. Dolinšek J, Goldschmidt F, Johnson DR. Synthetic microbial ecology and the dynamic interplay between microbial genotypes. *FEMS Microbiol Rev* 2016; **40**: 961–979.
8. Ghoul M, Mitri S. The Ecology and Evolution of Microbial Competition. *Trends Microbiol* 2016; **24**: 833–845.
9. Tecon R, Mitri S, Ciccarese D, Or D, van der Meer JR, Johnson DR. Bridging the Holistic-Reductionist Divide in Microbial Ecology. *mSystems* 2019; **4**: pii: e00265-18.
10. Ciccarese D, Johnson DR. Functional Microbial Landscapes. *Compr Biotechnol* 2019; 42–51.
110. Ciccarese D, Johnson DR. Functional Microbial Landscapes. *Compr Biotechnol* 2019; **6**: 42–51.
11. D. Ciccarese, A. Zuidema,V. Merlo, DR. Johnson. Interaction-dependent effects of surface structure on the spatial self-organization of microbial communities. *Philos Trans R Soc B* 2020.
12. Cutler NA, Chaput DL, Oliver AE, Viles HA. The spatial organization and microbial community structure of an epilithic biofilm. *FEMS Microbiol Ecol* 2015; **91**: pii: fiu027.
13. Liu W, Røder HL, Madsen JS, Bjarnsholt T, Sørensen SJ, Burmølle M. Interspecific bacterial interactions are reflected in multispecies biofilm spatial organization. *Front Microbiol* . 2016; **7** doi: 10.3389
14. Crespi BJ. The evolution of social behavior in microorganisms. *Trends Ecol Evol* . 2001; **16**:178-183.

15. Kerr B., Riley M.A., Feldman M.W., Bohannan B.J.M. Local dispersal promotes biodiversity in a real-life game of rock-paper-scissors. *Nature* 2002; **418**: 171–174.
- Kim W, Racimo F, Schluter J, Levy SB, Foster KR. Importance of positioning for microbial evolution. *Proc Natl Acad Sci U S A* 2014; **111**: E1639-47.
17. Kim W, Levy SB, Foster KR. Rapid radiation in bacteria leads to a division of labour. *Nat Commun* 2016; **7**:10508.
18. Flemming HC, Wingender J, Szewzyk U, Steinberg P, Rice SA, Kjelleberg S. Biofilms: An emergent form of bacterial life. *Nat Rev Microbiol*. 2016; **14**: 563-75.
19. Chacón JM, Möbius W, Harcombe WR. The spatial and metabolic basis of colony size variation. *ISME J* 2018; **12**: 669–680.
20. Nadell CD, Drescher K, Foster KR. Spatial structure, cooperation and competition in biofilms. *Nat Rev Microbiol* 2016; **14**: 589–600.
21. Ponomarova O, Patil KR. Metabolic interactions in microbial communities: untangling the Gordian knot. *Curr Opin Microbiol* 2015; **27**: 37–44.
22. Dai L, Vorselen D, Korolev KS, Gore J. Generic indicators for loss of resilience before a tipping point leading to population collapse. *Science (80-)* 2012; **336**: 1175–1177.
23. Hallatschek O, Hersen P, Ramanathan S, Nelson DR. Genetic drift at expanding frontiers promotes gene segregation. *Proc Natl Acad Sci* 2007; **104**: 19926–19930.
24. Gralka M, Hallatschek O. Environmental heterogeneity can tip the population genetics of range expansions. *Elife* 2019; **8**: 1–24.
25. Goldschmidt F, Regoes RR, Johnson DR. Successive range expansion promotes diversity and accelerates evolution in spatially structured microbial populations. *ISME J* 2017; **11**: 2112–2123.
- Lilja EE, Johnson DR. Metabolite toxicity determines the pace of molecular evolution within microbial populations. *BMC Evol Biol* 2017; **17**: 1–12.
27. Lilja EE, Johnson DR. Segregating metabolic processes into different microbial cells accelerates the consumption of inhibitory substrates. *ISME J* 2016; **10**: 1568–1578.
28. Goldschmidt F, Regoes RR, Johnson DR. Metabolite toxicity slows local diversity loss during expansion of a microbial cross-feeding community. *ISME J* 2018; **12**: 136-144.
29. Lilja EE, Johnson DR. Substrate cross-feeding affects the speed and trajectory of molecular evolution within a synthetic microbial assemblage. *BMC Evol Biol* 2019; **19**: 129.
30. Momeni B, Brileya KA, Fields MW, Shou W. Strong inter-population cooperation leads to

- partner intermixing in microbial communities. *Elife* 2013; **13**: 1–23.
31. Pielou EC. Species-diversity and pattern-diversity in the study of ecological succession. *J Theor Biol* 1966; **10**: 370–83.
 32. Hudson DJ. Fitting Segmented Curves Whose Join Points Have to Be Estimated. *J Am Stat Assoc* 1966; **61**, 1097–1129.
 33. Lee ML, Poon W-Y, Kingdon HS. A two-phase linear regression model for biologic half-life data. *J Lab Clin Med* 1990; **115**: 745–748.
 34. Atanasov D. Two-phase linear regression model. *MATLAB Central File Exchange*. <https://www.mathworks.com/matlabcentral/fileexchange/26804-two-phase-linear-regression-model..>
 35. Luria SE, Delbrück M. Mutations of Bacteria from Virus Sensitivity to Virus Resistance. *Genetics* 1943; **28**: 491–511.
 36. Fusco D, Gralka M, Kayser J, Anderson A, Hallatschek O. Excess of mutational jackpot events in expanding populations revealed by spatial Luria-Delbrück experiments. *Nat Commun* 2016; **7**: 1–9.
 37. Kayser J, Schreck CF, Yu Q, Gralka M, Hallatschek O. Emergence of evolutionary driving forces in pattern-forming microbial populations. *Philos Trans R Soc B Biol Sci* 2018; **373**: 20170106.

SUPPORTING MATERIAL

Statistical analysis

All statistical analyses were performed in Matlab R2017a. The two phase linear regression model for the intermixing index decay and surface ratio decay was calculated using a function available in File Exchange on matworks.com [34] with a general model defined as follow:

$$y \begin{cases} \alpha_1 + \beta_1 x, \\ \alpha_2 + \beta_2 x, \end{cases}$$

Mathematical modeling

We used a previously published mathematical model to simulate colony expansion using a pseudo two-dimensional numerical nutrient diffusion and an individual based representation of bacterial cells. Anaerobic phases are simulated using the same coefficients and conditions as described in (Chapter 3). To simulate aerobic phases, a carbon source was added to the simulation with a constant source boundary condition at the periphery (22 mM) which is consumed during both the aerobic and anaerobic phase. The concentration was chosen to reflect a 4% carbon concentration in defined media agar plates and does not reflect the total carbon in LB media (which primarily contains carbon in the form of amino acids). However, this concentration is sufficiently high and does not pose any limiting effect on community growth. Oxygen is not simulated explicitly as provision via the gas phase is three orders of magnitude faster compared to the agar phase. The total simulation includes six anaerobic and six aerobic phases such that no further change in resulting patterns is observed in the last fluctuations (i.e. the system reached steady state concerning spatial self-organization, congruent to the process used to determine the number of fluctuations in the experiment). Corresponding to the experiment, the duration of each phase is determined such that there are equal divisions expected during aerobic and anaerobic phases (in our case equal duration as growth rates for aerobic and anaerobic conditions are the same to exclude any coefficients bias). The total simulated time is 72h with each phase being 6h.

Diffusion time of conservative oxygen in agar

The incubation period in each redox condition was determined by taking into account a comparable yield during each redox phase, as well considering the diffusion time of oxygen into the agar. We conducted the experiment for fifteen cycle until no changes in pattern were recognized. We poured the LB agar on a petri dish with a microsensor oxygen needle (PreSens) positioned within the agar under anaerobic conditions. We then moved the agar plate outside the anaerobic chamber into ambient air. We maintained the agar plate in ambient air until the oxygen concentration within the agar stabilized. Finally, we returned the agar plate inside the anaerobic chamber and measured the decay of oxygen until it decreased below the analytical detection limit. We considered the oxygen within the agar as a conservative measure of available oxygen. This means that the time for oxygen to reach the detection limit is the assumed time when all available oxygen diffuses outside the agar.

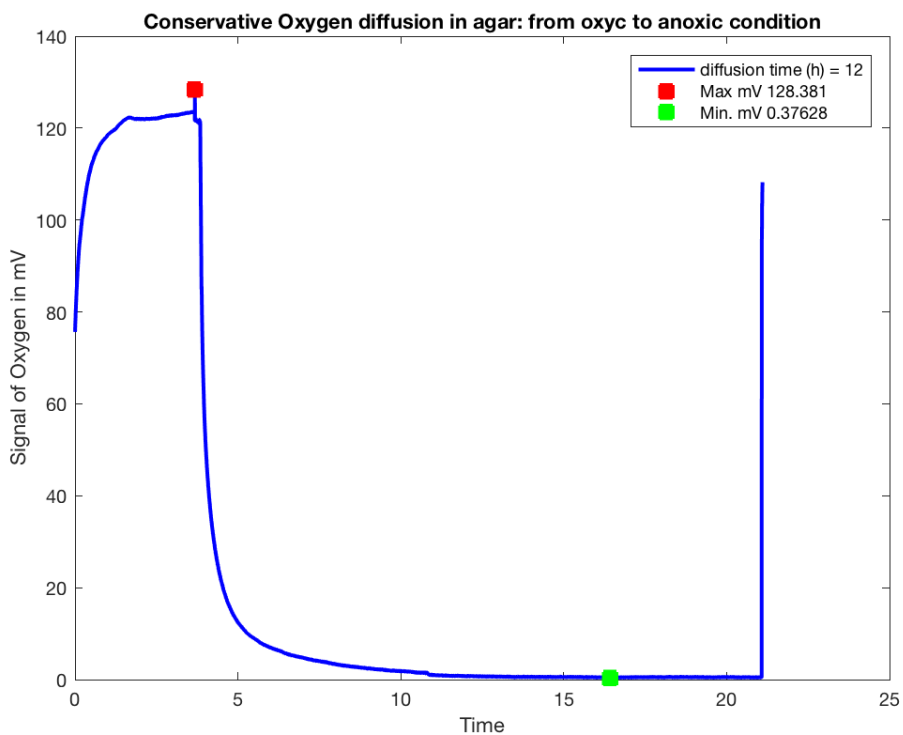


Figure S1 Diffusion time of conservative oxygen in agar. The red dot represents the maximum voltage value of oxygen measured into the agar (128.3 mV). The green dot is the zero value of oxygen (corresponding to the measured minimum 0.37 mv). The time between the maximum value and minimum value of oxygen is the diffusion time to diffuse all the detectable oxygen from the agar to the external atmosphere (~12h).

CHAPTER 5: Interaction-dependent effects of surface structure on the spatial self-organization of microbial communities.

A similar version of this chapter has been published as:

Ciccarese Davide, Zuidema Anita, Merlo Valeria, Johnson R David, (2020) Interaction-dependent effects of surface structure on the spatial self-organization of microbial communities. *Philos Trans R Soc B*. In press.

ABSTRACT

Surface-attached microbial communities consist of different cell-types that, at least to some degree, organize themselves non-randomly across space (referred to as spatial self-organization). While spatial self-organization can have important effects on the functioning, ecology, and evolution of communities, the underlying determinants of spatial self-organization remain unclear. Here, we hypothesize that the presence of physical objects across a surface can have important effects on spatial self-organization. Using pairs of isogenic strains of *Pseudomonas stutzeri*, we performed range expansion experiments in the absence or presence of physical objects and quantified the effects on spatial self-organization. We demonstrate that physical objects create local deformities along the expansion frontier, and these deformities increase in magnitude during range expansion. The deformities affect the densities of interspecific boundaries and diversity along the expansion frontier, and thus affect spatial self-organization, but the effects are interaction-dependent. For competitive interactions that promote sectorized patterns of spatial self-organization, physical objects increase the density of interspecific boundaries and diversity. In contrast, for cross-feeding interactions that promote dendritic patterns, they decrease the density of interspecific boundaries and diversity. These qualitatively different outcomes are likely caused by fundamental differences in the orientations of the interspecific boundaries. Thus, in order to predict the effects of physical objects on spatial self-organization, information is needed regarding the interactions present within a community and the general geometric shapes of spatial self-organization that emerge from those interactions.

INTRODUCTION

Surface-attached microbial communities are ubiquitous across our planet, contribute to all major biogeochemical processes, and have important roles in human health and disease [1-5]. These communities expand across space (*i.e.*, range expansion) as a consequence of growth and cell division (*i.e.*, cell shoving) [6-9] and active cell motility [3, 10]. During range expansion, different cell-types arrange themselves non-randomly across space and form spatial patterns [11-25], which is referred to as spatial self-organization [26-31]. Importantly, these patterns can be important determinants of community-level properties. For example, they can determine community-level productivity [13, 21, 32-35], the metabolic processes performed by communities [34, 36-39], the resistance and/or resilience of communities to environmental perturbations [40-42], and the evolutionary processes acting on communities [14, 22, 43-46]. Identifying the determinants of spatial self-organization is therefore important for our basic understanding of the structure, functioning and evolution of microbial communities [47].

One plausible determinant of spatial self-organization is the physical structure of the surface over which the microbial community expands [45, 48-52]. The majority of microbial range expansion studies have been conducted across smooth surfaces that lack physical objects [11-20, 22-26]. Yet, outside of controlled laboratory settings, physical objects are likely pervasive across surfaces. This then raises an important question: How do physical objects affect spatial self-organization? In other words, can we generalize results obtained with smooth surfaces to more complex surfaces that contain physical objects?

To address this question, consider a simplified community consisting of two cell-types with equivalent fitness. If a liquid suspension of the community is inoculated as a droplet onto a smooth surface containing no physical objects, the shape of the expansion frontier is approximately uniform and circular (*i.e.*, a circularity isoperimetric quotient [$\frac{\text{perimeter}^2}{4 \times \pi \times \text{area}}$] $\cong 1$ [53]) and can be described as the radius of curvature (R_c) of the inoculation area (Fig. 1A). In contrast, if a liquid suspension of the community is inoculated as a droplet onto a surface containing physical objects, where the physical objects are smaller than the inoculation area but larger than individual cells, then these physical objects can create deformities along the expansion frontier [45, 50, 51] (Fig. 1B). These deformities could result from two processes. First, if the physical objects lie behind the expansion frontier, the

objects could deform the expansion frontier as a consequence of liquid-surface interactions and create local regions with smaller R_c (R_{sc}) and inverted curvature (R_{ic}) [51] (Fig. 1C). Second, if the physical objects lie ahead of the expansion frontier, the expansion frontier could eventually collide with the physical objects and deform the expansion frontier [50]. In both cases, the deformed expansion frontier would have a larger perimeter-to-area ratio and a shape that deviates from circular (*i.e.*, a circularity isoperimetric quotient > 1) (Fig. 1B).

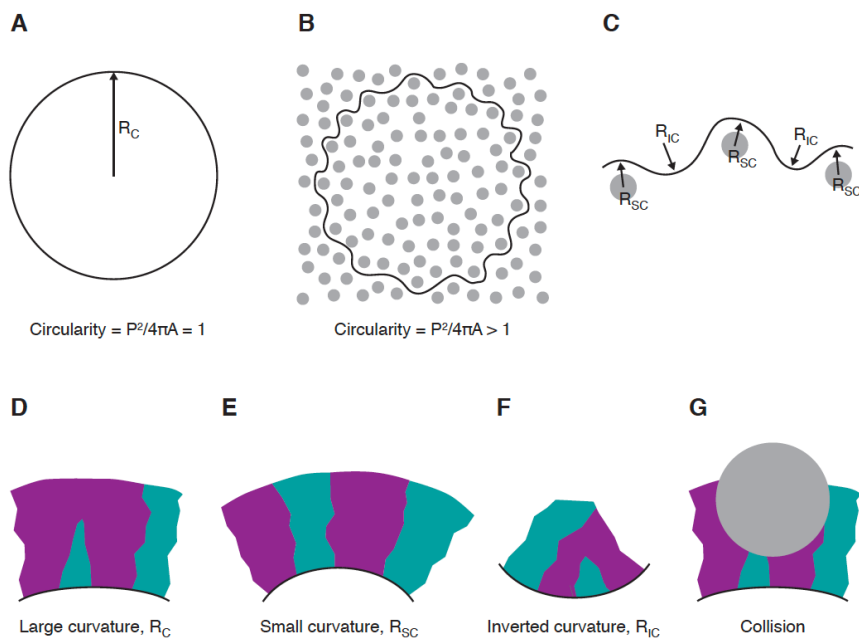


Figure 1. Effect of physical objects on spatial self-organization. *A)* In the absence of physical objects, the initial expansion frontier is approximately uniform and has a circularity isoperimetric quotient approximately equal to one. *B)* In the presence of physical objects (grey circles), the initial expansion frontier contains local deformities, deviates from circular, and has a circularity isoperimetric quotient greater than one. *C)* Magnification of deformities along the initial expansion frontier produced by the addition of physical objects (grey circles). The deformities consist of local regions of small R_C (R_{SC}) and inverted curvature (R_{IC}). *D)* At local regions of large R_C , the angle between neighboring interspecific boundaries is relatively small, which increases the probability of stochastic boundary coalescence and decreases interspecific mixing and diversity along the expansion frontier. *E)* At local regions of small R_C (R_{SC}), the angle between neighboring interspecific boundaries is relatively large, which decreases the probability of stochastic boundary coalescence and increases interspecific mixing and diversity along the expansion frontier. *F)* At local regions of inverted curvature (R_{IC}), neighboring interspecific boundaries are oriented towards coalescence, which decreases interspecific mixing and diversity along the expansion frontier. *G)* Collision of an expansion frontier into a physical object. If the physical object is larger than the length-scale of spatial self-organization, then the collision causes some interspecific boundaries to become lost and decreases interspecific mixing and diversity along the expansion frontier.

Do these deformities along the expansion frontier affect spatial self-organization? Theoretical considerations and experimental investigations indicate that this is likely the case [45, 50, 51]. Consider again a simplified community consisting of two cell-types with equivalent fitness. As the community expands across space, the cell-types demix as a consequence of random sampling at the expansion frontier and the stochastic coalescence of interspecific boundaries [12, 14] (Fig. 1D). Theoretical considerations predict that the probability of stochastic boundary coalescence is negatively related to R_c [51]. Importantly, if physical objects lie behind the expansion frontier, then they could create local regions of R_{sc} (Fig. 1C). The consequence is a larger angle between neighboring interspecific boundaries and a reduced probability of stochastic boundary coalescence, and we therefore expect more interspecific mixing and diversity along the expansion frontier [51] (Fig. 1E). In addition, the physical objects could also create local regions of R_{lc} (Fig. 1C). The consequence is that neighboring interspecific boundaries would be oriented towards coalescence, and we therefore expect the deterioration of interspecific mixing and diversity along the expansion frontier [51] (Fig. 1F). Finally, if physical objects lie ahead of the expansion frontier, the expansion frontier may eventually collide with those physical objects. The consequence is that some interspecific boundaries may become lost, and we therefore expect the deterioration of interspecific mixing and diversity along the expansion frontier [50] (Fig. 1G). Thus, the presence of physical objects can impose a variety of positive and negative effects on interspecific mixing and diversity.

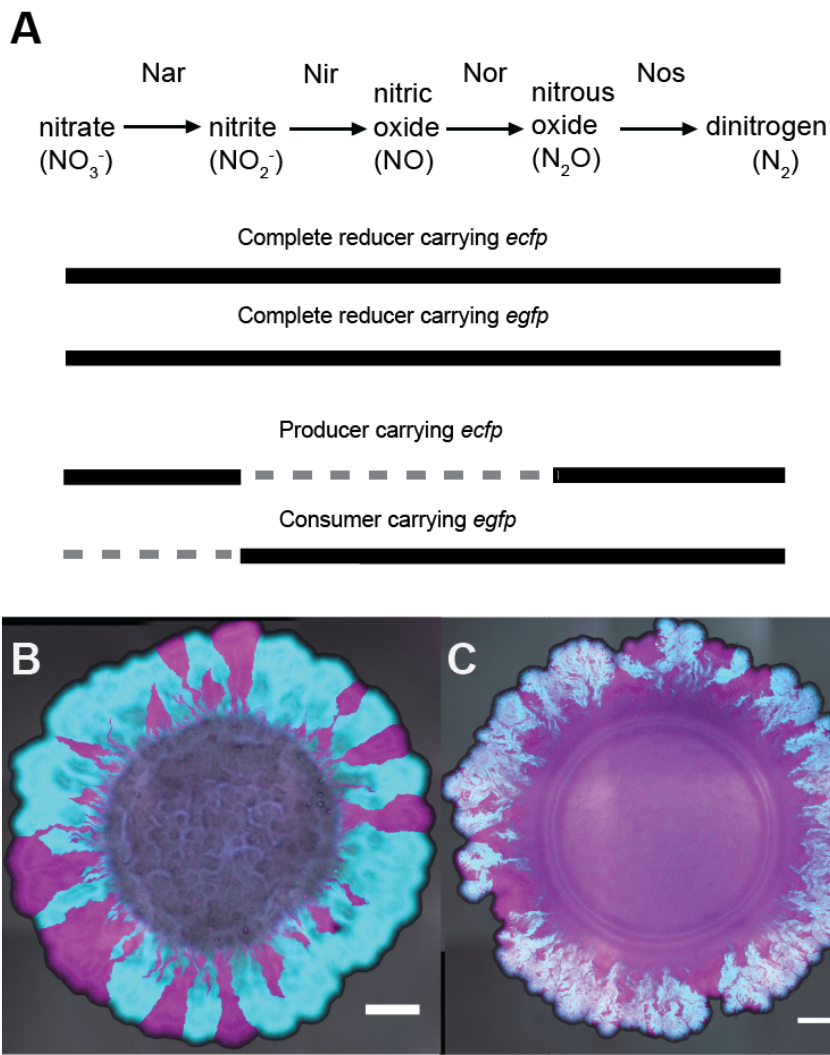


Figure 2. Experimental model system used in this study. A) Our experimental model system is composed of four isogenic mutant strains of *P. stutzeri*. The two complete reducer strains are genetically identical except that they express either the cyan fluorescent protein-encoding *ecfp* gene or the green fluorescence protein-encoding *egfp* gene. The producer contains a loss-of-function mutation in the *nirS* gene and can reduce nitrate (NO_3^-) but not nitrite (NO_2^-). The consumer contains a loss-of-function mutation in the *narG* gene and can reduce nitrite but not nitrate. In addition, the producer expresses the cyan fluorescence protein-encoding *ecfp* gene while the consumer expresses the green fluorescence protein-encoding *egfp* gene. When the two complete reducer strains are grown together with nitrate as the growth-limiting substrate, they have equivalent fitness and engage in a competitive interaction for nitrogen oxides. When the producer and consumer are grown together with nitrate as the growth-limiting substrate, they engage in a nitrite cross-feeding interaction. Thick arrows indicate the nitrogen oxides that can be reduced by each strain. Definitions: Nar, nitrate reductase; Nir, nitrite reductase; Nor, nitric oxide reductase;

Nos, nitrous oxide reductase. *B*) Pattern of spatial self-organization formed by pairs of complete reducers (1:1 initial cell number ratio) after two weeks of range expansion. One complete reducer carried the cyan fluorescent protein-encoding *ecfp* gene (shown in magenta) while the other carried the green fluorescent protein-encoding *egfp* gene (shown in green). *C*) Pattern of spatial self-organization formed by pairs of producer and consumer (1:1 initial cell number ratio) after two weeks of range expansion. The producer carried the cyan fluorescent protein-encoding *ecfp* gene (shown in magenta) while the consumer carried the green fluorescent protein encoding *egfp* gene (shown in green). The scale bars are equivalent to 1000 μm .

Our objectives here were three-fold. First, we sought to experimentally test whether the presence of physical objects do indeed create deformities along the expansion frontier. Second, we wanted to determine what types of deformities (*i.e.*, local regions of R_{SC} [Fig. 1E], local regions of R_{IC} [Fig. 1F], or collisions [Fig. 1G]) have the predominant effects on interspecific mixing, diversity, and spatial self-organization along the expansion frontier. Third, we wanted to test whether our results are generalizable to different types of microbial interactions that promote the formation of fundamentally different patterns of spatial self-organization. To achieve these objectives, we performed range expansion experiments with synthetic microbial communities consisting of pairs of isogenic mutant strains of the denitrifying bacterium *Pseudomonas stutzeri* A1501 (Fig. 2A). One pair consists of two strains that are genetically identical except that they express different fluorescent protein-encoding genes (referred to as complete reducers) [22, 54, 55] (Fig. 2A). When grown together in the absence of oxygen and with an exogenous supply of nitrate (NO_3^-) as the growth-limiting substrate, they have equivalent fitness and can completely reduce nitrate to dinitrogen gas (Fig. 2A). They therefore engage in a competitive interaction for nitrogen oxides [22, 54, 55]. The other pair consists of two strains that differ in their ability to reduce nitrogen oxides [22, 54, 56] (Fig. 2A). One strain contains a loss-of-function mutation in the *nirS* gene and can reduce nitrate but not nitrite (NO_2^-) (referred to as the producer) while the other strain contains a loss-of-function mutation in the *narG* gene and can reduce nitrite but not nitrate (referred to as the consumer) [22, 54, 56] (Fig. 2A). When grown together in the absence of oxygen and with an exogenous supply of nitrate as the growth-limiting substrate, the producer supports its growth via the reduction of nitrate to nitrite while the consumer supports its growth via the reduction of nitrite. They therefore engage in a nitrite cross-feeding interaction [22, 25, 54, 56]. Importantly, the two communities form fundamentally different patterns of spatial self-organization during range expansion (Figs. 2B and C). Namely, pairs of complete reducers (competitive interaction) form segregated or sectorized patterns where the interspecific boundaries are oriented approximately parallel to the axis of range expansion [22, 25] (Fig. 2B). In contrast, pairs of producer and consumer (nitrite cross-feeding interaction) form dendritic patterns where the dendrites originate from single points in the inoculation area and increase in width during range expansion, thus resulting in interspecific boundaries that are not oriented parallel to the axis of range expansion [22, 25] (Fig. 2C).

To address our main questions, we performed range expansion experiments in the presence or absence of physical objects for both pairs of complete reducers (competitive interaction) and for pairs of producer and consumer (nitrite cross-feeding interaction). We selected Nafion particles with a size distribution of 35-60 μm as physical objects, which is smaller than the size of the inoculation area [22, 25] but larger than the size of individual cells. Nafion particles are composed of a transparent and inert fluorocarbon polymer that is amenable to microscopic interrogation and have been successfully applied in other studies to create synthetic porous media [57-59]. While we could have used other particles as physical objects, such as spherical beads with precisely defined geometries, we selected Nafion particles due to their ability to mimic natural soils [57, 58]. After allowing the communities to expand, we then quantitatively compared how the presence of physical objects affect interspecific mixing, diversity, and spatial self-organization along the expansion frontier.

MATERIALS AND METHODS

Experimental model system

We described all of the strains used in this study in detail elsewhere [22, 54, 55]. For this study, our experimental model system is composed of four isogenic mutant strains of the bacterium *Pseudomonas stutzeri* A1501 (Fig. 2 and Supplementary Table S1). Briefly, the two complete reducers do not carry any disruptions in the denitrification pathway and can completely reduce nitrate (NO_3^-) to nitrite (NO_2^-), nitric oxide (NO), nitrous oxide (N_2O) and finally to dinitrogen gas (N_2) (Fig. 2 and Supplementary Table S1). In contrast, the producer carries a single loss-of-function deletion in the *nirS* gene and can reduce nitrate but not nitrite (Fig. 2 and Supplementary Table S1) while the consumer carries a single loss-of-function deletion in the *narG* gene and can reduce nitrite but not nitrate (Fig. 2 and Supplementary Table S1). Importantly, the two complete reducers, producer and consumer are all isogenic mutants of each other that differ at only single genetic loci [22, 54, 55], thus minimizing any potential confounding factors that could arise when using more distantly related strains. We reported complete descriptions for the deletion of the *narG* and *nirS* genes elsewhere [54].

In addition to the genetic changes described above, each strain contains two additional genetic changes. First, all of the strains contain a single loss-of-function deletion in the *comA* gene [54] (Supplementary Table S1). This minimizes the probability that the strains will take up extracellular DNA [60], and thus minimizes the probability that they will recombine with each other when grown together. Second, each strain contains either the IPTG-inducible green fluorescent protein-encoding *egfp* gene or the cyan fluorescent protein-encoding *ecfp* gene (Fig. 2 and Supplementary Table S1), which enables us to distinguish and quantify the abundances of each strain when grown together [22, 25, 56]. We reported complete descriptions for the deletion of the *comA* gene and the introduction of the fluorescent protein-encoding genes elsewhere [22, 54, 55]. We previously reported that there are no observable differential costs for expressing different fluorescent protein-encoding genes for our isolates [55].

Range expansion experiments

We performed anaerobic range expansion experiments as described in detail elsewhere [22, 25], which is a modified version a protocol developed for aerobic range expansions [12]. Briefly, we first grew the two complete reducers, producer, and consumer independently in aerobic lysogeny broth (LB) medium overnight in a shaking incubator at 37°C at 220 rpm. After reaching stationary phase, we adjusted the densities of each culture to an optical density at 600 nm of one (OD_{600}), centrifuged the cultures at 3600 $\times g$ for eight minutes at room temperature, discarded the supernatants, and suspended the cells in 1000 μl of 0.9% (w/v) saline solution. We then transferred the cultures into a glove box (Coy Laboratory Products, Grass Lake, MI) containing a nitrogen (N_2):hydrogen (H_2) (97:3) anaerobic atmosphere, mixed the two complete reducers together or the producer and consumer together at a volumetric ratio of 1:1, and deposited 1 μl of each mixture onto the center of a separate anaerobic LB agar plate amended with 1 mM of sodium nitrate ($NaNO_3$) and adjusted to pH 7.5 with 0.5 M NaOH. Because the complete reducers, producer and consumer are all isogenic mutants of each other and have identical optical properties, a volumetric ratio of 1:1 is equivalent to a cell number ratio of 1:1. We provided a complete description for the preparation of anaerobic LB agar plates elsewhere [22].

To assess the effects of physical objects on interspecific mixing, diversity, and spatial self-organization, we used Nafion particles with a size range of 35-60 μm (Sigma-Aldrich, Buchs, Switzerland). Briefly, after we inoculated the anaerobic LB agar plates with pairs of complete reducers or pairs of producer and consumer, we incubated the plates for 48 h. This allowed for the suspension liquid from the inoculum to dissipate and for individual cells to attach to the LB agar surface. After 48 hours, we then deposited approximately 5 mg of dry Nafion particles (*i.e.*, the particles were not suspended in solution) to the inoculation area of each plate that was assigned to the physical object treatment group and continued to incubate the plates for a total of two weeks. We note here that the growth-limiting substrate is nitrate (NO_3^-) for all of our experiments, which we exogenously added to the LB agar that resides below the Nafion particles. We therefore do not expect the Nafion particles, which reside on top of the LB agar, to constrain the diffusional supply of nitrate.

Microscopy and image analysis

We imaged the range expansions with a Leica TCS SP5 II confocal microscope (Leica Microsystems, Wetzlar, Germany) as described in detail elsewhere [22, 25]. Briefly, prior to imaging the range expansions, we exposed the LB agar plates to ambient air for 1 h to induce maturation of the fluorescent proteins [22, 25]. We then quantified the circularity of the range expansion area using the circularity isoperimetric quotient ($\frac{perimeter^2}{4 \times \pi \times area}$) [53]. We next quantified the number of interspecific boundaries between two complete reducers or between the producer and consumer by first plotting a line at 50 pixels from the leading edge of the range expansion area. We set this distance to avoid possible microscopy artefacts that could emerge due to uneven illumination at the expansion frontier. We then measured the number of color transitions along the internal end-joined line, where the number of color transitions are equivalent to the number of interspecific boundaries along the line. We note here that these measures are inherently one-dimensional in nature. The advantage of this approach is that we do not have to discriminate between the inoculation and expansion areas, which is technically difficult. The disadvantage, however, is that we cannot measure the number of boundary coalescence events, which would require discriminating between the inoculation and expansion areas and applying two-dimensional methodologies. Finally, we quantified the fractal dimension of the dendrites formed by the producer and consumer using the fractal box-counting method as described in detail elsewhere [22].

Statistical analysis

We used parametric methods for all of our statistical tests and considered a P-value < 0.05 to be statistically significant. We reported the type of statistical test, the sample size for each test, and the exact P-value for each test in the results section.

RESULTS

Physical objects create deformities along the expansion frontier

We first tested whether the addition of physical objects to a surface creates immediate deformities along an expansion frontier. To accomplish this, we assembled pairs of complete reducers together (1:1 initial cell number ratio) and deposited them onto separate replicated LB agar plates ($n = 18$). We then added Nafion particles as physical objects to half the plates, immediately interrogated the expansion frontier via microscopy, and quantified the immediate effects of physical objects on the shape of the expansion frontier.

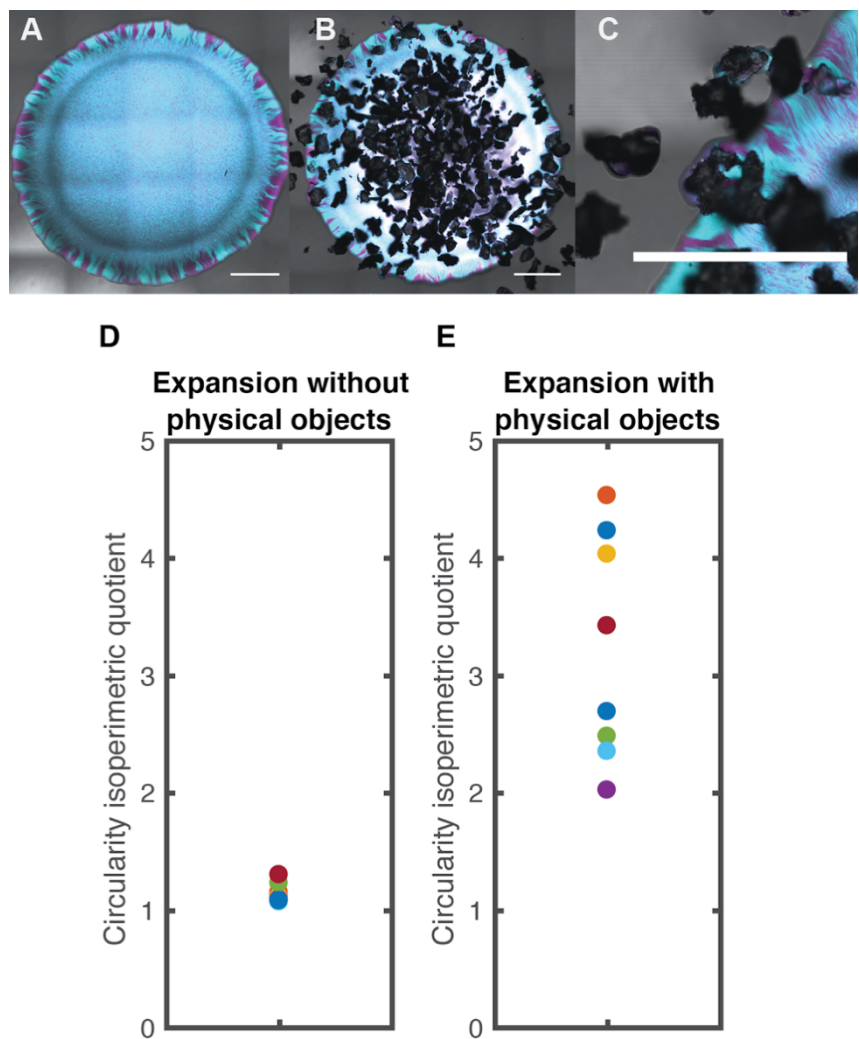


Figure 3. Circularity of the expansion frontier immediately after the addition of physical objects.

Patterns of spatial self-organization formed by pairs of complete reducers (1:1 initial cell number ratio) (competitive interaction) *A*) in the absence of physical objects or *B*) immediately after the addition of physical objects. One complete reducer carried the cyan fluorescent protein-encoding *ecfp* gene (shown in magenta) while the other carried the green fluorescent protein-encoding *egfp* gene (shown in green). The scale bars are equivalent to 1000 μm . The circularity isoperimetric quotients for range expansions *C*) in the absence of physical objects or *D*) immediately after the addition of physical objects.

We found that the addition of physical objects immediately created deformities along the expansion frontier. In the absence of physical objects, the expansion frontier slightly deviated from circular (Fig. 3A) with a mean circularity isoperimetric quotient among independent replicates of 1.14 ($\text{SD} = 0.081$, $n = 9$) (Fig. 3D). In the presence of physical objects, in contrast, the expansion frontier strongly

deviated from circular (Fig. 3B) with a mean circularity isoperimetric quotient among independent replicates of 3.22 ($SD = 0.96$, $n = 9$) (Fig. 3E). Overall, the addition of physical objects significantly increased the circularity isoperimetric quotient by nearly three-fold when compared to the absence of physical objects (two-sample two-sided t-test; $P = 3 \times 10^{-5}$, $n = 9$), indicating a significant increase in the perimeter-to-area ratio. Moreover, the presence of physical objects clearly created deformities along the expansion frontier that included both local regions of R_{SC} and R_{IC} (Fig. 3C). Thus, adding physical objects to the surface does indeed immediately create deformities along the expansion frontier.

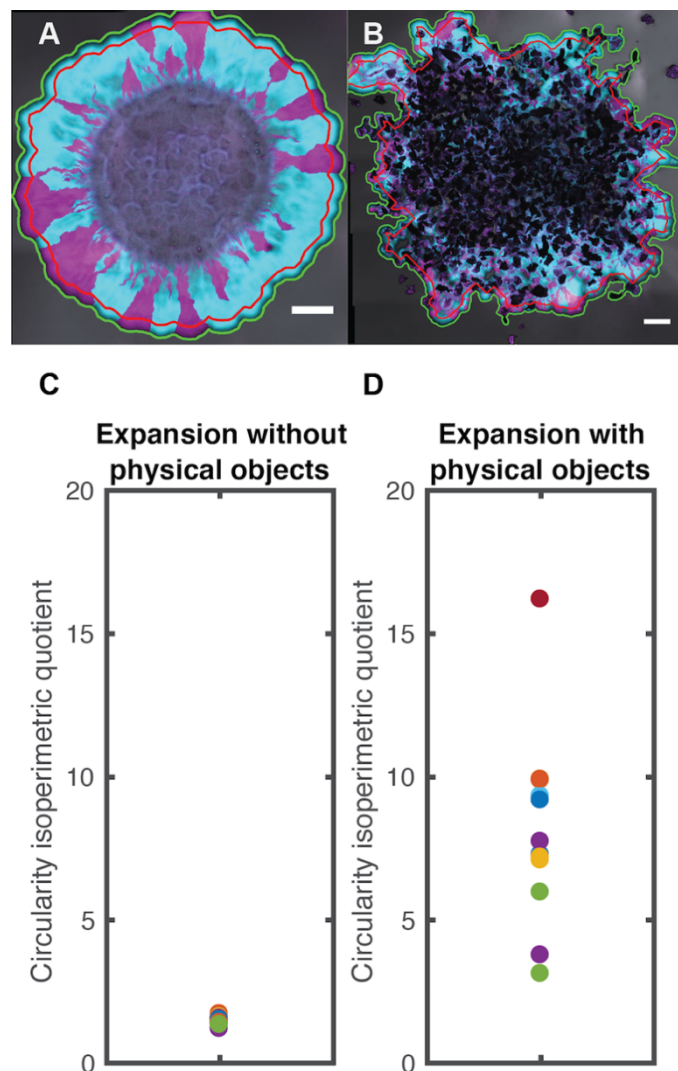


Figure 4. Circularity of the expansion frontier after two weeks of range expansion in the absence or presence of physical objects. Patterns of spatial self-organization formed by pairs of complete reducers (1:1 initial cell number ratio) (competitive interaction) after two weeks of range expansion *A*) in the absence of physical objects or *B*) in the presence of physical objects. One complete reducer carried the cyan fluorescent protein-encoding *ecfp* gene (shown in magenta) while the other carried the green fluorescent protein-encoding *egfp* gene (shown in green). The scale bars are equivalent to 1000 μm . The circularity isoperimetric quotients for range expansions of pairs of complete reducers ($n = 3$) and pairs of producer and consumer (1:1 initial cell number ratio) (nitrite cross-feeding interaction) ($n = 9$) *C*) in the absence of physical objects or *D*) immediately after the addition of physical objects.

We next tested whether deformities created immediately after the addition of physical objects persist as the communities expand across space. To accomplish this, we allowed pairs of complete

reducers (1:1 initial cell number ratio) ($n = 3$ without and with physical objects) or pairs of producer and consumer (1:1 initial cell number ratio) ($n = 9$ without and with physical objects) to expand for two weeks, interrogated the expansion frontier via microscopy, and quantified the shape of the expansion frontier. In the absence of physical objects, the expansion frontier continued to slightly deviate from circular (Fig. 4A) with a mean circularity isoperimetric quotient among independent replicates of 1.45 ($SD = 0.15$, $n = 12$) (Fig. 4C). In the presence of physical objects, in contrast, the expansion frontier strongly deviated from circular (Fig. 4B) with a mean circularity isoperimetric quotient among independent replicates of 8.04 ($SD = 3.3$, $n = 12$) (Fig. 4D). This latter value is significantly greater than the value observed immediately after the addition of physical objects (two-sample two-sided t-test; $P = 0.001$, $n_1 = 12$, $n_2 = 9$) (Fig. 3D). Overall, after two weeks of range expansion in the presence of physical objects, the circularity isoperimetric quotient significantly increased by more than five-fold when compared to range expansion in the absence of physical objects (two-sample two-sided t-test; $P = 9 \times 10^{-7}$, $n = 12$). Thus, the deformities created immediately after the addition of physical objects not only persist after the onset of range expansion, but also increase in magnitude during range expansion.

Effect of deformities on the general geometric shapes of spatial self-organization

We next tested whether the addition of physical objects affects the general geometric shapes of spatial self-organization that form as the communities expand across space. To accomplish this, we analyzed the geometric shapes of spatial self-organization that emerged after two weeks of range expansion using the same images obtained from the previously described experiment. Because we deposited physical objects both behind and in front of the initial expansion frontier (Fig. 3B) and allowed the communities to expand across space, deformities would be created that consist of local regions of R_{SC} (Fig. 1E) and R_{IC} (Fig. 1F) and by collisions with physical objects (Fig. 1G).

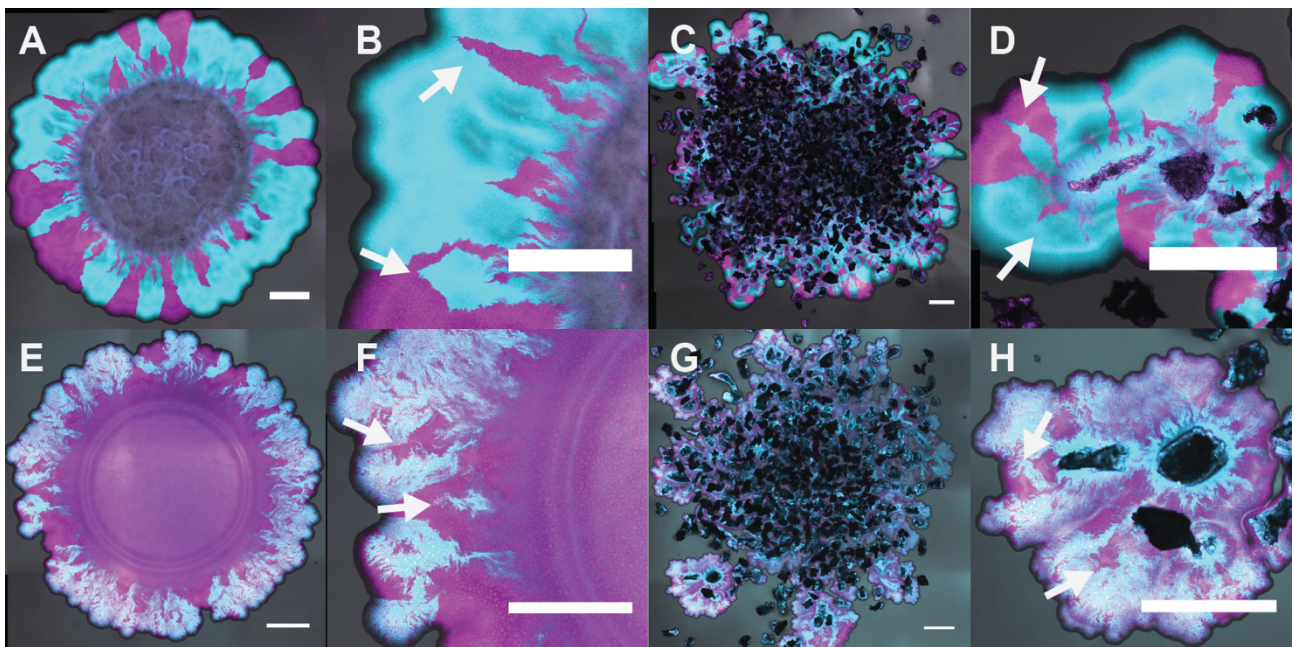


Figure 5. Effect of physical objects on the general geometric shapes of spatial self-organization.

Patterns of spatial self-organization formed by pairs of complete reducers (1:1 initial cell number ratio) (competitive interactions) after two weeks of range expansion *A-B*) in the absence of physical objects or *C-D*) in the presence of physical objects. One complete reducer carried the cyan fluorescent protein-encoding *ecfp* gene (shown in magenta) while the other carried the green fluorescent protein-encoding *egfp* gene (shown in green). Panels *B* and *D* are magnifications of panels *A* and *C*, respectively. Patterns of spatial self-organization formed by pairs of producer and consumer (1:1 initial cell number ratio) (nitrite cross-feeding interaction) after two weeks of range expansion *E-F*) in the absence of physical objects or *G-H*) in the presence of physical objects. The producer carried the cyan fluorescent protein-encoding *ecfp* gene (shown in magenta) while the consumer carried the green fluorescent protein-encoding *egfp* gene (shown in green). Panels *F* and *H* are magnifications of panels *E* and *G*, respectively. All scale bars are equivalent to 1000 µm. White arrows indicate events of stochastic boundary coalescence.

We first tested whether the deformities created by physical objects affect the general geometric shapes of spatial self-organization formed by pairs of complete reducers (1:1 initial cell number ratio) ($n = 3$ without and with physical objects). In the absence of physical objects, the two complete reducers rapidly segregated into sectors as they expanded and formed interspecific boundaries oriented approximately parallel to the axis of range expansion (Figs. 5*A* and 5*B*). This is consistent with our previously reported observations [22, 25] and with observations from similar experiments conducted with pairs of cell-types that have equivalent fitness [12, 14]. Moreover, the interspecific

boundaries underwent occasional stochastic boundary coalescence during range expansion (Fig. 5B, white arrows), indicating an increase in sector width and a reduction in interspecific mixing and diversity along the expansion frontier. In the presence of physical objects, the two complete reducers again rapidly segregated into sectors as they expanded and formed interspecific boundaries oriented approximately parallel to the axis of range expansion (Figs. 5C and 5D). As in the absence of physical objects, the interspecific boundaries also underwent occasional stochastic boundary coalescence during range expansion (Fig. 5D, white arrows), again indicating an increase in sector width and a reduction in interspecific mixing and diversity along the expansion frontier. Importantly, the geometric shapes of the sectors and interspecific boundaries were qualitatively similar regardless of whether physical objects were not or were present (Figs. 5B and 5D). Thus, deformities along the expansion frontier do not qualitatively affect the general geometric shapes of spatial self-organization formed by pairs of complete reducers.

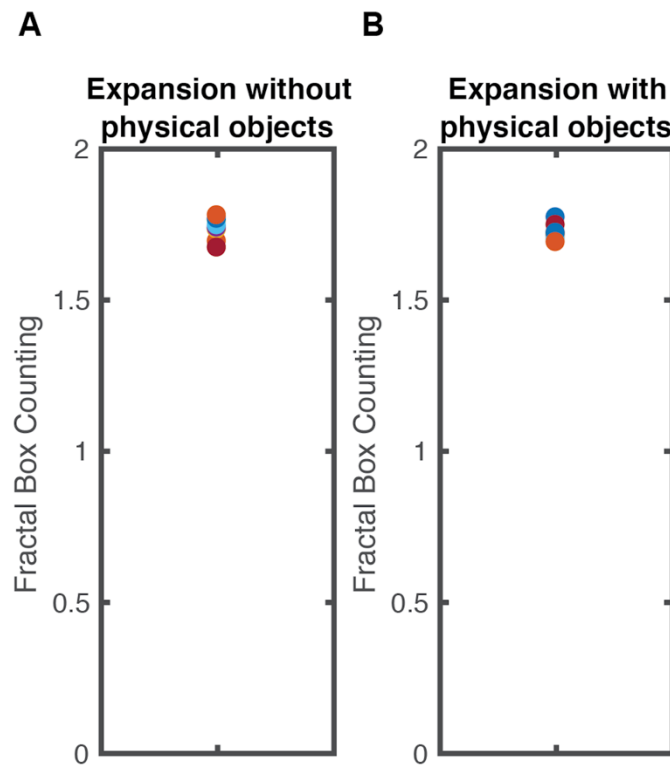


Figure 6. Fractal dimension of dendrites in the absence or presence of physical objects. The fractal dimension for pairs of producer and consumer (1:1 initial cell number ratio) (nitrite cross-feeding interaction) after two weeks of range expansion *A*) in the absence of physical objects or *B*) in the presence of physical objects. The fractal dimension was measured using the fractal box counting method.

We next tested whether the deformities created by physical objects affect the general geometric shapes of spatial self-organization formed by pairs of producer and consumer (1:1 initial cell number ratio) ($n = 9$ without and with physical objects). In the absence of physical objects, the producer and consumer did not form sectors but instead formed dendrites of the consumer that protruded into the producer (Figs. 5E and 5F), which is consistent with our previously reported observations [22, 25]. These dendrites tend to originate from single points in the inoculation area, increase in width during range expansion, and have interspecific boundaries that are not oriented parallel to the axis of range expansion (Fig. 5F), which are again features consistent with our previously reported observations [22, 25]. The dendrites display a fractal-like property with a mean fractal dimension among independent replicates of 1.73 ($SD = 0.034$, $n = 9$) (Fig. 6A), which is statistically indistinguishable from the fractal dimension for the dendrites described in our previous investigation with the same experimental system [22]. In the presence of physical objects, the producer and consumer again rapidly formed dendrites as they expanded (Fig. 5G and 5H).

Moreover, the mean fractal dimension of the dendrites formed in the presence of physical objects was 1.72 (SD = 0.024, n = 9) (Fig. 6B) and was statistically indistinguishable from the mean fractal dimension measured in the absence of physical objects (two-sample two-sided t-test; P = 0.33, n = 9) (Fig. 6). Thus, as with the general geometric shapes of spatial self-organization formed by pairs of complete reducers, deformities along the expansion frontier also do not affect the general geometric shapes of spatial self-organization formed by pairs of producer and consumer.

Effect of deformities on the density of interspecific boundaries

We next tested whether deformities created by physical objects affect the density of interspecific boundaries at the expansion frontier. The density of interspecific boundaries provides a measure of interspecific mixing and diversity along the expansion frontier. We chose to measure the density of interspecific boundaries rather than the absolute number of interspecific boundaries because the length of the expansion frontier dramatically increases in response to Nafion particles (Figs. 3 and 4). Thus, if we were to use the absolute number of interspecific boundaries, we would expect our experiments with Nafion particles to have more interspecific boundaries simply because of the longer expansion frontier. To achieve our objective, we first measured the numbers of interspecific boundaries after two weeks of range expansion using the same images obtained from the previously described experiment, all of which were conducted with pairs of complete reducers (1:1 initial cell number ratio) (n = 3 without and with physical objects) or with pairs of producer and consumer (1:1 initial cell number ratio) (n = 9 without and with physical objects). We then quantified the mean density of interspecific boundaries among independent replicates.

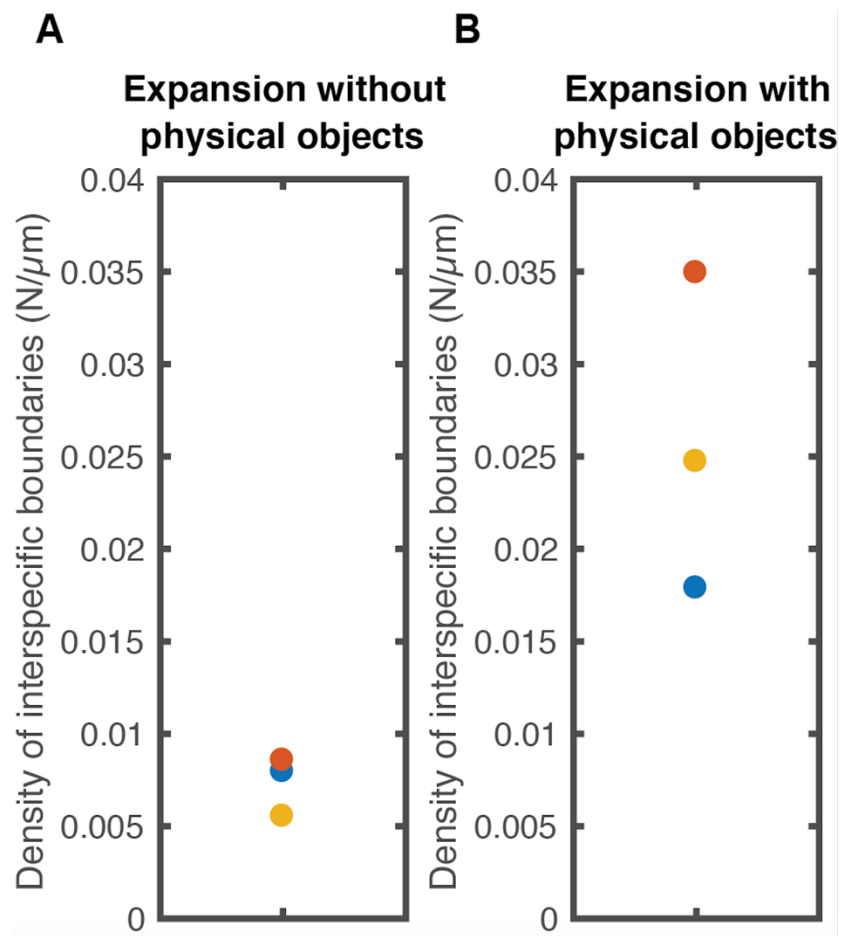


Figure 7. Density of interspecific boundaries for pairs of complete reducers (1:1 initial cell number ratio) (competitive interaction) in the absence or presence of physical objects. The density of interspecific boundaries is the number of boundaries per μM of expansion frontier after two weeks of range expansion. Densities are for range expansions *A*) in the absence of physical objects or *B*) in the presence of physical objects.

We first tested whether deformities created by physical objects affect the density of interspecific boundaries formed by pairs of complete reducers along the expansion frontier. We found that, in the absence of physical objects, the mean density of interspecific boundaries was 0.0073 boundaries per μm ($\text{SD} = 0.0016$, $n = 3$) (Fig. 7A). In the presence of physical objects, the mean density of interspecific boundaries was 0.0258 boundaries per μm ($\text{SD} = 0.0086$, $n = 3$) (Fig. 7B). Overall, we observed a significantly larger mean density of interspecific boundaries in the presence of physical objects than in the absence of physical objects (two-sample two-sided t-test; $P = 0.021$, $n = 3$) (Fig. 7). The theoretical considerations that we outlined in Fig. 1 predict that local regions R_{SC} should increase the density of interspecific boundaries along the expansion frontier (Fig. 1E) while local

regions of R_{IC} and particle collisions should both decrease the density of interspecific boundaries along the expansion frontier (Figs. 1F and 1G). Thus, because we experimentally observed that physical objects increase the density of interspecific boundaries along the expansion frontier, our results indicate that local regions of R_{SC} likely have the dominant effect while local regions of R_{IC} and collisions with physical objects likely have small effects on interspecific mixing, diversity, and spatial self-organization for pairs of complete reducers.

One alternative explanation for why physical objects might affect the density of interspecific boundaries for pairs of complete reducers (competitive interaction) along the expansion frontier is that physical objects also affect the initial cell density along the expansion frontier. Briefly, we used the same number of cells for experiments conducted without and with physical objects. The addition of physical objects, however, increased the length of the expansion frontier (*i.e.*, physical objects increased the circularity isoperimetric quotient [Fig. 3]). The initial cell density along the expansion frontier would therefore have been smaller, as the same number of cells were distributed along a longer length of frontier. The smaller initial cell density along the expansion frontier should have either no effect on [12] or result in a smaller number of interspecific boundaries [19]. However, we observed the opposite outcome, where physical objects increased rather than decreased the density of sectors along the expansion frontier. Thus, the effect of physical objects on the length of the expansion frontier, and thus on the initial cell density along the expansion frontier, cannot explain our results for pairs of complete reducers.

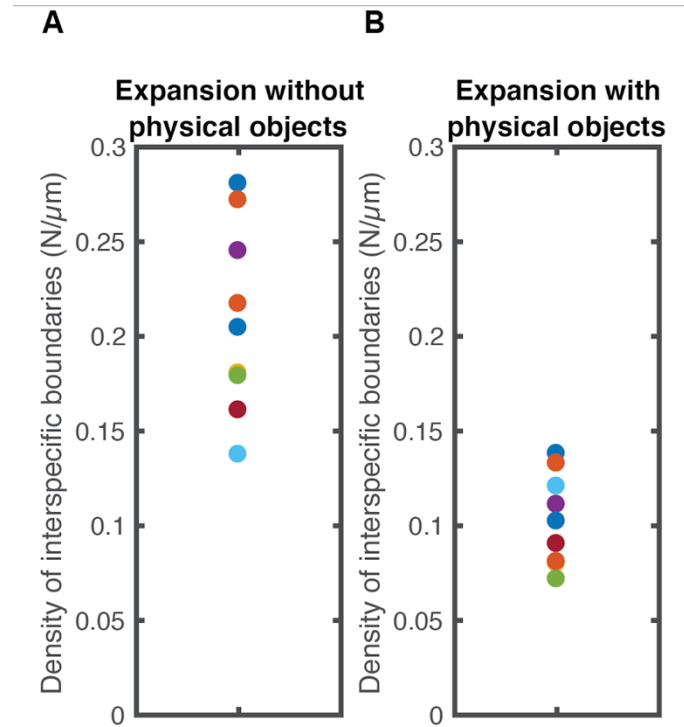


Figure 8. Density of interspecific boundaries for pairs of producer and consumer (1:1 initial cell number ratio) (nitrite cross-feeding interaction) in the absence or presence of physical objects.

The density of interspecific boundaries is the number of boundaries per μM of expansion frontier after two weeks of range expansion. Densities are for range expansions *A*) in the absence of physical objects or *B*) in the presence of physical objects.

We finally tested whether deformities created by physical objects affect the density of interspecific boundaries formed by pairs of producer and consumer along the expansion frontier. We found that, in the absence of physical objects, the mean density of interspecific boundaries was 0.208 boundaries per μm ($\text{SD} = 0.050$, $n = 9$) (Fig. 8A). In the presence of physical objects, the mean density of interspecific boundaries was 0.103 boundaries per μm ($\text{SD} = 0.024$, $n = 9$) (Fig. 8B). Overall, we observed a significantly smaller mean density of interspecific boundaries in the presence of physical objects than in the absence of physical objects (two-sample two-sided t-test; $P = 3 \times 10^{-5}$, $n = 9$) (Fig. 8), which is qualitatively opposite to what we observed for pairs of complete reducers (Fig. 7). Again, the theoretical considerations that we outlined in Fig. 1 predict that local regions R_{SC} should increase the density of interspecific boundaries along the expansion frontier (Fig. 1E) while local regions of R_{IC} and particle collisions should both decrease the density of interspecific boundaries along the expansion frontier (Fig. 1F and 1G). Thus, because we experimentally observed that physical objects decrease the density of interspecific boundaries along the expansion frontier, our results indicate

that local regions of R_{SC} have relatively small effects while local regions of R_{IC} and/or collisions with physical objects likely have the dominant effects on interspecific mixing, diversity, and spatial self-organization for pairs of producer and consumer.

DISCUSSION

We show here that physical objects can have important effects on the interspecific mixing, diversity, and spatial self-organization of microbial communities. Perhaps surprisingly, the effects of physical objects on the density of interspecific boundaries depends on the type of interaction that occurs between the resident cell-types. Competitive interactions that promote segregation and the formation of sectors with interspecific boundaries oriented approximately parallel to the axis of range expansion are positively affected by physical objects, where physical objects result in increased numbers of interspecific boundaries (Fig. 7). Conversely, cross-feeding interactions that promote the formation of dendrites with interspecific boundaries not oriented parallel to the axis of range expansion are negatively affected by physical objects, where physical objects result in decreased numbers of interspecific boundaries (Fig. 8). Thus, in order to make even qualitative predictions regarding the effects of physical objects on interspecific mixing, one needs information regarding the interactions that are present within a community and the general geometric shapes of spatial self-organization likely to emerge from those interactions.

Why do physical objects have interaction-dependent effects on interspecific mixing within microbial communities? One plausible explanation is that different interactions result in different orientations of the interspecific boundaries [22, 25]. Consider local regions of R_{SC} formed by physical objects (Fig. 1E). We expect these local regions to have potentially profound effects at preventing or delaying the coalescence of interspecific boundaries formed by competitive interactions. Briefly, when the competing cell-types have equivalent fitness, sectors form and the boundaries are oriented approximately parallel to the axis of range expansion [12, 14] (Figs. 2 and 5). Stochastic processes then act on the boundaries resulting in a random walk-like behavior [12, 14]. Given sufficient time, this random walk-like behavior can result in the stochastic coalescence of neighboring boundaries [12, 14] (Fig. 5). Local regions of R_{SC} increase the angle between these neighboring boundaries (Fig. 1E), which would decrease the probability of stochastic boundary coalescence [51]. In contrast, we expect local regions of R_{SC} to have relatively small effects at preventing the coalescence of the

interspecific boundaries formed by cross-feeding interactions. Cross-feeding interactions promote the formation of dendrites that do not have boundaries oriented parallel to the axis of range expansion. Instead, the boundaries diverge from each other as the dendrites expand across space [22, 25] (Figs. 2 and 5). Because the boundaries are not oriented parallel to the axis of range expansion, a subset of the neighboring boundaries will inevitably be oriented towards coalescence regardless of the radius of curvature of the expansion frontier. Thus, interactions that form interspecific boundaries oriented parallel to the axis of range expansion will be more affected by local regions of R_{SC} than interactions that form interspecific boundaries not oriented parallel to the axis of range expansion, thus providing an explanation for why local regions of R_{SC} have larger effects for pairs of complete reducers (competitive interaction) than for pairs of producer and consumer (nitrite cross-feeding interaction).

Similar arguments can be made for local regions of R_{IC} formed by physical objects (Fig. 1F). We expect these local regions to have smaller effects at promoting the coalescence of interspecific boundaries formed by competitive interactions than those formed by nitrite cross-feeding interactions. As discussed above, the boundaries formed by competitive interactions are oriented approximately parallel to the axis of range expansion [12, 14] (Figs. 2 and 5), and local regions of R_{IC} will inevitably orient them towards coalescence (Fig. 1F). However, it will take a relatively long period of time for coalescence to occur, as they nevertheless remain oriented parallel to the axis of range expansion. In contrast, the boundaries formed by nitrite cross-feeding interactions are not oriented parallel to the axis of range expansion [22, 25] (Figs. 2 and 5), and a subset of the neighboring boundaries will inevitably be oriented towards coalescence regardless of whether they occur within a local region of R_{IC} or not. If they are located within a local region of R_{IC} , these neighboring boundaries will be oriented even more sharply towards coalescence, thus resulting in a relatively short period of time for coalescence to occur. Thus, interactions that form interspecific boundaries oriented parallel to the axis of range expansion will be less affected by local regions of R_{IC} than interactions that form interspecific boundaries not oriented parallel to the axis of range expansion, thus providing another explanation for why local regions of R_{SC} have smaller effects for pairs of complete reducers (competitive interaction) than for pairs of producer and consumer (nitrite cross-feeding interaction).

What can our results tell us about the maintenance of diversity within microbial communities? We used the number of interspecific boundaries as a measure of diversity. Briefly, the number of interspecific boundaries is a proxy measure for how many individuals migrated out of the inoculation area and contributed to range expansion [12, 14]. If genetic heterogeneity occurs within populations, then more of that genetic heterogeneity will be maintained during range expansion as the number of interspecific boundaries increases. Thus, because physical objects affect the number of interspecific boundaries, physical objects also affect the diversity of microbial communities. Physical objects may therefore not only be an important determinant of spatial self-organization, but also be an important determinant of the diversity of spatially structured microbial communities.

Under what environmental conditions do we expect the presence of physical objects to have effects? We can address this question by considering what types of interactions are likely to occur under different environmental conditions. In our case, we investigated a linear metabolic pathway (*i.e.* denitrification) where a competitive interaction occurs between completely denitrifying strains while a cross-feeding interaction occurs between partially denitrifying strains. Importantly, previous theoretical studies predict that low substrate supply selects for completely consuming strains (and thus competitive interactions) while high substrate supply selects for partially consuming strains (and thus cross-feeding interactions) [61, 62]. Combined with these theoretical studies, our results therefore lead to the following prediction. In environments with low substrate supply, we expect competitive interactions to predominate. The presence of physical objects would then increase interspecific mixing and diversity along the expansion frontier. In contrast, in environments with high substrate supply, we expect cross-feeding interactions to predominate. The presence of physical objects would then decrease interspecific mixing and diversity along the expansion frontier. Importantly, this prediction is experimentally testable and generalizable across a wide variety of metabolic processes, environments, and microbial communities.

ACKNOWLEDGEMENTS

We thank Benedict Borer, Emanuel A. Fronhofer, Sara Mitri, Dani Or, and Jan Roelof van der Meer for helpful discussions.

REFERENCES

1. Davey ME, O'Toole GA. Microbial biofilms: from ecology to molecular genetics. *Microbiol. Mol. Biol. Rev.* 2000; **64**, 847–867.
2. Hall-Stoodley L, Costerton JW, Stoodley P. Bacterial biofilms: from the natural environment to infectious diseases. *Nat. Rev. Microbiol.* 2004; **2**, 95-108.
3. Kolter R, Greenberg EP. The superficial life of microbes. *Nature* 2006; **441**, 300–302.
4. Flemming HC, Wingender J, Szewzyk U, Steinberg P, Rice SA, Kjelleberg S. Biofilms: an emergent form of bacterial life. *Nat. Rev. Microbiol.* 2016; **14**, 563-575.
5. Flemming HC, Wuertz S. Bacteria and archaea on Earth and their abundance in biofilms. *Nat. Rev. Microbiol.* 2019; **17**, 247-260.
6. Asally M, Kittisopkul M, Rué P, Du Y, Hu Z, Çağatay T, Robinson AB, Lu H, Garcia-Ojalvo J, Süel GM. Localized cell death focuses mechanical forces during 3D patterning in a biofilm. *Proc. Natl. Acad. Sci. USA* 2012; **109**, 18891-18896.
7. Lloyd DP, Allen RJ. Competition for space during bacterial colonization of a surface. *J. R. Soc. Interface* 2015; **12**, 0608.
8. Delarue M, Hartung J, Schreck C, Gniewek P, Hu L, Herminghaus S, Hallatschek O. Self-driven jamming in growing microbial populations. *Nat. Phys.* 2016; **12**, 762-766.
9. Ghosh P, Mondal J, Ben-Jacob E, Levine H. Mechanically-driven phase separation in a growing bacterial colony. *Proc. Natl. Acad. Sci. USA* 2016; **112**, E2166-E2173.
10. Harshey RM. Bacterial motility on a surface: many ways to a common goal. *Annu. Rev. Microbiol.* 2003; **57**, 249-273.
11. Kerr B, Riley MA, Feldman MW, Bohannan BJM. Local dispersal promotes biodiversity in a real-life game of rock-paper-scissors. *Nature* 2002; **418**, 171-174.
12. Hallatschek O, Hersen P, Ramanathan S, Nelson DR. Genetic drift at expanding frontiers promotes gene segregation. *Proc. Natl. Acad. Sci. USA* 2007; **104**, 19926-19930.
13. Kim HJ, Boedicker JQ, Choi JW, Ismagilov RF. Defined spatial structure stabilizes a synthetic multispecies bacterial community. *Proc. Natl. Acad. Sci. USA* 2008; **105**, 18188-18193.
14. Hallatschek O, Nelson DR. Life at the front of an expanding population. *Evol.* 2010; **64**, 193-206.
15. Momeni B, Brileya KA, Fields MW, Shou W. Strong inter-population cooperation leads to partner intermixing in microbial communities. *eLife* 2013; **2**, e00230.

16. Momeni B, Waite AJ, Shou W. Spatial self-organization favors heterotypic cooperation over cheating. *eLife* 2013; **2**, e00960.
17. Rudge TJ, Federici F, Steiner PJ, Kan A, Haseloff J. Cell polarity-driven instability generates self-organized, fractal patterning of cell layers. *ACS Synth. Biol.* 2013; **2**, 705-714.
18. Müller MJ, Neugeboren BI, Nelson DR, Murray AW. Genetic drift opposes mutualism during spatial population expansion. *Proc. Natl. Acad. Sci. USA* 2014; **111**, 1037–1042.
19. van Gestel J, Weissing FJ, Kuipers OP, Kovács AT. Density of founder cells affects spatial pattern formation and cooperation in *Bacillus subtilis* biofilms. *ISME J.* 2014; **8**, 2069-2079.
20. Mitri S, Clarke E, Foster KR. Resource limitation drives spatial organization in microbial groups. *ISME J.* 2015; **10**, 1471-1482.
21. Nadell CD Xavier JB, Foster KR. The sociobiology of biofilms. *FEMS Microbiol. Rev.* 2009; **33**, 206–224.
22. Goldschmidt F, Regoes RR, Johnson DR. Successive range expansion promotes diversity and accelerates evolution in spatially structured microbial populations. *ISME J.* 2017; **11**, 2112-2123.
23. Tecon R, Or D. Cooperation in carbon source degradation shapes spatial self-organization of microbial consortia on hydrated surfaces. *Sci. Rep.* 2017; **7**, 43726.
24. Giometto A, Nelson DR, Murray AW, Physical interactions reduce the power of natural selection in growing yeast colonies. *Proc. Natl. Acad. Sci. USA* 2018; **115**, 11448-11453.
25. Goldschmidt F, Regoes RR, Johnson DR. Metabolite toxicity slows local diversity loss during expansion of a microbial cross-feeding community. *ISME J.* 2018; **12**, 136-144.
26. Ben-Jakob E, Shmueli H, Shochet O, Tenenbaum A. Adaptive self-organization during growth of bacterial colonies. *Physica A* 1992; **187**, 378-424.
27. Rohani P, Lewis TJ, Grünbaum D, Ruxton GD. Spatial self-organization in ecology: pretty patterns or robust reality? *Trends Ecol. Evol.* 1997; **12**, 70-74.
28. Ben-Jakob E. Bacterial self-organization: co-enhancement of complexification and adaptability in a dynamic environment. *Philos. Trans. A Math Phys. Eng. Sci.* 2003; **361**, 1283-312.
29. Solé RV, Bascompte J. Self-organization in complex ecosystems. Princeton University Press, Princeton, NJ. 2006
30. Lion S, Baalen MV. Self-structuring in spatial evolutionary ecology. *Ecol. Lett.* 2008; **11**, 277-295.
31. Rietkerk M, van de Koppel J. Regular pattern formation in real ecosystems. *Trends Ecol. Evol.* 2008; **23**, 169–75.

32. Brenner K, Arnold FH. Self-organization, layered structure, and aggregation enhance persistence of a synthetic biofilm consortium. *PLOS One* 2011; **6**, e16791.
33. Bernstein HC, Paulson SD, Carlson RP. Synthetic *Escherichia coli* consortia engineered for syntrophy demonstrate enhanced biomass productivity. *J. Biotechnol.* 2012; **157**, 159-166.
34. Drescher K, Nadell CD, Stone HA, Wingreen NS, Bassler BL. Solutions to the public goods dilemma in bacterial biofilms. *Curr. Biol.* 2014; **24**, 50–55.
35. Røder HL, Sørensen SJ, Burmølle M. Studying bacterial multispecies biofilms: where to start? *Trends Microbiol.* 2016; **24**, 503-513.
36. Kindaichi T, Tsushima I, Ogasawara Y, Shimokawa M, Ozaki N, Satoh H, Okabe S. *In situ* activity and spatial organization of anaerobic ammonium-oxidizing (anammox) bacteria in biofilms. *Appl. Environ. Microbiol.* 2007; **73**, 4931-4939.
37. Satoh H, Miura Y, Tsushima I, Okabe S. Layered structure of bacterial and archaeal communities and their *in situ* activities in anaerobic granules. *Appl. Environ. Microbiol.* 2007; **73**, 7300-7307.
38. Breugelmans P, Barken KB, Tolker-Nielsen T, Hofkens J, Dejonghe W, Springael D. Architecture and spatial organization in a triple-species bacterial biofilm synergistically degrading the phenylurea herbicide linuron. *FEMS Microbiol. Ecol.* 2008; **64**, 271-282.
39. Estrela S, Libby E, Van Cleve J, Débarre F, Deforet M, Harcombe WR, Peña J, Brown SP, Hochberg ME. Environmentally mediated social dilemmas. *Trends Ecol. Evol.* 2019; **34**, 6-18.
40. Vega NM, Gore J. Collective antibiotic resistance: mechanisms and implications. *Curr. Opin. Microbiol.* 2014; **21**, 28-34.
41. Estrela S, Brown SP. Community interactions and spatial structure shape selection on antibiotic resistant lineages. *PLOS Comput. Biol.* 2018; **14**, e1006179.
42. Frost I, Smith WPJ, Mitri S, Milan AS, David Y, Osborne JM, Pitt-Francis JM, MacLean RC, Foster KR. Cooperation, competition and antibiotic resistance in bacterial colonies. *ISME J.* 2018; **12**, 1582-1593.
43. Xavier JB, Martinez-Garcia E, Foster KR. Social evolution of spatial patterns in bacterial biofilms: when conflict drives disorder. *Am. Nat.* 2009; **174**, 1-12.
44. Madsen JS, Burmølle M, Hansen LH, Sørensen SJ. The interconnection between biofilm formation and horizontal gene transfer. *FEMS Immunol. Med. Microbiol.* 2012; **65**, 183-195.
45. Gralka M, Hallatschek O. Environmental heterogeneity can tip the population genetics of range expansions. *eLife* 2019; **8**, e44359.
46. Gralka M, Stiewe F, Farrel F, Möbius W, Waclaw B, Hallatschek O. Allele surfing promotes

- microbial adaptation from standing variation. *Ecol. Lett.* 2016; **19**, 889-898.
47. Elias S, Banin E. Multi-species biofilms: living with friendly neighbors. *FEMS Microbiol. Rev.* 2012; **36**, 990-1004.
48. Burton OJ, Travis JMJ. Landscape structure and boundary effects determine the fate of mutations occurring during range expansion. *Heredity* 2008; **101**, 329-340.
49. Wang G, Or D. Trophic interactions induce spatial self-organization of microbial consortia on rough surfaces. *Sci. Rep.* 2014; **4**, 6757.
50. Möbius W, Murray AW, Nelson DR. How obstacles perturb population fronts and alter their genetic structure. *PLOS Comput. Biol.* 2015; **11**, e1004615.
51. Beller DA, Alards KMJ, Tesser F, Mosna RA, Toschi F, Möbius W. Evolution of populations expanding on curved surfaces. *EPL* 2018; **123**, 58005.
52. Borer B, Tecon R, Or D. Spatial organization of bacterial populations in response to oxygen and carbon counter-gradients in pore networks. *Nat. Comm.* 2018; **9**, 769.
53. Croft HT, Falconer KJ, Guy RK. Unresolved Problems in Geometry. Springer-Verlag, New York, NY 1991.
54. Lilja EE, Johnson DR. Segregating metabolic processes into different microbial cells accelerates the consumption of inhibitory substrates. *ISME J.* 2016; **10**, 1568-1578.
55. Lilja EE, Johnson DR. Metabolite toxicity determines the pace of molecular evolution within microbial populations. *BMC Evol. Biol.* 2017; **17**, 52.
56. Lilja EE, Johnson DR. Substrate cross-feeding affects the speed and trajectory of molecular evolution within a synthetic microbial assemblage. *BMC Evol. Biol.* 2019; **19**, 129.
57. Leis AP, Schlicher S, Franke H, Strathmann M. Optically transparent porous medium for nondestructive studies of microbial biofilm architecture and transport dynamics. *Appl. Environ. Microbiol.* 2005; **71**, 4801–4808.
58. Downie H, Holden N, Otten W, Spiers AJ, Valentine TA, Dupuy LX. Transparent soil for imaging the rhizosphere. *PLOS One* 2012; **7**, e44276.
59. Drescher K, Shen Y, Bassler BL, Stone HA. Biofilm streamers cause catastrophic disruption of flow with consequences for environmental and medical systems. *Proc. Natl. Acad. Sci. USA* 2013; **110**, 4345–4350.
60. Meier P, Berndt C, Weger N, Wackernagel W. Natural transformation of *Pseudomonas stutzeri* by single-stranded DNA requires type IV pili, competence state and *comA*. *FEMS Microbiol. Lett.* 2002; **207**, 75-80.

61. Pfeiffer T, Bonhoeffer S. Evolution of cross-feeding in microbial populations. *Am. Nat.* 2004; **163**, E126-135.
62. Costa E, Pérez J, Kreft JU. Why is metabolic labour divided in nitrification? *Trends Microbiol.* 2006; **14**, 213-219.

CHAPTER 6: The strength of a metabolic interaction determines the establishment, proliferation, and spatial organization of local microbial populations

Ciccarese Davide, Vulin Clément, Borer Benedict, Or Dani, Johnson R David

ABSTRACT

Metabolic interactions are important determinants of microbial community assembly, functioning and behavior. However, it is unclear how the strength of a metabolic interaction affects the spatial organization of microbial communities. Here, we used a synthetic microbial community consisting of two nitrite (NO_2^-) cross-feeding genotypes to study how interaction strength affects the establishment and proliferation of individuals. We imposed a strong mutualism between the two genotypes by growing them at pH 6.5 where nitrite is strongly toxic. In this case, one strain produces nitrite while the other strain consumes nitrite and detoxifies the local environment. We imposed a weak mutualism between the two genotypes by growing them at pH 7.5 where nitrite is relatively non-toxic. In this case, one strain produces nitrite while the other strain consumes nitrite, but this does not provide any benefits to the producing strain. We found that the number of individuals that develop into colonies, colony size, and interspecific distance to the nearest neighbor all depend on interaction strength. However, the number of colonies and the interspecific distance are determined by the mutualistic component of the interaction while colony size is determined by the competitive component of the interaction. Our results highlight that net interactions include multiple components (i.e. mutualism and competition), and these individual components can change in predominance and affect different community properties.

INTRODUCTION

Ecological communities consist of individuals that interact with each other [1–7]. These interactions are typically mediated by molecules, where individuals may release, consume, or respond to a molecule produced by another individual [8–10]. Such molecule-mediated interactions could occur across a range of spatial scales depending on the production, consumption, and mass transfer (*i.e.*, diffusion, advection, *etc.*) of the molecules, ranging from interacting with its nearest neighbor to interacting with a spatially distant member of the community [3, 11–17]. Importantly, these molecule-mediated interactions can be important determinants of the emergent properties of the community as a whole, where they can determine the spatial organization of the community, enable community-level functions, and modulate community-level stability and resilience [10, 16, 18–23].

Here, we propose that the distance between interacting individuals is an emergent property itself of a microbial community [24–26]. As an example, consider the random inoculation of individuals of two cell-types across a surface, where one cell-type produces a molecule (referred to as the producer) that is toxic to itself but a nutrient for another cell-type (referred to as the consumer). Under mass transfer-limited conditions, only those consumers located within a threshold distance from a producer will receive sufficient amounts of the molecule to proliferate and divide. Conversely, only those producers located within a threshold distance from a consumer will receive sufficient amounts of localized detoxification to proliferate and divide. Thus, while the initial distribution of interspecific distances between individuals of the producer and consumer will be determined by the initial inoculation process, the distribution of interspecific distances will change as individuals with advantageous distances proliferate and displace those with disadvantageous distances. We refer to the change in the distribution of interspecific distances as a community process and the final distribution of interspecific distances as an emergent community property [22, 27, 28].

We tested this hypothesis using a synthetic microbial community consisting of two cross-feeding strains of the bacterium *Pseudomonas stutzeri* A1501. One strain reduces nitrate (NO_3^-) to nitrite (NO_2^-) (referred to as the producer) while the other strain consumes the released nitrite [29, 30]. At pH 6.5, nitrite has toxic effects. Thus, the consumer depends on the producer to provide its growth-limiting nutrient nitrite while the producer depends on the consumer to consume nitrite

and mitigate its toxic effects (referred to as a strong mutualism). The maximum interspecific distance that still supports growth and proliferation is the distance that provides sufficient nitrite to the consumer while also enabling consumption of nitrite below inhibitory levels. Thus, the system consists of a metabiosis, where one cell type creates a favorable environment for other cell types to grow [31]. At pH 7.5, however, nitrite has no observable toxic effects. Thus, the consumer depends on the producer to provide its growth-limiting nutrient nitrite but the producer does not depend on the consumer (referred to as a weak mutualism). The maximum interspecific distance that still supports growth and proliferation is therefore simply the distance that provides sufficient nitrite to the consumer. Using this system, we propagated the microbial communities at pH 6.5 (*i.e.*, where nitrite is highly toxic and a strong mutualism occurs) and 7.5 (*i.e.*, where nitrite is relatively non-toxic and a weak mutualism occurs) on agar plates and measured the consequences on the ability to form colonies, colony sizes, and the emergent interspecific distances.

MATERIALS AND METHODS

Bacterial strains

The two strains that compose the trophically interacting consortium are isogenic mutants of the bacterium *Pseudomonas stutzeri* A1501 [29, 30]. The strain referred to as the producer has a loss-of-function deletion in the *nirS* gene and cannot reduce nitrite (NO_2^-) to nitrous oxide (N_2O). The interacting counterpart, which is referred to as consumer, has a loss-of function deletion in the *narG* gene and cannot reduce nitrate (NO_3^-) to nitrite. Under anaerobic conditions with nitrate as the growth-limiting resource, the two strains engage in a mutualistic interaction [29, 30]. The producer provides nitrite to the consumer while the consumer removes nitrite from the system. At pH 6.5, nitrite is highly toxic, and we therefore refer to the interaction as a strong mutualism [29, 30]. At pH 7.5, in contrast, nitrite is relatively non-toxic, and we therefore refer to the interaction as a weak mutualism [29, 30]. Details of the methods to delete *narG* and *nirS* are described in detail elsewhere [30]. To avoid natural transformation and recombination between the strains when grown together, both strains carry a loss-of-function deletion of the gene *comA* [30]. Finally, to distinguish the two strains when grown together, the strains carry either an IPTG-inducible green or cyan fluorescent protein-encoding gene [29, 32].

Colony forming unit experiment

We performed a colony forming unit (CFU) experiment with agar plates containing 20 ml of a modified version of a defined asparagine-citrate synthetic medium (ACS medium) [30]. The modifications include the following additions: 1mM sodium nitrate (NaNO_3), 22 mM citrate, 10 $\mu\text{g ml}^{-1}$ gentamicin, 0.1 mM IPTG, and agar to a final concentration of 2% (w/v). We adjusted the pH of the medium with 1 M HCl or 0.5 M NaOH to either pH 6.5 or 7.5.

To perform the CFU experiment, we first grew the producer and consumer separately in aerobic ACS liquid medium overnight in a shaking incubator at 37°C at 220 rpm until reaching stationary phase. We then centrifuged the cultures for eight minutes at 7000 rpm at room temperature, discarded the supernatants, and suspended the cells in saline solution (0.89% NaCl, v/w) to reach an optical density of 1 at 600 nm (OD_{600}). We next mixed the producer and consumer suspensions together to a ratio of 1:1, diluted the mixtures by 10^5 , and spread 50 μl of the diluted mixtures onto the surfaces of agar plates using sterile hockey sticks (Lazy-L Spreader, Sigma Aldrich). Finally, we incubated the agar plates for one week at room temperature (~21°C) in a glove box (Coy Laboratory Products, Grass Lake, USA) containing an anaerobic nitrogen (N_2):hydrogen (H_2) atmosphere (97:3). In total, we performed five replicates for each interaction strength (strong mutualism at pH 6.5 and weak mutualism at pH 7.5). We decided on one week of incubation because no further colonies developed after that time.

Microscopy and image analysis

We imaged the agar plates using a Leica TCS SP5 II confocal microscope mounted with an HCX FL Plan 2.5x/0.07na Objective (Etzlar, Germany) with settings as described in detail elsewhere [32]. We scanned over the entire plate surface at the end of one week of incubation. We exposed the plates to aerobic conditions for 1 h before acquiring images in order to allow the maturation of the fluorescent proteins [32]. After image acquisition, we first segmented the images in ilastik-1.2 [33] and measured the spatial positioning, centroids, and sizes of colonies in KNIME 3.5.3 (<https://www.knime.com/>). We estimated colony size as the colony radius. We plotted all data in Matlab R2017a and R [34] using the coordinates of the centroids of the colonies.

Statistical analyses

We performed all statistical analyses using Matlab R2017a and R studio [34]. We used the two-sample two-sided t-test for all pairwise comparisons. We report the sample size, the exact P, and the statistical methods used for each test in the results section. We considered $P < 0.05$ to be statistically significant.

RESULTS

Effect of interaction strength on the relative abundances of producer and consumer CFUs.

We first tested whether interaction strength affects the relative abundances of producer and consumer CFUs that successfully develop across the inoculation area. To test this, we mixed the producer and consumer together at an initial ratio of 1:1 (cell number/cell number) and inoculated them onto replicated agar plates at pH 6.5 (strong mutualistic conditions) or pH 7.5 (weak mutualistic conditions) ($n = 5$ each). Our expectations are four-fold. First, if the producer strongly depends on the consumer to remove nitrite (*i.e.*, when grown at pH 6.5 where nitrite is highly toxic and a strong mutualism occurs), then only those producer CFUs located within close spatial proximity of a consumer CFU can grow. We therefore expect a smaller relative CFU abundance of the producer at pH 6.5. Second, if the producer only weakly depends on the consumer to remove nitrite (*i.e.*, when grown at pH 7.5 where nitrite is relatively non-toxic and a weak mutualism occurs), then all producer CFUs can grow regardless of whether they are in close spatial proximity of a consumer CFU or not. We therefore expect a larger relative CFU abundance of the producer at pH 6.5. Third, at pH 6.5 where nitrite is highly toxic and a strong mutualism occurs, the producer cannot grow without the consumer. We therefore expect approximately equivalent relative CFU abundances of the producer and consumer. Finally, at pH 7.5 where nitrite is relatively non-toxic and a weak mutualism occurs, the producer can grow without the consumer. We therefore expect the relative CFU abundance of the producer to be greater than that for the consumer.

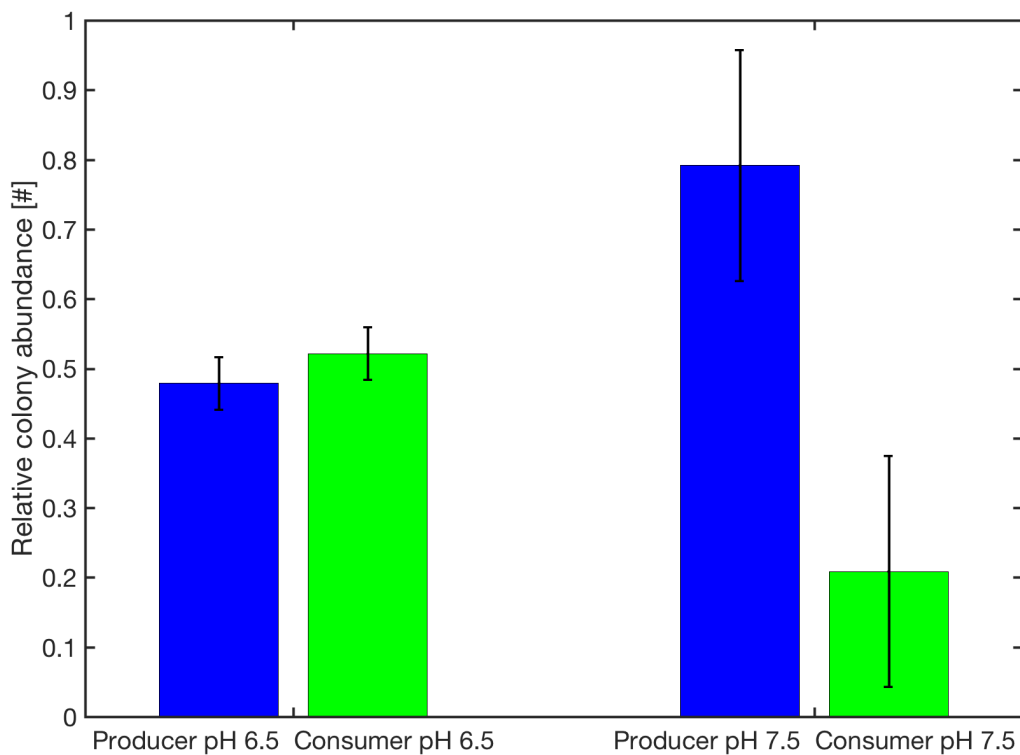


Figure 1. Relative abundances of producer and consumer CFUs. At pH 6.5 (strong mutualistic conditions), the producer achieves a mean relative CFU abundance of 0.5 ($SD = 0.04$, $n = 5$) while the consumer also achieves a mean relative CFU abundance of 0.5 ($SD = 0.04$, $n = 5$). At pH 7.5 (weak mutualistic conditions), the producer achieves a mean relative CFU abundance of 0.8 ($SD = 0.2$, $n=5$) while the consumer achieves a mean relative CFU abundance of 0.2 ($SD = 0.2$, $n=5$).

Our results support all four of these expectations. To address the first two expectations, we found that the relative CFU abundance of the producer is smaller at pH 6.5 (*i.e.*, where nitrite is highly toxic and a strong mutualism occurs) than at pH 7.5 (*i.e.*, where nitrite is highly toxic and a strong mutualism occurs) (Fig. 1). The producer attained a mean relative CFU abundance of 0.5 ($SD = 0.04$, $n = 5$) at pH 6.5 and a mean relative CFU abundance of 0.8 ($SD = 0.2$, $n = 5$) at pH 7.5 (Fig. 1), and these two means are significantly differ from each other (two-sample two-sided t-test; $P = 0.0034$, $n = 5$). To address the third expectation, we found that the producer and consumer attained equivalent relative CFU abundances at pH 6.5 (*i.e.*, where nitrite is highly toxic and a strong mutualism occurs) (Fig. 1). The producer attained a mean relative CFU abundance of 0.5 ($SD = 0.04$, $n = 5$) while the consumer also attained a mean relative CFU abundance of 0.5 ($SD = 0.04$, $n = 5$) (Fig. 1), and these two means do not significantly differ from each other (two-sample two-sided t-test; P

$= 0.1$, $n = 5$). To address the fourth expectation, we found that the producer attained a larger relative CFU abundance than the consumer at pH 7.5 (*i.e.*, where nitrite is relatively non-toxic and a weak mutualism occurs) (Fig. 1). The producer attained a mean relative CFU abundance of 0.8 (SD = 0.2, $n = 5$) while the consumer also attained a mean relative CFU abundance of 0.2 (SD = 0.2, $n = 5$) (Fig. 1), and these two means significantly differ from each other (two-sample two-sided t-test; $P = 5 \times 10^{-4}$, $n = 5$). Thus, our data demonstrate that interaction strength determines the relative CFU abundances of metabolically-interacting strains, where fewer individuals of the producer are able to develop into CFU as nitrite toxicity increases.

Effect of interaction strength on the sizes of producer and consumer CFUs

We next tested whether interaction strength affects the sizes of the producer and consumer CFUs that successfully develop across the inoculation area from the same experiment described above. Here, our expectation is three-fold. First, because fewer producer CFUs develop at pH 6.5 (*i.e.*, where nitrite is highly toxic and a strong mutualism occurs) than at pH 7.5 (*i.e.*, where nitrite is relatively non-toxic and a weak mutualism occurs) (Fig. 1), there are also more resources available per producer CFU at pH 6.5 than at pH 7.5. We therefore expect the size of the producer CFUs to be larger at pH 6.5 than at pH 7.5. Second, the biomass yields from reducing nitrate (NO_3^-) to nitrite (NO_2^-) or nitrite to nitrous oxide are approximately equivalent (both reduction steps accept two electrons), and the reduction of one mol of nitrate produces one mol of nitrite [35]. Assuming all the nitrogen oxides are consumed, we expect the sizes of the producer and consumer CFUs that develop at pH 6.5 (*i.e.*, where nitrite is highly toxic and a strong mutualism occurs) to be equivalent. This is because there are equivalent numbers of producer and consumer CFUs under these conditions (Fig. 1), and there are therefore equivalent amounts of resources available per CFU for the producer and consumer. Third, we expect the sizes of the producer CFUs to be smaller than the sizes of the consumer CFUs at pH 7.5 (*i.e.*, where nitrite is relatively non-toxic and a weak mutualism occurs). This is because there are larger numbers of producer CFUs than consumer CFUs under these conditions, and there are therefore less resources available per producer CFU than per consumer CFU (Fig. 2).

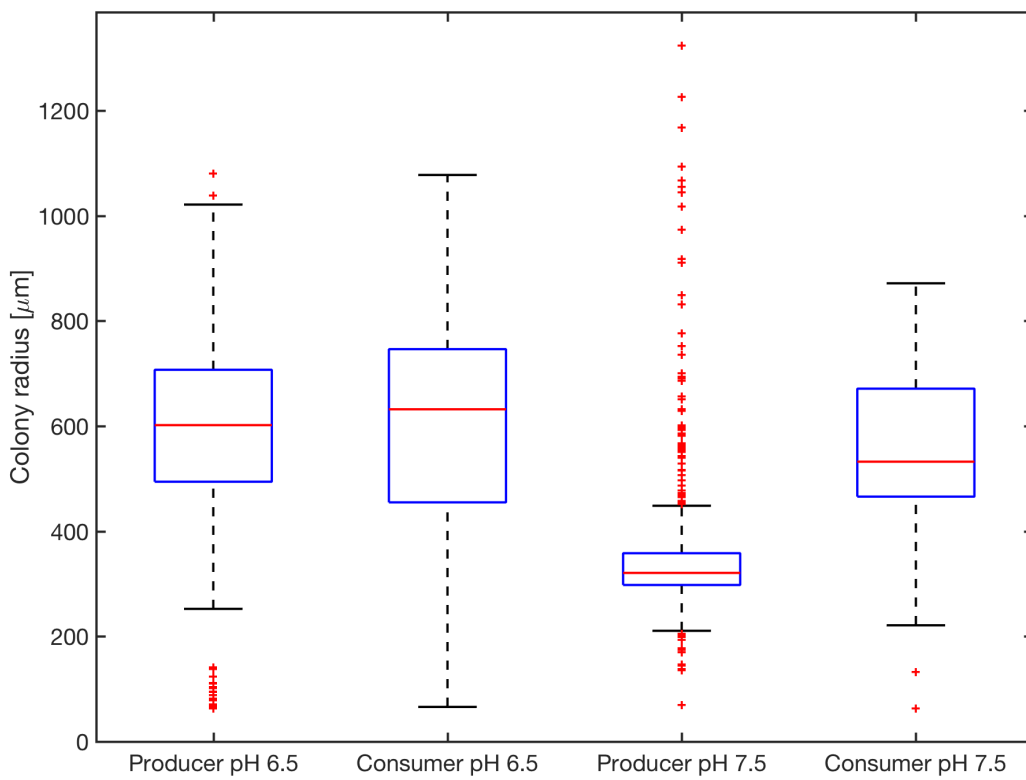


Figure 2. Sizes of producer and consumer CFUs. At pH 6.5 (strong mutualistic conditions), the producer CFUs have a mean radius of 579.1 μm ($\text{SD} = 204 \mu\text{m}$, $n = 287$) while the consumer CFUs have a similar mean radius of 603.7 μm ($\text{SD} = 205.9 \mu\text{m}$, $n = 313$). At pH 7.5 (weak mutualistic conditions), the producer CFUs have a mean radius = 355.8 μm ($\text{SD} = 138.6 \mu\text{m}$, $n = 566$) while the consumer CFUs have a larger mean radius of 555.1 μm ($\text{SD} = 132.8 \mu\text{m}$, $n = 119$). Data are presented as Tukey boxplots.

Our results again support all three of these expectations. To address the first expectation, we found that the size of producer CFUs at pH 6.5 (*i.e.*, where nitrite is highly toxic and a strong mutualism occurs) is larger than that at pH 7.5 (*i.e.*, where nitrite is relatively non-toxic and a weak mutualism occurs) (Fig. 2). The producer CFUs had a mean radius of 579.1 μm ($\text{SD} = 205 \mu\text{m}$, $n = 287$) at pH 6.5 and a mean radius of 355.8 μm ($\text{SD} = 138.6 \mu\text{m}$, $n = 566$) (Fig. 2) at pH 7.5 and these two means are significantly differ from each other (two-sample two-sided t-test; $P = 1.84\text{e-}66$, $n_1 = 287$, $n_2 = 566$). To address the second expectation, we found that the sizes of producer and consumer CFUs at pH 6.5 (*i.e.*, where nitrite is highly toxic and a strong mutualism occurs) are equivalent (Fig. 2). The producer CFUs had a mean radius of 579.1 μm ($\text{SD} = 205 \mu\text{m}$, $n = 287$) while the consumer CFUs had a similar mean radius of 603.7 μm ($\text{SD} = 205.9 \mu\text{m}$, $n = 313$) (Fig. 2), and these two means do not

significantly differ from each other (two-sample two-sided t-test; $P = 0.1$, $n_1 = 287$ x, $n_2 = 313$). To address the third expectation, we found that the sizes of the producer CFUs are smaller than those of the consumer CFUs at pH 7.5 (*i.e.*, where nitrite is highly toxic and a strong mutualism occurs) (Fig. 2). The producer CFUs had a mean radius of 355.8 μm ($SD = 138.6 \mu\text{m}$, $n = 566$) while the consumer CFUs had a mean radius of 555.1 μm ($SD = 132.8 \mu\text{m}$, $n = 119$) (Fig. 3), and these two means significantly differ from each other (two-sample two-sided t-test; $P = 4 \times 10^{-41}$, $n_1 = 566$, $n_2 = 119$). Thus, our data demonstrate that interaction strength not only determines the relative CFU abundances of metabolically-interacting strains, but also the sizes of those CFUs.

Effect of interaction strength on interspecific distances to the nearest neighbor

We next tested the effects of interaction strength on the interspecific distances to the nearest neighbor (*i.e.*, distance from a producer CFU to the nearest consumer CFU and vice versa) again using the same experiment as described above. Our expectations are four-fold. First, at pH 6.5 where nitrite is highly toxic and a strong mutualism occurs, we expect only those producer CFUs located within a certain threshold distance from a consumer CFU to develop. We therefore expect a smaller interspecific distance to the nearest neighbor. Second, at pH 7.5 where nitrite is highly toxic and a strong mutualism occurs, we expect all producer CFUs to develop regardless of their distance from a consumer CFU. We therefore expect a larger interspecific distance to the nearest neighbor. Third, at pH 6.5 there are relatively fewer producer CFUs per consumer CFU (Fig. 1). We therefore expect a larger interspecific distance for the consumer, as each consumer CFU is less likely to be in close spatial proximity to a producer CFU. Fourth, at pH 7.5 there are relatively more producer CFUs per consumer CFU (Fig. 1). We therefore expect a smaller interspecific distance for the consumer, as each consumer CFU is more likely to be in close spatial proximity to a producer CFU.

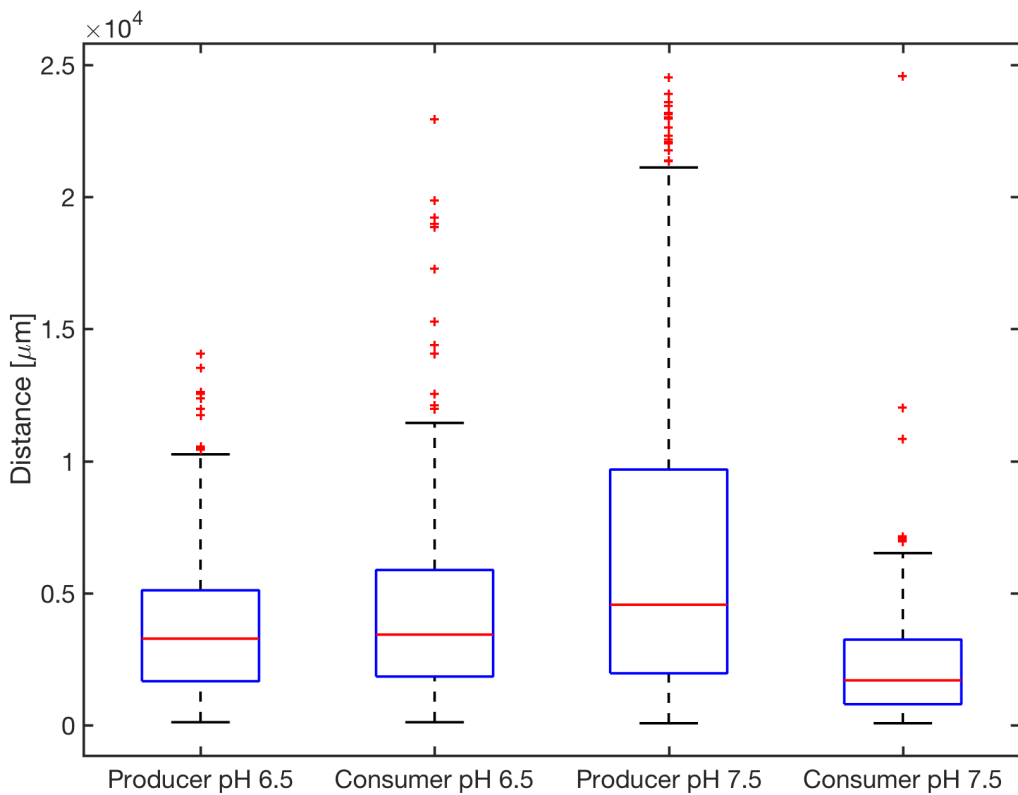


Figure 3. Interspecific distances to nearest neighbors. The interspecific distance to the nearest neighbor was measured using the Euclidean distance. At pH 6.5 (strong mutualistic conditions), the mean interspecific distance for the producer is 3.8 mm ($SD = 2.8$ mm, $n = 287$) and for the consumer is 4.4 mm ($SD = 3.6$ mm, $n = 313$). At pH 7.5 (weak mutualistic conditions), the mean interspecific distance for the producer is 6.4 mm ($SD = 5.6$ mm, $n = 566$) and for the consumer is 2.6 mm ($SD = 2.9$ mm, $n = 119$). Data are presented as Tukey boxplots.

Our results provide evidence supporting all of these expectations. To address the first two expectations, we found that the interspecific distance to the nearest neighbor for the producer is smaller at pH 6.5 (*i.e.*, where nitrite is highly toxic and a strong mutualism occurs) than that at pH 7.5 (*i.e.*, where nitrite is relatively non-toxic and a weak mutualism occurs) (Fig. 3). The mean interspecific distance is 3.8 mm ($SD = 2.8$ mm, $n = 287$) at pH 6.5 and 6.4 mm ($SD = 5.6$ mm, $n = 566$) at pH 7.5 (Fig. 3), and these two means are significantly differ from each other (two-sample two-sided t-test; $P = 5.6e-13$, $n_1 = 287$, $n_2 = 566$). To address the second two expectations, we found that the interspecific distance to the nearest neighbor for the consumer is larger at pH 6.5 (*i.e.*, where nitrite is highly toxic and a strong mutualism occurs) than that at pH 7.5 (*i.e.*, where nitrite is relatively non-toxic and a weak mutualism occurs) (Fig. 3). The mean interspecific distance is 4.4 mm ($SD = 3.6$ mm

, n = 313) at pH 6.5 and 2.6 mm (SD = 2.9 mm, n = 119) at pH 7.5 (Fig. 3), and these two means are also significantly differ from each other (two-sample two-sided t-test; P = 1.8e-06, n₁ = 313, n₂ = 119).

Interspecific distances associate positively with CFU size

We next reasoned that the interspecific distances to the nearest neighbors should conditionally associate with CFU sizes. At pH 6.5 when nitrite is highly toxic and a strong mutualism occurs, both the producer and consumer should benefit from close spatial proximity to each other. We therefore expect negative associations between CFU radius and interspecific distance. In contrast, at pH 7.5 when nitrite is relatively non-toxic and a weak mutualism occurs, only the consumer should benefit from close spatial proximity to the producer. We therefore expect a negative association between CFU radius and interspecific distance for the consumer but no association between CFU radius and interspecific distance for the producer.

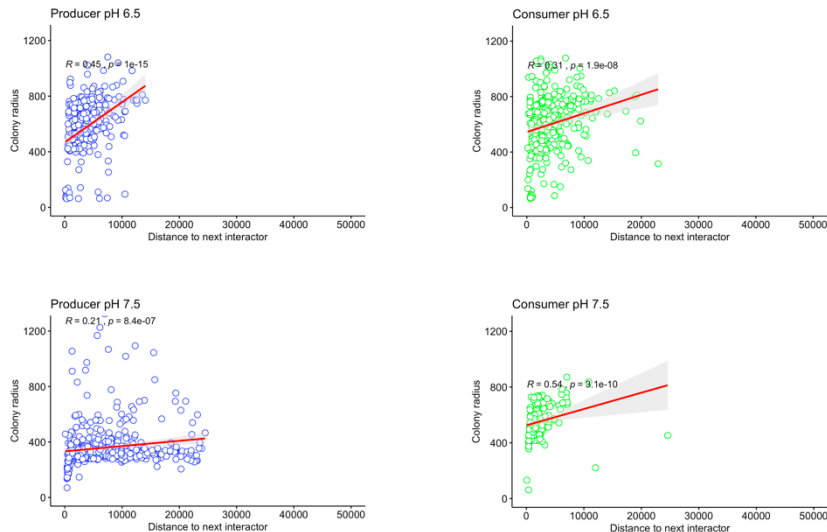


Figure 4. Association between colony size and interspecific distance to the nearest neighbor. At pH 6.5 (strong mutualistic conditions), the producer CFU radius is positively associated with the interspecific distance (Spearman rank correlation test; $R= 0.45$, $P = 1 \times 10^{-15}$, $n = 287$). This is also true for the consumer radius (Spearman rank correlation coefficient $R= 0.31$, $P = 2 \times 10^{-8}$, $n = 313$). At pH 7.5 (weak mutualistic conditions), the producer CFU radius is again positively associated with the interspecific distance (Spearman rank correlation coefficient $R= 0.21$, $P = 8 \times 10^{-5}$, $n = 566$). This is again also true for the consumer radius (Spearman rank correlation coefficient $R= 0.54$, $P = 3 \times 10^{-10}$, $n = 119$)

Unexpectedly, our data does not support either of these expectations. We did not observe negative associations between colony radii and interspecific distances for either the producer or consumer and for either pH 6.5 (*i.e.*, where nitrite is highly toxic and a strong mutualism occurs) or pH 7.5 (*i.e.*, where nitrite is relatively non-toxic and a weak mutualism occurs) (Fig. 4). Instead we observed

statistically significant positive associations (Spearman rank correlation tests; Spearman rank correlation tests; R 0.21-0.45, $P < 10^{-5}$) (Fig. 4). Thus, both producer and consumer CFUs achieve larger sizes as the interspecific distances increase to the nearest neighbor.

Intraspecific distances also associate positively with CFU size

What could be the cause of the observed positive associations between CFU sizes and interspecific distances between nearest neighbors? This appears to be counter to intuitive expectations for genotypes that mutualistically interact [36]. We propose here that the positive associations must emerge due to interspecific competition for other shared resources that develops over time [8, 24, 37]. Briefly, immediately after inoculation, the producer and consumer will primarily interact via nitrate cross-feeding and will be free of competition for secondary shared resources, as those other resources will initially be in excess. Producer CFUs that lie close to consumer CFUs will then be more likely to proliferate at pH 6.5 (*i.e.*, where nitrite is highly toxic and a strong mutualism occurs), which is consistent with our experimental results (Figs. 1 and 2). However, at later times, the producer and consumer may begin to compete for these other shared resources, which would switch the interaction from predominantly mutualistic to predominantly competitive [8]. At this time, producer CFUs that lie further from consumer CFUs will be more likely to proliferate.

If this expectation were correct, we would also expect a positive association between colony size and intraspecific distances to nearest neighbors, where larger intraspecific distances indicate less competition for shared resources. Indeed, this is what we observed when we analyzed the intraspecific distances. We again did not observe negative associations between colony radii and intraspecific distances for either the producer or consumer and for either pH 6.5 (*i.e.*, where nitrite is highly toxic and a strong mutualism occurs) or pH 7.5 (*i.e.*, where nitrite is relatively non-toxic and a weak mutualism occurs) (Fig. 5). Instead we observed statistically significant positive associations (Spearman rank correlation tests; R 0.21-0.45, $P < 10^{-5}$) (Fig. 5). Thus, both producer and consumer CFUs achieve larger sizes as the intraspecific distances increase to the nearest neighbor and competition for shared resources is reduced.

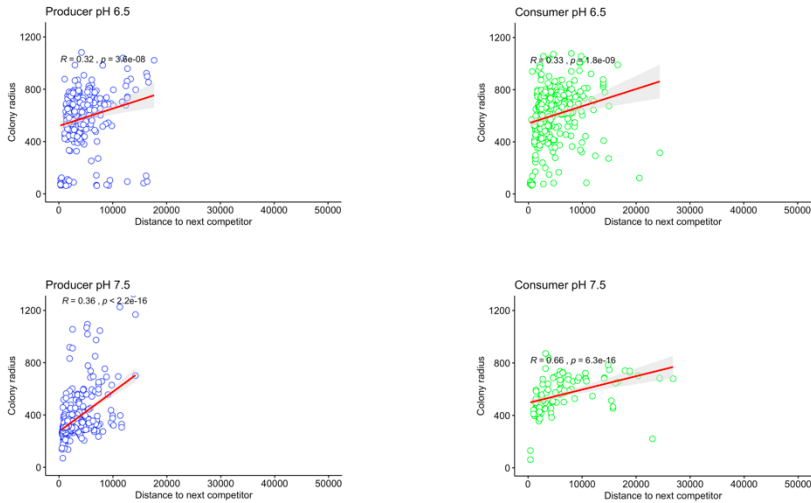


Figure 5. Association between colony size and intraspecific distance to the nearest neighbor. At pH 6.5 (strong mutualistic conditions), the producer CFU radius is positively associated with the intraspecific distance (Spearman rank correlation test; $R= 0.32$, $P = 4 \times 10^{-8}$, $n = 566$). This is also true for the consumer radius (Spearman rank correlation coefficient $R= 0.33$, $P = 2 \times 10^{-9}$, $n = 119$). At pH 7.5 (weak mutualistic conditions), the producer CFU radius is again positively associated with the intraspecific distance (Spearman rank correlation coefficient $R= 0.36$, $P = 2 \times 10^{-16}$, $n = 287$). This is again also true for the consumer radius (Spearman rank correlation coefficient $R= 0.66$, $P = 6 \times 10^{-16}$, $n = 313$).

DISCUSSION

Our data highlights what we view as an important consideration when defining microbial interactions; we typically define interactions using absolute and simplistic terminology [38]. For example, we may define a microbial interaction as mutualistic or competitive [18, 39, 40]. Then, given the type of interaction, we may try to predict the pattern of spatial self-organization likely to emerge [27] or the community properties and behaviors likely to be expressed [41]. Here, we show that even for a simple engineered mutualism, the interaction may become competitive over time and that multiple interactions may therefore occur simultaneously and contribute to community composition and behavior. While we found that producers are more likely to develop into CFUs when in close spatial proximity to consumers (Figs. 1 and 2), they are also more likely to achieve smaller CFU sizes (Fig. 3). Thus, the mutualistic component of the net interaction appears to determine the probability of a CFU establishing, but the competitive component of the net interaction determines how well the CFU is likely to proliferate after developing. This highlights the

danger of using simple absolute definitions of interactions and not considering that net interactions may include disparate individual components, and that these individual components may dynamically change in relative importance [8, 21].

Our results also reveal interspecific distances between individuals as an emergent property of a microbial community. We initially deposited individuals randomly across a surface. Yet, under certain conditions, only those individuals with particular interspecific distances were able to proliferate into CFUs. Thus, given an initial distribution of interspecific distances, the distribution changes as a consequence of the mutualistic interaction, which is a self-selecting process. The initial distribution of interspecific distances may therefore be a key factor that governs microbial spatial self-organization and the emergence of other community-level behaviors and properties [19, 37, 41].

How generalizable are our results? How likely is an interaction to be composed of more than one component that can change in predominance? We suggest that this may be the rule rather than the exception. All mutualistic interactions must, at least to some extent, contain competitive components at the same time [38]. These competitive components may be for other shared resources or could be for physical space to proliferate within[8]. As these other shared resources become depleted and become growth-limiting, the competitive components will increase in magnitude until, at some point, they predominate over the mutualistic component. Because nearly every microbial community will eventually become resource limited [42, 43], we suggest that the dynamics of a mutualistic interaction will eventually be driven by these competitive components rather than the mutualistic component, thus having profound impacts on how we predict community dynamics in nature [44, 45].

ACKNOWLEDGEMENTS

We thank Sara Mitri, Jan Roelof van der Meer and Robin Tecon for helpful discussions.

REFERENCES

1. van Vliet S, Dal Co A, Winkler AR, Spriewald S, Stecher B, Ackermann M. Spatially Correlated Gene Expression in Bacterial Groups: The Role of Lineage History, Spatial Gradients, and Cell-Cell Interactions. *Cell Syst* 2018; **6**: 496-507.e6.
2. Stump SMC, Johnson EC, Klausmeier CA. Local interactions and Self-Organized spatial patterns stabilize microbial Cross-Feeding against cheaters. *J R Soc Interface* 2018; **15**: 20170822.
3. Stubbendieck RM, Vargas-Bautista C, Straight PD. Bacterial communities: Interactions to scale. *Front Microbiol* 2016; **7**: 1-19.
4. Hartmann R, Singh PK, Pearce P, Mok R, Song B, Díaz-Pascual F, et al. Emergence of three-dimensional order and structure in growing biofilms. *Nat Phys* 2019; **15**: 251–256.
5. Ozgen VC, Kong W, Blanchard AE, Liu F, Lu T. Spatial interference scale as a determinant of microbial range expansion. *Sci Adv* 2018; **4**: 1–10.
6. Kim W, Racimo F, Schluter J, Levy SB, Foster KR. Importance of positioning for microbial evolution. *Proc Natl Acad Sci U S A* 2014; **111**: E1639-47.
7. van Gestel J, Kolter R. When We Stop Thinking about Microbes as Cells. *J Mol Biol* 2019; **431**: 2487–2492.
8. Harcombe WR, Riehl WJ, Dukovski I, Granger BR, Betts A, Lang AH, et al. Metabolic resource allocation in individual microbes determines ecosystem interactions and spatial dynamics. *Cell Rep* 2014; **7**: 1104–1115.
9. Dal Co A, Ackermann M, Vliet S van. Metabolic activity affects response of single cells to a nutrient switch in structured populations. *BioRxiv* 2019; **16**: 580563.
10. Cordero OX, Datta MS. Microbial interactions and community assembly at microscales. *Curr Opin Microbiol*. 2016; **31**: 227-234.
11. Drescher K, Nadell CD, Stone HA, Wingreen NS, Bassler BL. Solutions to the public goods dilemma in bacterial biofilms. *Curr Biol* 2014; **24**: 50–55.
12. Nadell CD, Foster KR, Xavier JB. Emergence of spatial structure in cell groups and the evolution of cooperation. *PLoS Comput Biol* 2010; **6**: e1000716.
13. Datta MS, Sliwerska E, Gore J, Polz MF, Cordero OX. Microbial interactions lead to rapid micro-scale successions on model marine particles. *Nat Commun* 2016; **7**: 11965.
14. Ebrahimi A, Schwartzman J, Cordero OX. Cooperation and spatial self-organization determine

- rate and efficiency of particulate organic matter degradation in marine bacteria. *Proc Natl Acad Sci U S A* 2019; **116**: 23309–23316.
15. Allen B, Gore J, Nowak MA. Spatial dilemmas of diffusible public goods. *Elife* 2013; **2**: 1–11.
 16. Dal Co A, van Vliet S, Kiviet DJ, Schlegel S, Ackermann M. Short-range interactions govern cellular dynamics in microbial multi-genotype systems. *bioRxiv* 2019; 530584.
 17. Dechesne A, Or D, Smets BF. Limited diffusive fluxes of substrate facilitate coexistence of two competing bacterial strains. *FEMS Microbiol Ecol* 2008; **64**: 1–8.
 18. Mitri S, Richard Foster K. The Genotypic View of Social Interactions in Microbial Communities. *Annu Rev Genet* 2013; **47**: 247–273.
 19. Kerr B., Riley M.A., Feldman M.W., Bohannan B.J.M. Local dispersal promotes biodiversity in a real-life game of rock-paper-scissors. *Nature* 2002; **418**: 171–174.
 20. Rietkerk M, van de Koppel J. Regular pattern formation in real ecosystems. *Trends Ecol Evol* 2008; **23**: 169–175.
 21. Estrela S, Libby E, Van Cleve J, Débarre F, Deforet M, Harcombe WR, et al. Environmentally Mediated Social Dilemmas. *Trends Ecol Evol* 2019; **34**: 6–18.
 22. Madsen JS, Sørensen SJ, Burmølle M. Bacterial social interactions and the emergence of community-intrinsic properties. *Curr Opin Microbiol*. 2018. Elsevier Ltd. , **42**: 104–109
 23. Marchal M, Goldschmidt F, Derksen-Müller SN, Panke S, Ackermann M, Johnson DR. A passive mutualistic interaction promotes the evolution of spatial structure within microbial populations. *BMC Evol Biol* 2017; **17**: 1–14.
 24. P. LD, J. AR. Competition for space during bacterial colonization of a surface. *J R Soc Interface* 2015; **12**: 20150608.
 25. Flemming HC, Wingender J, Szewzyk U, Steinberg P, Rice SA, Kjelleberg S. Biofilms: An emergent form of bacterial life. *Nat Rev Microbiol*. 2016; **14**: 563–75.
 26. Dal Co A, van Vliet S, Ackermann M. Emergent microscale gradients give rise to metabolic cross-feeding and antibiotic tolerance in clonal bacterial populations. *Philos Trans R Soc B Biol Sci* 2019; **374**: 20190080.
 27. Ciccarese D, Johnson DR. Functional Microbial Landscapes. *Compr Biotechnol* 2019; **6**: 42–51.
 28. Flemming H-C, Wingender J, Szewzyk U, Steinberg P, Rice SA, Kjelleberg S. Biofilms: an emergent form of bacterial life. *Nat Rev Microbiol* 2016; **14**: 563–575.
 29. Lilja EE, Johnson DR. Metabolite toxicity determines the pace of molecular evolution within microbial populations. *BMC Evol Biol* 2017; **17**: 1–12.

30. Lilja EE, Johnson DR. Segregating metabolic processes into different microbial cells accelerates the consumption of inhibitory substrates. *ISME J* 2016; **10**: 1568–1578.
31. Gram L, Ravn L, Rasch M, Bruhn JB, Christensen AB, Givskov M. Food spoilage - Interactions between food spoilage bacteria. *Int J Food Microbiol* 2002; **78**: 79–97.
32. Goldschmidt F, Regoes RR, Johnson DR. Successive range expansion promotes diversity and accelerates evolution in spatially structured microbial populations. *ISME J* 2017; **11**: 2112–2123.
33. Berg S, Kutra D, Kroeger T, Straehle CN, Kausler BX, Haubold C, et al. ilastik: interactive machine learning for (bio)image analysis. *Nat Methods* 2019; **16**: 1226-1232.
34. R Development Core Team R. R: A Language and Environment for Statistical Computing. *R Foundation for Statistical Computing*. 2011.
35. Strohm TO, Griffin B, Zumft WG, Schink B. Growth yields in bacterial denitrification and nitrate ammonification. *Appl Environ Microbiol* 2007; **73**: 1420-4.
36. Hynes WF, Chacón J, Segrè D, Marx CJ, Cady NC, Harcombe WR. Bioprinting microbial communities to examine interspecies interactions in time and space. *Biomed Phys Eng Express* 2018; **7**: 1104–1115.
37. Chacón JM, Möbius W, Harcombe WR. The spatial and metabolic basis of colony size variation. *ISME J* 2018; **12**: 669–680.
38. Dolinšek J, Goldschmidt F, Johnson DR. Synthetic microbial ecology and the dynamic interplay between microbial genotypes. *FEMS Microbiol Rev* 2016; **40**: 961–979.
39. Crespi BJ. The evolution of social behavior in microorganisms. *Trends Ecol Evol*. 2001; **16**:178-183
40. Ghoul M, Mitri S. The Ecology and Evolution of Microbial Competition. *Trends Microbiol* 2016; **24**: 833–845.
41. Yanni D, Márquez-Zacarías P, Yunker PJ, Ratcliff WC. Drivers of Spatial Structure in Social Microbial Communities. *Curr Biol.* Cell Press. 2019; **29**: R545–R550
42. Mitri S, Clarke E, Foster KR. Resource limitation drives spatial organization in microbial groups. *ISME J* 2016; **10**: 1471–1482.
43. Freilich S, Zarecki R, Eilam O, Segal ES, Henry CS, Kupiec M, et al. Competitive and cooperative metabolic interactions in bacterial communities. *Nat Commun* 2011; **13**: 589.
44. Pande S, Kaftan F, Lang S, Svato A, Germerodt S, Kost C. Privatization of cooperative benefits stabilizes mutualistic cross-feeding interactions in spatially structured environments. *ISME J*

- 2016; **10**: 1413–1423.
45. Hoek TA, Axelrod K, Biancalani T, Yurtsev EA, Liu J, Gore J. Resource Availability Modulates the Cooperative and Competitive Nature of a Microbial Cross-Feeding Mutualism. *PLoS Biol* 2016; **14**: e1002540.

CHAPTER 7: Discussion and outlook

The causes and consequences of spatial self-organization in the face of temporal and spatial heterogeneity

In this thesis, I have shown how different types of heterogeneities can influence the spatial arrangement and ultimately the functioning, ecology, and genetic diversity of a cross-feeding community. In Chapters 3 and 4, I focused my work on range expanding communities. The interesting aspect of any microbial community that undergoes range expansion is that the genotypes will organize themselves creating patterns that will display community level properties [1–7]. This universal aspect highlights the relevance of range expansion experiments as a model to study the emergence of microbial structures and their ecological and evolutionary dynamics [8–11].

In Chapters 3 and 4, I showed that in range expanding communities of metabolically dependent strains, the initial spatial positioning of cells plays a crucial role in determining the development of the community and maintaining its metabolic function. This is relevant both under static atmospheric conditions (anaerobic incubation) [4, 12] and under temporal fluctuations. When cycling from anaerobic to aerobic conditions, the cross-feeding community rearranges itself in space, from sequential (anaerobic conditions) to simultaneous expansion (aerobic conditions). In this changing condition, I found that the spatial positioning of the consumer determines its persistence at the expanding edges. I have therefore shown that the localization of consumer cells at the edge represents spatial jackpot events (Chapter 3). In our model system, these rare events do not have a genetic basis (Goldschmidt et al., in review), a fundamental difference from what is reported elsewhere [13], and instead depends on a combination of factors such as the initial spatial positioning of individuals and local concentrations of metabolites resulting from the strength of metabolic interaction (Chapter 4). For instance, the development of the colony and its interactions with the surrounding environment can impact the genetic diversity at the expanding edge (Chapter 3 and 4). In this respect, I have shown that genetic diversity could be influenced due to changes in the local environment as a result of the diffusion of metabolites (Chapter 3 and 4). I have also shown that physical obstacle on the surface influence the interspecific diversity depending on the trophic interactions (Chapter 5).

Finally, I have shown how the community assembles when cross feeding strains are separated by distance, thus investigating the effect of initial positioning on the colonization process (Chapter 6). The focus of this work was to test the hypothesis that the strength of interaction can influence community compositions and spatial organization when cross-feeding cells are spatially separated and the interaction is mediated through diffusion. This project unveils that the final community composition depends on different types of interactions that operate positively at the scale of the community level (mutualistic interaction) and negatively at local scale (competitive interaction). In conclusion, together all my results show that the different types of heterogeneities (abiotic factors) influence the development of spatial arrangements of our cross-feeding model system, with different impact on the community composition.

AVENUES FOR FUTURE RESEARCH

Controlling the biotic factor to explore spatial community assembly

In order to answer the main research question of this thesis work, I defined specific abiotic factors (spatial and temporal heterogeneities) and investigated their effects on biotic factors (spatial self-organization). I propose that a possible further development of this research work would potentially aim to understand how the biotic factor could be controlled deterministically with the use of specific abiotic factors. This would allow us to confirm the mechanisms that give rise to specific bacterial interactions and pattern formation observed in this thesis work. More specifically, it would help to better understand the dynamics of population genetics in range expanding communities by enabling one to selectively manipulate the abiotic factors that control spatial arrangement at the expanding edge.

This new research direction could aim to fill the gap of knowledge of the mechanisms that drive microbial assembly and thus understand basic principles that could enable rational community engineering [14]. In Chapter 5, I described that when the local curvature (R_c) at the colony edge decreases, this enable the presence of higher numbers of interspecific boundaries. In this chapter, I tested the general impact of physical objects on the colony edge curvature, with no control over the spatial arrangement of the physical objects on the surface.

A possible alternative to gain more control on the biotic factor is to instead use defined geometric space [15]. The use of defined geometric space, referred to as a microhabitat [16] could serve for instance to explore the effect of small curvature edges (R_c) on the spatial positioning at the expanding frontier and ultimately study population dynamics under defined structured environment. In Figure 1 I report an example on how to control the boundary curvature. This approach could enable the exploration of two interrelated aspects; the influence of small curvatures on local diversity and the emergence of jackpot events. Reducing the curvature of the edge may lead to more interspecific boundaries [6, 17]; therefore, this should potentially increase the chance to have the consumer positioned at the expanding edge with higher probability of observing the emergence of jackpot events.

In the example illustrated in Figure 1, I designed a defined geometric space with the objective to control the shape of the edge of the colony specifically to observe the effect of reduced curvature and control the spatial arrangement at the expanding edge. The geometrical defined space (also referred to as microhabitat 14, 15) was obtained by printing PDMS on a filter (0.2 Millipore GTTP02) and the method is reported elsewhere [18, 19]. The agar plate and the inoculum were prepared as reported in Chapter 5. In total, I produced 4 replicates and incubated them for 4 weeks under anaerobic conditions (the agar plates were prepared as reported in Chapter 5).

In this example (Fig.1), a geometrical defined space (with 8 channels) were designed to control the curvature of the colony edge expansion (Fig.1 C). In our cross feeding model system (weak mutualism, pH 7.5), the producer and consumer expand sequentially [20]. With a small R_c , producer and consumer cells have a higher chance to be localized together at the leading edge. Reducing the curvature of the edge of the colony increases the probability for the consumer to further advance side by side with the producer, thus breaking the sequential expansion. Consequently, this could also increase the probability of observing the emergence of jackpot events on a defined spatial position, located at every channels (Fig.1 A-B). This should be expected since it is predicted that the emergence of jackpot event should be promoted by the preferential spatial positioning of consumer at the edge of the colony (Chapter 3). Across all 4 replicates, I indeed observed the appearance of a jackpot event positioned at the channel.

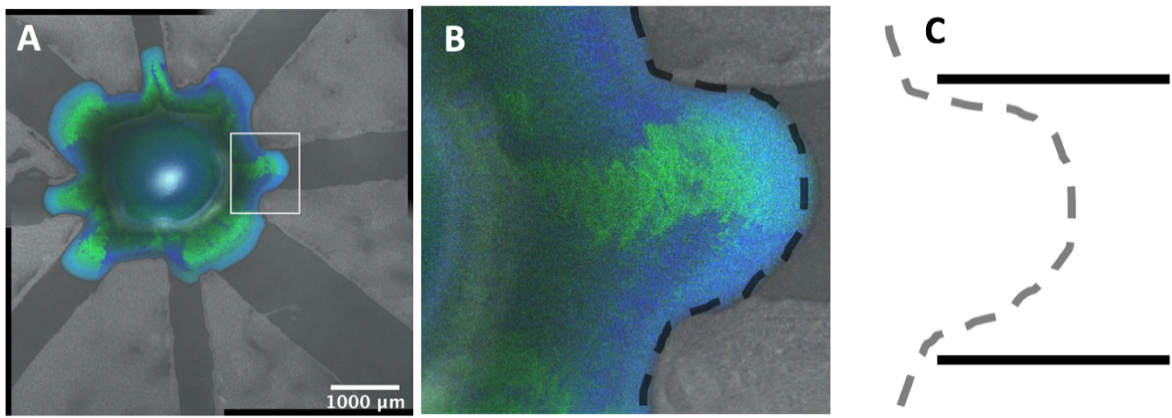


Figure 1 Filter PDMS to induce inflation of colony edge. A) PDMS filter with defined spatial geometry. A geometrical defined space was printed with PDMS on a filter membrane. A mixture of 1:1 ratio of consumer and producer was inoculated at the center of the 8 channels. B) Close up of the colony edge, (gray dashed line was manually drawn to mark the edge of the colony). When the colony expanded towards the channel, the inflation of the edge dramatically reduced the radius of expansion (R_c). C) scheme of inflation of the expansion edge. The gray dashed line marks the edge of the colonies with a small R_c , whereas the black solid line represent the border of the channel.

The above preliminary results were obtained using PDMS micropattern on filter membrane. Yet, the use of membranes could potentially lead to surface frictions and introduce possible cofounding factors that influence the pattern formation. In addition, the use of a filter membrane would have surface conditions very different from the agar surface, thus making it difficult to compare with previous work [4, 20]. A possible improvement could be obtained using 3 D engraved plexiglass micropatterns (Fig. 2). This allows to directly shape the agar in defined geometries instead of using PDMS printed on membranes, thus opening up new possible ecological explorations.

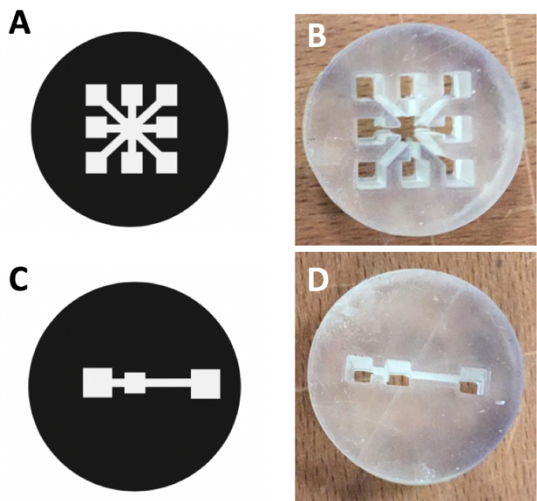


Figure 2 Schemes and prototype of 3-D engraved plexiglass micropatterns. A) Scheme of 3-D engraved plexiglass micropatterns with a central patch connected to other patches. A possible exploration of the emergence of jackpot events under the influence of external competition (other consumer colonies) or positive interactions (other producer colonies) with distant patches. B) 3-D engraved plexiglass micropatterns. C) Scheme of 3-D engraved plexiglass micropatterns. A central patch is connected with two distant patches. The example shows a configuration in which the two external patches have different distances.

Range expansion and jackpot events within a metapopulation landscape

The microbial world is an incredibly crowded environment composed of multiple species [21]. In this context, there is still a lack of knowledge regarding the dynamics of pattern formation during range expansion in the presence of other species. More specifically, it is unknown whether jackpot events are likely to emerge or not in such environments. In Chapters 3 and 4, I highlighted the importance of jackpot events to maintain the functionality of a cross feeding system under static and fluctuating condition. Therefore, it is relevant to understand the dynamics of emergence of jackpot events in light of multiple species context.

In particular, in the presence of other nearby beneficial or competitive colonies, the dynamics of local populations (cell to cell interactions within the biofilm) could be potentially influenced to the point that might modify the local spatial arrangement. It is important to understand the role of spatial structure to maintain diversity in multispecies context, and possibly it poses a new perspective population dynamics in range expanding communities.

In Figure 3 a possible approach to study the expansion of a mixed cross-feeding population in the presence of other competitive or mutualistic near populations (metapopulation landscape). To test interactions with near populations, one could use the same isogenic mutants (either consumer and producer) of the range expanding community to avoid any possible cofounding effect that would otherwise be observed when using distantly related strains.

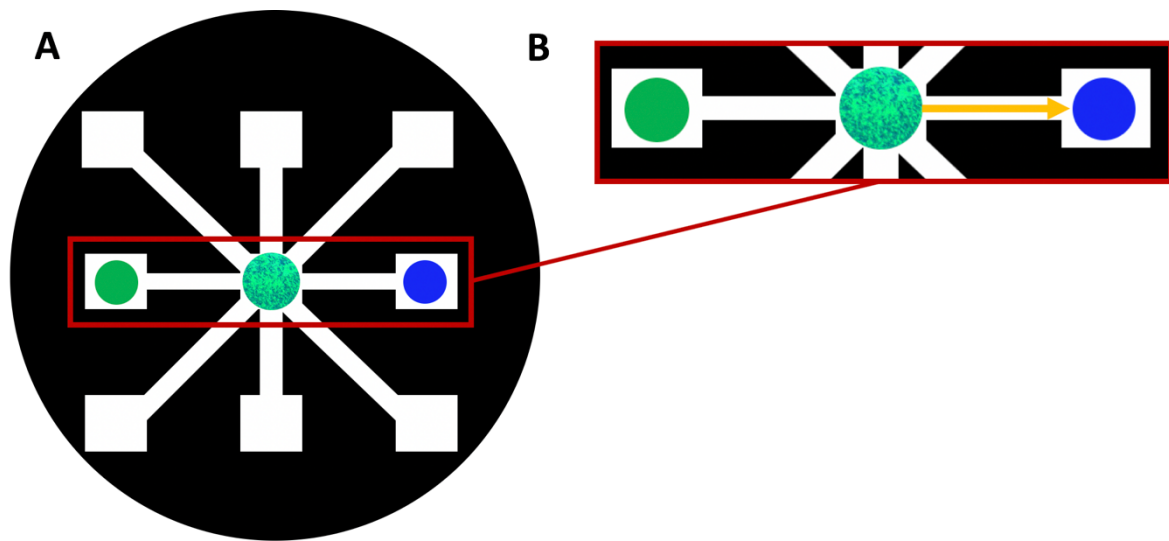


Figure 3. Example of preferential expansion in a metapopulation landscape. A) Range expansion in microhabitat within a metapopulation. At the center is inoculated a mixture of consumer and producer (equal volumetric ratio). On the sides in green is a population of consumer (competitive population) and in blue a population of producer (mutualistic population). B) Example of preferential expansion towards a mutualistic colony. In yellow an arrow points in the directions of expansion towards a mutualistic population of producer. In this case a potential jackpot event could emerge and grow preferentially towards the producer patch.

For instance, in the central patch (Fig. 3A) one could inoculate a mixed community of producer and consumer (volumetric ratio of 1:1 ratio) and in the connected patches, inoculate either a population with only producer or only with consumer. This would enable one to study the emergence of jackpot events under the influence of external negative or positive interactions. Thus, testing only the emergence of pattern formation with competitive or mutualistic interaction, one could ask: Does the emergence of jackpot events increase when influenced by external positive interactions with near beneficial populations? Or conversely, decrease with near competitive interaction?

Using micropatterning one can create multiple patches that enable the investigation of range expansion and genetic drift within a metapopulation landscape [22] (Fig. 2A and C scheme and B and D Plexiglas prototype). Another benefit of using a defined geometric space aside from controlling the local population at the expanding edge (Fig. 3A and B) is to better detect and measure the preferential expansion of jackpot events towards the direction of one specific patch (with mutualistic species of producer) or repulsion towards a competitive patch (with competitive species of consumer) (Fig. 3B). Interestingly, in the first scenario (beneficial interaction), this type of exploration enables to study the influence of beneficial but also competitive effects simultaneously, since the producer cells that surround the jackpot event will compete with the near colony of consumer (a similar eclipse effect, discussed in Chapter 5). Conversely, in absence of defined structure (i.e. without channels at the expanding edge) the preferential expansion of a local community would be hardly identified in a circular colony, as well it would be difficult to control the spatial location of jackpot events. Ultimately, this new experimental system will enable us to understand the relevance of genetic drift within a multiple populations context. The use of channels enables to control better the expanding edge, where decreasing the R_c enables the probability to obtain the emergence of a jackpot event in a precise location.

Spatio-temporal environmental heterogeneity

In this thesis work, I decomposed heterogeneities into defined classes: temporal fluctuations, geometrical heterogeneity and interspecific spatial distances. The goal was to study the influence of specific heterogeneities on pattern formation. However, in the natural environment, temporal and spatial heterogeneities in abiotic factors occur together to influence community composition [21, 23, 24]. Therefore, one possible further advancement in the exploration of the influence of the environment on community assembly would be to more realistically mimic the abiotic complexity of natural habitats [24, 25]. An interesting approach would be to recreate a three-dimensional porous environment similar to the soil. This could have multiple interesting features. For instance, fluctuating water content in soil creates cycles of saturated and unsaturated conditions, serving as temporal changes between anaerobic and aerobic conditions [26, 27]. A three-dimensional porous environment also opens the possibility to explore the effect of niche partitioning and distance interactions within a geometrical heterogeneous space [28, 29].

A possible approach is to create small soil habitats in microfluidic chambers to enable the study of spatial arrangement under the microscope with continuous observation (a similar device is reported in [30]). Using Nafion particles will gain complete optical accessibility to the spatial arrangement of the bacterial structure within the porous environment [31]. This device could also be used to fluctuate between saturated and unsaturated conditions to mimic fluctuating conditions [25]. These abiotic conditions offer together an overlap of spatial and temporal conditions that allow to explore the different questions illustrated during this thesis work in a complex context that mimics the natural environment. Finally, the abiotic factors that were chosen in this thesis work could be immediately reproduced. This is fundamental to bridge the gap of knowledge between laboratory conditions and the natural environmental where different types of abiotic factors often overlap [23, 26].

Another question then is if a spatially structured environment will enable a better partitioning of resources, reducing local competition and the potential eclipse effect. For instance, in Chapter 6 I have shown that when distances separate the interacting strain via diffusion, local interactions display competition between cross-feeding strains due to the eclipse effect [32]. In Chapter 4 I have shown that the emergence of jackpot events enable the persistence of the consumer. When moving into a three-dimensional porous space, one could ask: do the same rules and principles governing the pattern formation on agar plates also occur in soil-like space? One additional complication could be the dispersal of cells through the liquid interface which could interfere with the above observations. A possible solution would be to track the cells to differentiate between the two subpopulation (the residential and the migrant). However, dispersal may play a role to position local consumer populations at the edge of expanding producer populations. Overall this approach could open new possibilities to study defined metabolic interactions and population dynamics under overlapping spatiotemporal heterogeneity.

CONCLUSION

In this thesis work, I explored spatial and temporal heterogeneities, where I divided them into discrete classes. This approach enabled me to study the link between the dynamics of microbial assembly and the environment. Over the course of all the thesis chapters, one fundamental finding emerged as a common element of all the research projects here presented: there is a strong

connection between local interactions within the microbial community and environmental conditions [7, 33, 34]. In this thesis, I showed how environmental heterogeneities are a key factor that influence local interactions. The combined effect of interactions that occur at local scales determine the properties of the community as whole [9, 35–37]. These community properties are then a result of environmental drivers. This work has further highlighted the importance of understanding how environmental factors influence microbial community function. To fill this knowledge gap, the use of synthetic ecology has proven to be essential to understanding the basic principles and mechanisms that power the microbial world [14, 15, 38–41].

ACKNOWLEDGEMENTS

We thank Clément Vulin for helping on creating the microhabitat and Jacopo Caracci for helping on creating the of 3-D engraved plexiglass micropatterns.

REFERENCES

1. Müller MJI, Neugeboren BI, Nelson DR, Murray AW. Genetic drift opposes mutualism during spatial population expansion. *Proc Natl Acad Sci U S A* 2014; **111**: 1037–42.
2. Hallatschek O, Hersen P, Ramanathan S, Nelson DR. Genetic drift at expanding frontiers promotes gene segregation. *Proc Natl Acad Sci* 2007; **104**: 19926–19930.
3. Giometto A, Nelson DR, Murray AW. Physical interactions reduce the power of natural selection in growing yeast colonies. *Proc Natl Acad Sci* 2018; **115**: 11448–11453.
4. Goldschmidt F, Regoes RR, Johnson DR. Metabolite toxicity slows local diversity loss during expansion of a microbial cross-feeding community. *ISME J* 2018; **12**: 136-144.
5. Mitri S, Clarke E, Foster KR. Resource limitation drives spatial organization in microbial groups. *ISME J* 2016; **10**: 1471–1482.
6. Kayser J, Schreck CF, Gralka M, Fusco D, Hallatschek O. Collective motion conceals fitness differences in crowded cellular populations. *Nat Ecol Evol* 2019; **3**: 125–134.
7. Yanni D, Márquez-Zacarías P, Yunker PJ, Ratcliff WC. Drivers of Spatial Structure in Social Microbial Communities. *Curr Biol* . 2019; **29**: R545-R550.
8. Mitri S, Xavier JB, Foster KR. Social evolution in multispecies biofilms. *Proc Natl Acad Sci* 2011; **108**: 10839–10846.
9. Nadell CD, Foster KR, Xavier JB. Emergence of spatial structure in cell groups and the evolution of cooperation. *PLoS Comput Biol* 2010; **6**: e1000716.
10. Flemming HC, Wingender J. The biofilm matrix. *Nat Rev Microbiol*. 2010; **8**: 623-33.
11. Van Gestel J, Kolter R. When We Stop Thinking about Microbes as Cells. *J Mol Biol*. 2019; **431**: 2487-2492.
12. Goldschmidt F, Regoes RR, Johnson DR. Successive range expansion promotes diversity and accelerates evolution in spatially structured microbial populations. *ISME J* 2017; **11**: 2112-2123.
13. Fusco D, Gralka M, Kayser J, Anderson A, Hallatschek O. Excess of mutational jackpot events in expanding populations revealed by spatial Luria-Delbrück experiments. *Nat Commun* 2016; **7**: 1–9.
14. Said S Ben, Or D. Synthetic microbial ecology: Engineering habitats for modular consortia. *Front Microbiol* 2017; **8**: 1125.
15. Johns NI, Blazejewski T, Gomes ALC, Wang HH. Principles for designing synthetic microbial

- communities. *Curr Opin Microbiol.* 2016; **31**: 146-153.
- 16. Vulin C, Evenou F, Di Meglio JM, Hersen P. Micropatterned porous membranes for combinatorial cell-based assays. *Methods in Cell Biology..* Academic Press Inc. 2014; **121**: 155–169.
 - 17. Beller DA, Alards KMJ, Tesser F, Mosna RA, Toschi F, Möbius W. Evolution of populations expanding on curved surfaces(a). *Epl* 2018; **123**: 58005.
 - 18. Vulin C, Di Meglio J-M, Lindner AB, Daerr A, Murray A, Hersen P. Growing Yeast into Cylindrical Colonies. *Biophys J* 2014; **106**: 2214–2221.
 - 19. Vulin C, Evenou F, Di Meglio JM, Hersen P. Micropatterned porous membranes for combinatorial cell-based assays. *Methods in Cell Biology.* 2014; **121**: 155–169.
 - 20. Goldschmidt F, Regoes RR, Johnson DR. Successive range expansion promotes diversity and accelerates evolution in spatially structured microbial populations. *ISME J* 2017; **11**: 2112–2123.
 - 21. Curtis TP, Sloan WT. Prokaryotic diversity and its limits: Microbial community structure in nature and implications for microbial ecology. *Curr Opin Microbiol.* 2004; **7**: 221-6.
 - 22. Keymer JE, Galajda P, Muldoon C, Park S, Austin RH. Bacterial metapopulations in nanofabricated landscapes. *Proc Natl Acad Sci U S A* 2006; **103**: 17290-5.
 - 23. Tecon R, Mitri S, Ciccarese D, Or D, van der Meer JR, Johnson DR. Bridging the Holistic-Reductionist Divide in Microbial Ecology. *mSystems* 2019; **4**: pii: e00265-18.
 - 24. Widder S, Allen RJ, Pfeiffer T, Curtis TP, Wiuf C, Sloan WT, et al. Challenges in microbial ecology: building predictive understanding of community function and dynamics. *ISME J* 2016; **10**: 2557–2568.
 - 25. Tecon R, Ebrahimi A, Kleyer H, Erev Levi S, Or D. Cell-to-cell bacterial interactions promoted by drier conditions on soil surfaces. *Proc Natl Acad Sci* 2018; **115**: 9791–9796.
 - 26. Tecon R, Or D. Biophysical processes supporting the diversity of microbial life in soil. *FEMS Microbiol Rev.* 2017; **41**: 599-623.
 - 27. Griffiths RI, Thomson BC, James P, Bell T, Bailey M, Whiteley AS. The bacterial biogeography of British soils. *Environ Microbiol* 2011; **13**: 1642-54.
 - 28. Borer B, Tecon R, Or D. Spatial organization of bacterial populations in response to oxygen and carbon counter-gradients in pore networks. *Nat Commun* 2018; **9**: 769.
 - 29. Baran R, Brodie EL, Mayberry-Lewis J, Hummel E, Da Rocha UN, Chakraborty R, et al. Exometabolite niche partitioning among sympatric soil bacteria. *Nat Commun* 2015; **6** :8289.

30. Drescher K, Shen Y, Bassler BL, Stone HA. Biofilm streamers cause catastrophic disruption of flow with consequences for environmental and medical systems. *Proc Natl Acad Sci* 2013; **110**: 4345–4350.
31. Downie H, Holden N, Otten W, Spiers AJ, Valentine TA, Dupuy LX. Transparent Soil for Imaging the Rhizosphere. *PLoS One* 2012; **7**: e44276.
32. Harcombe WR, Riehl WJ, Dukovski I, Granger BR, Betts A, Lang AH, et al. Metabolic resource allocation in individual microbes determines ecosystem interactions and spatial dynamics. *Cell Rep* 2014; **7**: 1104–1115.
33. Estrela S, Libby E, Van Cleve J, Débarre F, Deforet M, Harcombe WR, et al. Environmentally Mediated Social Dilemmas. *Trends Ecol Evol* 2019; **34**: 6–18.
34. Stubbendieck RM, Vargas-Bautista C, Straight PD. Bacterial communities: Interactions to scale. *Front Microbiol* 2016; **7**: 1–19.
35. D’Souza GG. Phenotypic variation in spatially structured microbial communities: ecological origins and consequences. *Curr Opin Biotechnol* 2020; **62**: 220–227.
36. Ciccarese D, Johnson DR. Functional Microbial Landscapes. *Compr Biotechnol* 2019; 42–51.
37. Madsen JS, Sørensen SJ, Burmølle M. Bacterial social interactions and the emergence of community-intrinsic properties. *Curr Opin Microbiol* 2018; **42**: 104–109.
38. Großkopf T, Soyer OS. Synthetic microbial communities. *Curr Opin Microbiol* 2014; **18**: 72–77.
39. Vrancken G, Gregory AC, Huys GRB, Faust K, Raes J. Synthetic ecology of the human gut microbiota. *Nat Rev Microbiol*. Nature Publishing Group. 2019; **17**: 754–763
40. De Roy K, Marzorati M, Van den Abbeele P, Van de Wiele T, Boon N. Synthetic microbial ecosystems: an exciting tool to understand and apply microbial communities. *Environ Microbiol* 2014; **16**: 1472–1481.
41. Solden L, Lloyd K, Wrighton K. The bright side of microbial dark matter: Lessons learned from the uncultivated majority. *Curr Opin Microbiol* . 2016; **31**: 217-226.

Acknowledgements

I would like to thank Dave for having taught me how to approach the unknown and read the biological complexities objectively without any biases dictated by preconception. More importantly, for having guided me till here and give me the tools to go beyond.

I thank Dani Or for his guidance and tremendous support over the past years. I want to thank him for having challenged me and taught me how to think as scientist. I'm honored for having been hosted in his group, where he is always able to create superb conditions for collaboration and learning within an incredible culturally reach environment.

An enormous thanks to Benedict Borer, who "lived on the train" with me for all these years. And who certainly helped me to shape my research in ways I could never think to reach by myself. Thanks to his incredible sense of curiosity and for his fantastic and never ending thirst for knowledge. Thank you for being there as colleague and friend.

Thanks to Gabriele Micali who taught me how to read the data and opened my eyes to the realm of physics, through his strikingly clear and effective explanations.

A special thanks to Clement Vulin, who always found time to invent new approaches, pushing me to explore new scientific directions with patience and dedication.

Thanks to Robin Tecon, who found always the time to talk about science and exchange fundamental ideas that improve significantly this research work.

Thanks to Sara Mitri for the precious tips on how to navigate the academic world and how to shape my future goals.

Thanks to Jan Dolinšek for having been a fantastic "stubborn" lab companion. I thank him for having taught me many valuable tricks that I will carry with me in the next labs. Also, I thank him for having set an extraordinary sound system in the lab which without, I couldn't get through the very long lab days.

Thanks to Jan Van Der Meer, who boss and mentor and shapes human beings with an incredible passion. I will always thank him for having gave me the life changing opportunity to be a scientist, in an unique and special environment in which I have learn the meaning of science.

Thanks to Vladimir, for being such a great human and for having taught me how to survive in the lab and in the life.

Thanks to Erika Yashiro, who taught me precision and the rigors of the scientific method.

Thanks to Lisa Neu that have always found the time to help me survive over these years. Thanks for being able to extinguish any of my problems and doubt even before they actually become problems. Also for being able to do so with a fantastic smile.

Thanks to the Eawag's running team (especially Brian) that taught me to push and go further.

Thanks to Fredrik Hammes for all the discussions about the beauty of food fermentations, the importance of home science, but most importantly how to defend and enjoy the most important day of a PhD student.

Thanks to Jordi van Gestel for every jokes and brilliant conversations. I'm gonna miss every of those precious moments of super intense fun. Those blast of laugh are still echoing in the corridor.

Thanks to Glen Dsouza for always give me tips, suggestions and exchange always gold worth information about the scientific community.

Thanks to Micheal Daniels for being always there for me any time I needed.

A special thanks to the dream team of Eawag: Annette, Teresa, Thomi, Jurg, Teresa, Kim and Lea. I always felt like I was never alone in the lab. More importantly, you always had a smile for me.

